

Intelligent Distribution Voltage Control in The Presence of Intermittent Embedded Photo- Voltaic Generation

A thesis submitted
in fulfilment of the requirements for the degree of
Doctor of Philosophy

Kai Cheung Peter Wong
B.Sc.(Eng.), CPEng, FIEAust, SMIEEE, MIET

**College of Engineering and Science
Victoria University**

PO Box 14428
Melbourne
Victoria, Australia, 8001
March 2017



To my beloved family,

Thank you for your support and encouragement during the course of the PhD study.

Without your support, this thesis will not be possible.



Table of Contents

Declaration of Originality	i
Acknowledgments	ii
List of Figures	iii
List of Tables	vii
List of Nomenclature	ix
List of Publications	xiii
Abstract	xi
Chapter 1 - Introduction	1
1.1 Overview	1
1.2 Key Objectives	4
1.3 Design and Methodology	5
1.3.1 Literature Review	5
1.3.2 Methodology	6
1.4 Research Significance	7
1.5 Original Contribution	7
1.6 Thesis Organisation.....	8
1.7 Summary	9
Chapter 2 - Literature Review	10
2.1 Overview	10
2.2 Quality of Supply in the Low Voltage Networks.....	10
2.3 Impact of Grid Connected PV Systems.....	11
2.4 Voltage Quality Data from Smart Meters	12
2.5 Network Modelling Techniques.....	13
2.6 Methods to Increase the Hosting Capacity of LV Networks for PV Generators	15
2.7 Key Issues Identified.....	17
2.8 Summary	18
Chapter 3 - Exploratory Analysis of Smart Meter Voltage Quality Data	19
3.1 Overview	19
3.2 Smart Meter Rollout Program	19
3.3 Forms of Smart Meter Voltage Quality Data	20
3.4 Exploratory Analysis of Smart Meter Voltage Quality Data	21
3.4.1 Data Set.....	21
3.4.2 Analysis of Undervoltage Events.....	22
3.4.3 Analysis of Overvoltage Events.....	26

3.4.4	Relationship Between Overvoltage and Embedded Photovoltaic Generation	30
3.4.5	Relationship Between Voltage Non-compliance and Customer Complaints	32
3.5	Linking Voltage Quality Events to Supply Substations	32
3.5.1	Undervoltage Sites	33
3.5.2	Overvoltage Sites	35
3.5.3	Sites Experiencing both Overvoltage and Undervoltage.....	37
3.6	A Big Data Problem	38
3.7	Summary	38
Chapter 4 - A PV Generator Model Suitable for Practical Utility Applications		41
4.1	Overview	41
4.2	Survey of Existing PV Generator Models	42
4.2.1	Solar Cell Modelling [26, 27, 62-67]	42
4.2.2	Inverter Modelling [67-70].....	47
4.2.3	Solar Irradiance Modelling [67, 71, 72]	47
4.2.4	Overall PV generator model.....	48
4.2.5	Need for a Simplified Generator Model for Residential Roof-top PV Systems .	48
4.3	Simplified Generator Model for Residential Roof-top PV Systems	49
4.3.1	Insight from Smart Meter Data	49
4.3.2	Derivation of a Simplified PV Generator Model	52
4.4	Applications of the Simplified PV Generator Model	54
4.4.1	Solar Irradiance Data at PV Locations	54
4.4.2	Modelled and Actual Output of a PV System	57
4.4.3	Power Quality Investigations	59
4.4.4	Gross and Net Load Profiles	60
4.5	Summary	62
Chapter 5 - LV Network Model for Simulation Studies		64
5.1	Overview	64
5.2	Network Asset Data	65
5.3	Derivation of Line Impedances	66
5.3.1	The Need to Model Neutral Conductor and Earth.....	66
5.3.2	Calculating LV Line Impedances Considering Neutral Conductor and Earth	67
5.4	Derivation of Loads and Generation	70
5.4.1	Load Modelling	70
5.4.2	Generation Modelling	72
5.5	Modelling of Voltage Control Devices	73

5.6	Modelling Software.....	73
5.7	Network Scenarios Modelled.....	76
5.8	Summary	80
Chapter 6 - Analysis of Simulation Results.....		81
6.1	Overview	81
6.2	Effect of MV Voltage Regulation Control.....	82
6.2.1	OLTC Flat Voltage Control	82
6.2.2	Line Drop Compensation	85
6.2.3	Mixed Load Types	86
6.3	Effect of LV Voltage Regulation Control.....	87
6.3.1	LV Model to Include Effects of Circuit unbalance, Load Unbalance and Ground Connections.....	87
6.3.2	LV PV Generation Caused Localized Voltage Rise and Voltage Unbalance	88
6.4	Phase Voltage Unbalance, Its Effect and Applicable Standards	88
6.5	Optimal Solar Generator Placement to Reduce Voltage Unbalance	90
6.6	Smart Grid Voltage Control Technologies.....	93
6.6.1	Smart Grid Distribution Transformer fitted with On-load Tap Changer (OLTC) and Automatic Voltage Control Scheme.....	93
6.6.2	Smart PV Inverters	95
6.6.3	Connect Battery Storage to PV Generator	101
6.7	Future Scenario of Higher PV Penetration.....	104
6.8	Summary	108
Chapter 7 - Conclusions and Future Research		109
7.1	Overview	109
7.2	Conclusions	109
7.3	Future Work and Recommendation	115
7.4	Concluding Remarks	116
Appendices – OpenDSS & MatLab Codes.....		118
A.	OpenDSS codes for network model	118
B.	MATLAB Codes for Phase Voltage Analysis	121
C.	MATLAB Codes for Voltage Unbalance Analysis.....	128
References		135

Declaration of Originality

I, Kai Cheung Peter Wong, declare that the PhD thesis entitled “Intelligent Distribution Voltage Control in The Presence of Intermittent Embedded Photo-Voltaic Generation” is no more than 100,000 words in length including quotes and exclusive of tables, figures, appendices, bibliography, references and footnotes. This thesis contains no material that has been submitted previously, in whole or in part, for the award of any other academic degree or diploma. Except where otherwise indicated, this thesis is my own work.

Signature

Date

A large black rectangular redaction box covering the signature area.

Kai Cheung Peter Wong

15 March 2017

Acknowledgment

Someone once said that a Doctoral research was a lonely journey. In the pursuit of extending the boundary of human understanding, a PhD candidate often finds himself or herself in places where no one has ever been before. I am fortunate to have pick a research topic that is in the front of minds of many engineers practising in the electricity supply industry. Discussions with these engineers during my course of employment and in industry conferences have all contributed to ideas presented in this thesis. To these “unnamed” engineers I offer my gratitude.

I would like to thank Professor Akhtar Kalam of Victoria University for persuading me to take up the research and offering me sound advice along the way. Dr Robert Barr, principal of Electric Power Consulting, agreed to be my industry supervisor and his practical insight has been invaluable. My employer, Jemena, has been very supportive of my academic research and has contributed relevant industry data. To my cohort of PhD students at Victoria University, their comradeship and practical help has been outstanding.

No success, however, will come without the emotional support of my family. I would like to thank my wife Ada who has gracefully accepted my many working weekends and working holidays so progress can be made in my PhD research while I am employed full-time. My son Geoffrey has offered practical help around the house when I am desk-bound and his sense of humour has brightened up many stressful situations. To Engineers Australia who awarded me the John Madsen Medal for the best paper published in the Australian Journal of Electrical & Electronics Engineering (2015) – it’s like a shot of adrenalin in the arm close to the finishing line!

Last but not least, the human minds have been created with the capacity to pursue knowledge and understanding about the natural laws that govern the behaviour of things on earth. To this Creator I offer my deepest gratitude.

List of Figures

Fig. 1.1. A residential roof-top PV installation	2
Fig. 1.2. Augmentation expenditure of JEN.....	2
Fig. 1.3. Typical load curves for three classes of customers during summer peak	3
Fig. 2.1. Long-term national power quality survey result for steady state voltages of LV sites (2013-14).....	11
Fig. 2.2. Typical voltage regulation schemes in Australia	16
Fig. 3.1. Advanced Metering Infrastructure installed by Jemena Electricity Networks	20
Fig. 3.2. Example of event list for overvoltage events.....	20
Fig. 3.3. Parameters associated with a voltage quality event	21
Fig. 3.4. Number of active undervoltage sites during the 6-day period	23
Fig. 3.5. Number of undervoltage events versus maximum daily ambient temperature	24
Fig. 3.6. Number of undervoltage events versus start times	25
Fig. 3.7. Number of undervoltage events versus duration (minutes)	25
Fig. 3.8. Minimum voltage of undervoltage events	26
Fig. 3.9. Number of active overvoltage sites during the 6-day period	27
Fig. 3.10. Percentage of sites giving overvoltage events versus maximum daily ambient temperature.....	28
Fig. 3.11. Number of overvoltage events versus start times	29
Fig. 3.12. Number of overvoltage events versus duration (minutes)	29
Fig. 3.13. Maximum voltage of overvoltage events.....	30
Fig. 3.14. Growth of residential PV systems in JEN.....	31
Fig. 3.15. Analysis of customer voltage complaints	32
Fig. 3.16. Linking OV sites to upstream supply substations.....	33

Fig. 4.1. Equivalent circuit of a PV cell (5-parameter model)	42
Fig. 4.2. Simplified 4-parameter model of a PV cell	43
Fig. 4.3. Example of data required to set up a PV output model in a commonly used engineering software package.....	46
Fig. 4.4. I-V and P-V characteristics of a PV array at different irradiance levels.....	46
Fig. 4.5. Energy demand data of a customer with a 1kW PV system	49
Fig. 4.6. Consumption data for a customer	50
Fig. 4.7. PV generation data for a customer.....	50
Fig. 4.8. Maximum power output of a number of PV sites over the course of one year.....	51
Fig. 4.9. Map of Jemena Electricity Networks.....	54
Fig. 4.10. Daily correlation coefficients for the 1kW PV customer site	55
Fig. 4.11. Components of solar irradiance on a day where strong correlation is found between solar irradiance and PV generation	56
Fig. 4.12. Components of solar irradiance on a day where weak correlation is found between solar irradiance and PV generation	56
Fig. 4.13. Actual and estimated output of a 1kW PV system on a relatively cloudy day	58
Fig. 4.14. Actual and estimated output of a 1kW PV system on a relatively clear sky day.....	59
Fig. 4.15. Model voltage output of a 5 kW PV system in a power quality investigation.....	60
Fig. 4.16. Estimated and measured load profile for the 1kW PV site	62
Fig. 5.1. LV Distribution Circuits from Cypress Stillia Distribution Substation.....	66
Fig. 5.2. Details of LV Distribution Circuit #4	66
Fig. 5.3. Concepts of conductor images used in Carson's equations	68
Fig. 5.4. Weekly loadshapes used in the simulation based on SCADA and smart meter measurements.....	71

Fig. 5.5. Loadshapes used in the simulation for 15 February 2015 based on SCADA and smart meter measurements.....	72
Fig. 5.6 Output of solar generator PV1 between 15 to 21 February 2015	72
Fig. 5.7. Example OpenSS codes for converting a 4-wire LV line construction into impedance matrix	74
Fig. 5.8. Output of OpenDSS codes for a 4-wire LV line.....	74
Fig. 5.9. Single-line presentation of network model	76
Fig. 5.10. SCADA readings of loads on SHM Zone Substation and SHM14 feeder.....	77
Fig. 5.11. Commercial and industrial loadshapes for the period 15 to 21 Feb 2015.....	78
Fig. 6.1. Red phase voltage on 433V side of distribution substation showing the effect of various MV voltage control schemes (Scenarios 1, 2, 4, 5 & 6).....	84
Fig. 6.2. Voltages at the end of LV distribution circuit #4.....	84
Fig. 6.3. The use of Line Drop Compensation has improved the voltage at the 433V side of the distribution substation (Bus9)	85
Fig. 6.4. The use of Line Drop Compensation has improved the voltage at the end of LV circuit #4 (Bus17).....	85
Fig. 6.5. Red phase voltage on 433V side of distribution substation showing the effect of different load profiles on SHM 22kV bus.....	86
Fig. 6.6. Voltages at the end of LV distribution circuit #4, with MV and LV network modelled as 3-wire balanced network	87
Fig. 6.7. Voltages at the end of LV distribution circuit #4.....	88
Fig. 6.8. Modelled results with PV1 and PV2 both connected to red phase	92
Fig. 6.9. Modelled results with PV1 connected to white phase and PV2 connected to blue phase	93
Fig. 6.10. Voltages at 415V bus (Bus9) with OLTC distribution transformer.....	94

Fig. 6.11. Voltages at end of distribution circuit #4 (Bus17) with OLTC distribution transformer	94
Fig. 6.12. Voltage unbalance on various load buses with OLTC distribution transformer.....	94
Fig. 6.13. Volt-Watt characteristics of smart inverter used in the simulation.....	96
Fig. 6.14. Effect of Smart Inverter Volt-Watt control on phase voltages	97
Fig. 6.15. Effect of Smart Inverter Volt-Watt control on voltage unbalance.....	97
Fig. 6.16. Volt-Var characteristics of smart inverter used in the simulation.....	98
Fig. 6.17. Effect of Smart Inverter Volt-Var control on phase voltages	99
Fig. 6.18. Effect of larger inverter rating on Smart Inverter Volt-Var control.....	100
Fig. 6.19. Effect of larger inverter rating on voltage unbalance.....	100
Fig. 6.20. Charging & discharging characteristics of the 4.4kW/25kWh battery.	102
Fig. 6.21. Battery energy and charging status during the simulation.	103
Fig. 6.22. Voltages at Bus20 without storage battery	104
Fig. 6.23. Voltages at Bus20 with storage battery.....	104
Fig. 6.24. Voltage unbalance on the load buses with storage battery	104
Fig. 6.25. Voltages at the various load buses with four PV	105
Fig. 6.26. Voltages at the various load buses with four PV and after phase optimisation	106
Fig. 6.27. Voltages at the various load buses with four PV and after phase optimisation and application of LDC.....	107

List of Tables

Table 3.1 Undervoltage events.....	23
Table 3.2 Analysis of the 6,131 undervoltage sites.....	23
Table 3.3 Overvoltage events.....	27
Table 3.4 Analysis of the 6,131 overvoltage sites.....	27
Table 3.5 Proportion of overvoltage events generated by sites with PV installation.....	31
Table 3.6 20 distribution substations with the highest percentage of undervoltage sites in the 6-day period.....	34
Table 3.7 Ten worst zone substations which supply distribution substations with undervoltage events	35
Table 3.8 20 distribution substations with the highest percentage of overvoltage sites in the 6-day period.....	36
Table 3.9 Ten worst zone substations which supply distribution substations with overvoltage events	37
Table 3.10 Seven worst distribution substations whose customers have experienced both overvoltage and undervoltage events in the 6-day period.....	37
Table 4.1 Summary of correlation coefficients	55
Table 5.1 Network Characteristics (provided by Jemena Electricity Networks)	65
Table 5.2 Derivation of base loads and load shapes.....	71
Table 5.3 Voltage Control Devices	73
Table 5.4 Impedance Matrix for 4-wire 19/3.25AAC LV Overhead Line.....	75
Table 5.5 Network Scenarios for MV Voltage Control	79
Table 5.6 Network Scenarios for LV Voltage Control	79
Table 6.1 Voltage Control Settings	83

Table 6.2 Network Voltage Unbalance Factor for Different Combinations of Phase Connection of Generators PV1 and PV2	92
Table 6.3 Network Voltage Unbalance Factor for Different Combinations of Phase Connection of Generators PV1 and PV2, with PV3 and PV4 connected to Customer 6 (W-phase) and Customer 2 (B-phase)	106

List of Nomenclature

AC	Alternating Current
ADMD	After Diversity Maximum Demand
AMI	Advanced Metering Infrastructure
BOM	Bureau of Meteorology
COM	Component Object Model
DC	Direct Current
DSTATCOM	Distribution Static Compensator
GIS	Geographical Information System
HANA	High Performance Analytical Appliance, an in-memory processing database in the SAP suite of products
IEC	International Electrotechnical Commission
JEN	Jemena Electricity Networks
kVA	Kilo-Volt-Ampere, a measure of energy
kW	Kilo-Watt, a measure of active power
kWh	Kilo-Watt hour, a measure of active energy
LDC	Line Drop Compensation
LV	Low Voltage
MATLAB	Matrix Laboratory, a multi-paradigm numerical computing environment and fourth-generation programming language
MEN	Multiple Earthed Neutral
MPPT	Maximum Power Point Tracking
MV	Medium Voltage
MVA	Mega-Volt-Ampere, a measure of energy
MWh	Mega-Watt hour, a measure of active energy
NOCT	Nominal Operating Cell Temperature
OLTC	On-Load Tap Changer
OpenDSS	Open Distribution System Simulator

OV	Overvoltage
PDF	Probability Density Function
POA	Plane-of-array
POC	Point of Connection
PQ Loads	Loads expressed in active power (P) and reactive power (Q)
PV	Photo-Voltaic
SAP	Systems, Applications and Products, a software for enterprise resource planning and data management
SCADA	Supervisory Control and Data Acquisition
STC	Standard Test Conditions
TMY	Typical Meteorological Year
UV	Undervoltage
VRR	Voltage Regulating Relay

List of Publications

1. **P.K.C. Wong**, R.A. Barr and A. Kalam, “Analysis of Voltage Quality Data from Smart Meters”, Australasian Universities Power Engineering Conference, 2012
2. R.A. Barr, **P. Wong** and A. Baitch, “New Concepts for Steady State Voltage Standards”, IEEE International Conference on Harmonics & Quality of Power, 2012
3. **P.K.C. Wong**, R.A. Barr and A. Kalam, “Using smart meter data to improve quality of voltage delivery in public electricity distribution networks”, Saudi Arabia Smart Grid Conference, 2012
4. **Peter K.C. Wong**, Akhtar Kalam and Robert Barr, “A Big Data Challenge – Turning Smart Meter Voltage Quality Data into Actionable Information”, 22nd International Conference on Electricity Distribution (CIRED), 2013
5. **Peter K.C. Wong**, Robert A. Barr, Akhtar Kalam, “Voltage Rise Impacts and Generation Modeling of Residential Roof-top Photo-Voltaic Systems”, IEEE International Conference on Harmonics & Quality of Power, 2014
6. **Peter K.C. Wong**, Akhtar Kalam and Robert Barr, “Generation Modeling of Residential Roof-top Photo-Voltaic Systems”, 23rd International Conference on Electricity Distribution (CIRED), 2015
7. **Peter K.C. Wong**, Robert A. Barr & Akhtar Kalam, “Generation modelling of residential rooftop photovoltaic systems and its applications in practical electricity distribution networks”, Australian Journal of Electrical and Electronics Engineering, 12:4, 332-341. The paper was awarded the John Madsen Medal for the best paper published in AJEEE in 2015.
8. **Peter K.C. Wong**, Akhtar Kalam and Robert Barr, “Modelling and Analysis of Practical Options to Improve the Hosting Capacity of Low Voltage Networks for Embedded Photo-Voltaic Generation”, accepted for publication in the IET (Institution of Engineering & Technology) Journal of Renewable Power Generation. Doi: 10.1049/iet-rpg.2016.0770.
9. **Peter K.C. Wong**, Akhtar Kalam, Robert A. Barr, “Increase the hosting capacity of four-wire low-voltage supply network for embedded solar generators by optimising generator and load placement on the three supply phases”, 24th International Conference & Exhibition on Electricity Distribution (CIRED), 2017

Abstract

Dwindling fossil fuel resources and the concern for greenhouse gas emissions resulting from the burning of fossil fuels have led to significant development of renewable energy in many countries. While renewable energy takes many forms, solar and wind resources are being harvested in commercial scale in many parts of the world. Government incentives such as Renewable Energy Certificates and Feed-in Tariffs have contributed to the rapid uptake.

Australia, per capita of population, has topped the world in the penetration of residential roof-top solar generation systems. With electricity consumers of only 10 million, there are almost 1.5 million grid connected residential solar installations approaching 5,000MW of installed capacity in June 2016, and the number continues to grow. These residential PV generations are embedded in the Low Voltage (LV) networks that were traditionally designed to take one-way flow of electricity only. As the number of embedded solar generators increases, customers begin to experience voltage quality problems.

Public electricity supply networks are required to deliver voltages within narrow ranges. This ensures that the supply voltages are compatible with the design parameters of consumer electrical equipment. Supply voltage non-compliance has high societal costs as it impacts on the efficiency, performance and life expectancy of electrical equipment.

Except for large commercial or industrial customers, however, direct monitoring of the quality of voltage delivered is not possible due to the relatively high cost of providing measurement at each customer's point of supply. Electricity distribution utilities generally adopt a reactive approach of responding to customer voltage complaints. This approach could be appropriate if it is expected that supply voltages are within declared range for most customers and most of the time. This is because customers generally only complain of high or low voltage when they can observe something abnormal. Hidden costs such as lower equipment efficiency and shortened equipment life are not obvious to most customers.

The rollout of residential smart meters with voltage monitoring function has brought about challenges and opportunities for electricity distribution utilities. For the first time, utilities receive information about the energy consumption and voltage at the point of supply for every residential customer. Utilities are no longer ignorant of the voltages they

supply to customers hence there is an obligation to fix voltage non-compliance. At the same time smart meters improve the utility's visibility of the Low Voltage network and opens up the opportunity to monitor the impact of embedded generators on supply quality. To make sense of the vast quantity of LV network voltage quality data requires utilities to implement "Big Data" analytic tools. With the results of this analysis, corrective action can be taken where necessary. This is a new horizon for many utilities, with new roles such as "data scientist" and "data analytics engineer" appearing in utility's organisation charts. The research for this thesis has benefited from smart meter voltage quality data provided by Jemena Electricity Networks (JEN), an electricity distribution company in the state of Victoria, Australia. Analysis of voltage quality data has confirmed that, firstly, voltage quality data are a form of "Big Data" as defined by Gartner, having characteristics of three "V" – Volume, Velocity and Variety – and secondly, LV supply voltages are on the high side most of the time (though low supply voltages also occur at times of peak demand), and thirdly, there is indication that higher proportion of LV customers with grid connected solar installations have experienced overvoltages. The last point does not come as a surprise as PV generator will raise the voltage at the point of supply in order to inject excess generation into the supply grid.

But how many Photo-Voltaic (PV) generators can a distribution circuit accommodate before voltage rise or other voltage quality parameters exceed the regulatory limits? To answer this question a distribution engineer requires an accurate LV network model so the effect of PV attributes such as generation output, relative location, interaction with other PV systems and loads can be simulated. Accurate LV network models have traditionally been lacking due to the lack of data and real-time monitoring by utilities. Mass rollout of smart meters to residential customers makes it possible to accurately identify the phase and circuit connection, as well as consumption, of every LV customer, allowing an accurate LV network model to be established.

Integral to the network model is PV generation output prediction. Models of PV generators have been developed by various researchers. While these complex models provide accurate output prediction, they require extensive data collection which is possible in a laboratory setting but impractical for PV systems installed in customer premises. This research has developed a model that treats the PV installation as a system, not individual components, and requires only panel DC rating at standard test conditions

(STC). Input environmental parameter requirements are simplified to global solar irradiance and ambient temperature only thus making the model very efficient to use.

The PV output model developed is then incorporated in a 4-wire LV network model set up in the Open Distribution System Simulator™ (OpenDSS). Other parameters for the network model are obtained from utilities' Geographical Information System (GIS), with time series load data from the Supervisory Control and Data Acquisition (SCADA) system and smart meter system, and environmental data from a nearby weather station. Traditional utility voltage control schemes, namely voltage regulation applied to on-load tap changing transformers at primary (MV) substations and MV switched shunt capacitor installations, are modelled. MATLAB® is used to drive load flow simulations from which voltage and current profiles on various parts of the distribution network are analysed.

It is concluded that modification to existing voltage regulation schemes will be required to lower the nominal voltage delivered to customers, in accordance with recommendations made in AS 61000.3.100, a relatively new Australian Standard on steady-state voltage limits in public electricity systems. In addition, an effective method of dealing with voltage rise is required to minimise voltage unbalance between supply phases in the LV supply network. This can be achieved by minimising the *Network Voltage Unbalance Factor* (defined in the thesis) through judicious placement of PV generation to the appropriate supply phases. These practical, cost effective approaches will go a long way in improving the hosting capacity of LV network for PV generation. Lastly, the effect of smart grid technologies such as on-load tap changing LV distribution transformers, smart PV inverters and battery storage on hosting capacity are demonstrated using network simulation.

Index Terms: *Rooftop photovoltaic systems, renewable energy resources, steady-state voltage, voltage standards, voltage quality, smart meter, solar output model, Low Voltage network modelling, voltage control, phase imbalance, PV hosting capacity, smart grid technologies.*

Chapter 1 - Introduction

1.1 Overview

Concern for greenhouse gas emission and the resultant focus on de-carbonisation has resulted in significant changes to the electricity supply industry. Renewable energy resources, such as wind and solar, are being harvested in commercial scale in many parts of the world. Due to the requirement of large land area for deployment, wind and solar farms are generally located in sparsely populated areas where significant investment in electricity infrastructure is required to transmit the renewable energy to the load centres. The intermittent nature of wind and solar also challenges power system operation when these renewable generations displace traditional base load power stations run on fossil fuels. In the urban landscape, wind turbines are rarely found but rooftop PV systems have found wide acceptance especially in countries where favourable government policies such as feed-in tariffs exist. In Australia the penetration of residential rooftop PV systems is among the highest in the world. With electricity consumers of only 10 million, there are almost 1.5 million grid connected residential PV installations approaching 5,000MW of installed capacity (June 2016), and the number continues to grow. A residential rooftop PV installation is shown in Figure 1.1.



Fig. 1.1. A residential roof-top PV installation

These residential PV generations are embedded in the LV networks. LV networks are traditionally designed with a ‘fit and forget’ approach and receive relatively little additional investment once they are built. Advancement in remote monitoring is seldom applied to LV networks hence they lack observability [1]. An example of historic and forecast augmentation expenditure for JEN is shown in Figure 1.2. It can be seen that minimal investment goes into LV augmentation once the circuits are built.

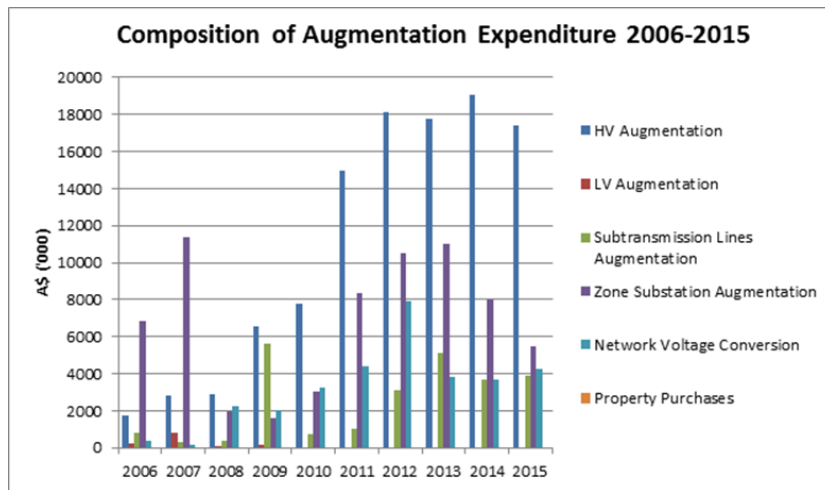


Fig. 1.2. Augmentation expenditure of JEN

Historically, lack of vigour in LV data capture means that LV circuit data (conductor size, number of phases, line geometry) are not accurate and customer information such as supply phase is either missing or cannot be relied upon.

In this environment, planning of LV networks incorporates significant assumptions of customer homogeneity. JEN estimates customer load consumption during the summer peak using three daily load curves shown in Figure 1.3: residential, commercial and industrial. Aggregation of customer loads to upstream supply circuit and distribution

substation is based on the use of After Diversity Maximum Demand (ADMD). ADMD for residential customers are taken to be 4.5kVA per customer. For commercial and industrial customers, the ADMD is determined based on appliance information supplied by the customers and an assumed diversity of usage. The addition of a new customer to an existing LV circuit is based on rule-of-thumb or simple calculation without reverting to detailed network modelling. This planning approach represents good industry practice when LV network monitoring facilities are absent, customers are passive users and fairly homogenous.

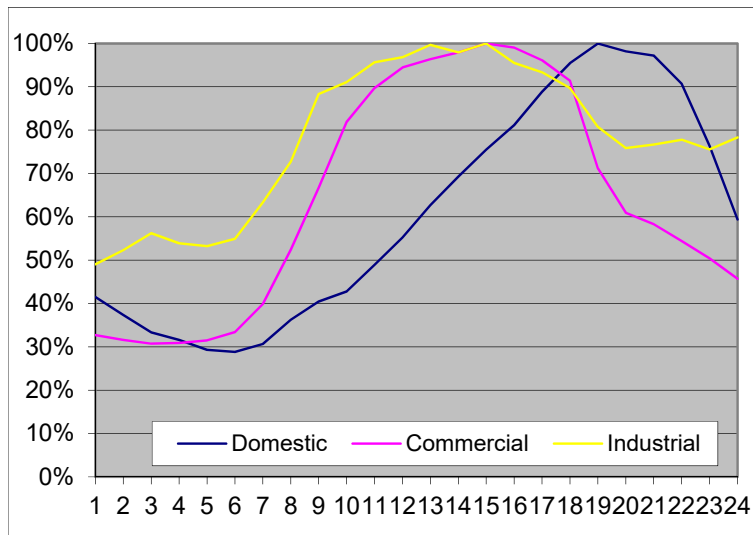


Fig. 1.3. Typical load curves for three classes of customers during summer peak

The assumptions of “typical customers” no longer hold true when customer behaviour starts to diverge from the norm. A new term “Prosumer” has been used to describe a customer who is, at different times, both a consumer and generator of electricity. This term applies to residential customers who have installed roof-top PV systems except when a control system has been installed to prevent reverse power flow, or the generation output of the PV system is always consumed by the local load. Customer behaviour will increasingly diverge as they adopt new forms of energy devices and services such as fuel cells, electric vehicles, battery storage, demand response and peer-to-peer energy trading. Emerging challenges are occurring on the parts of the supply network that are least prepared for them. A perfect storm is coming to the supply utilities!

This research is motivated by the desire to find practical, cost effective solutions that can be adopted by supply utilities to accommodate the increasing penetration of roof-top PV

systems, and in this way preserve or even increase the value of the supply network to the modern-day customers.

1.2 Key Objectives

The key objectives of this research are synthesised as follows:

- Perform exploratory analysis of voltage quality data collected by smart meters and develop, on a macro level, insight about steady-state voltage delivery to customers;
- Determine, based on anecdotal evidence and smart meter voltage quality data analysis, how grid connected residential PV systems contribute to voltage quality issues;
- Develop a Low Voltage network model which can be used to simulate the effect of PV on steady-state voltage levels. The model shall be accurate enough for network planning purposes and incorporate data sets that can be reasonably collected by supply authorities:
 - Simplified PV output model based on panel DC rating, inverter AC rating, panel orientation and environmental parameters collected by public weather stations;
 - 4-wire LV network design comprising single-phase loads connected between phase and neutral conductors as well as three-phase loads within a Multiple Earthed Neutral (MEN) system;
 - Time series load and generation data collected by smart meters and Supervisory Control and Data Acquisition (SCADA) system;
 - Conventional utility voltage control systems consisting of voltage regulating schemes acting on transformers with on-load tap changers, substation switched shunt capacitor banks and line switched shunt capacitor banks.
 - Smart grid voltage control systems consisting of on-load tap changing distribution transformer, smart PV inverter and battery storage system.
- Perform time series load flow simulation studies to obtain LV network voltage profiles for different network configurations and voltage control system scenarios, for different PV penetration levels.

- Make recommendations to supply authorities on changes to their network planning policies and adoption of smart network technologies in order to increase the capacity of their LV distribution networks to accommodate the increasing penetration of PV generation systems.

1.3 Design and Methodology

1.3.1 Literature Review

Interest in the behaviour of grid connected PV systems has intensified in recent years due to the continual decline in system costs making the systems more affordable and the number of installations has increased considerably. A body of knowledge has been developed on models that can accurately represent the various components of the PV systems and how the components interact to produce energy on an annual basis. Models with higher time resolution have also been developed to model the transient impact on the supply grid. These models generally require design parameters that can reasonably be collected for large systems connected to the Medium Voltage or High Voltage grids but will require significant simplification for small PV systems installed by residential customers.

The PV models developed have been used in system studies to determine the upper limit of PV penetration before serious issues arise. Due to the different assumptions of network characteristics and generally idealised installation conditions, these limits cannot be readily used by electricity supply companies.

While big data analytics techniques have been applied to many service industries such as finance and banking, smart meter data analytics is a relatively new research area as mass rollout of smart meters to residential customers started to occur only around mid 2000s. This area of research is primarily driven by supply utilities as they have access to the meter data and are keen to unlock the value of the data to improve planning and operational performance of their supply networks.

Supply utility voltage control techniques have remained fundamentally the same since electrification of societies occurred over 100 years ago. This is evidenced by the lack of research papers published on the topic. With the advance of small generators embedded in the distribution network, there is renewed research interest on improving utility voltage control to manage the impact of these small embedded generators. Some large-scale smart grid demonstration projects in the U.S. and Europe have specifically include the trial of

various advanced voltage control schemes to alleviate the impact of embedded generation on supply voltage quality.

The literature review focuses on scientific research papers on PV characteristics, technical journals and industry conferences where relevant results of industry research are disseminated.

1.3.2 Methodology

Smart meter voltage quality data (supplemented by energy consumption data where required) of approximately 100,000 residential customers over a 1-week period are collected for exploratory data analysis. The majority of these customers have a net metering scheme where the energy meter records the net consumption/generation over each 30-minute integration time interval. The exploratory data analysis yields macro-level insight on the existing voltage quality delivered to utility customers including customers who have installed grid connected PV generation systems.

Literature review is conducted to identify the appropriate PV generation output model that can be used in system studies. Simplification of the PV output model is attempted to reduce the number of model parameters in order to improve the practicality of the model for use in distribution system studies.

Accuracy of the simplified PV output model is tested on a number of PV customers who have gross metering schemes where the generation output and load consumption are metered separately.

To test the effect of various voltage control schemes on managing voltage issues caused by embedded PV generation, parameters of an actual LV distribution circuit are determined and then set up in a network model. This approach is preferred by supply utilities over the use of “typical” circuits and is becoming increasingly feasible with the mass rollout of smart meters. The circuit model is set up in OpenDSS™ where load flow simulations are run. MATLAB© interfaces with OpenDSS™ and is used to vary the PV penetration level and voltage control schemes, and to analyse the load flow results.

Based on the modelled results, recommendations are made for supply authorities on changes to their network planning policies and adoption of smart network technologies that will increase the capacity of their LV distribution networks to accommodate the increasing penetration of PV generation systems.

1.4 Research Significance

The installation of grid connected renewable generation systems, in particular PV systems, is an unstoppable trend worldwide. For the small grid connected PV systems, government regulators and customers are demanding a streamlined connection process which generally translates into automatic connection policy for systems under a certain kVA limit. Even small systems can cause localised voltage issues and when in aggregate, can affect the upstream supply network. Voltage quality non-compliance has high societal costs as this affects the performance, energy efficiency and longevity of customer electrical equipment. As LV networks are generally not observable to utility engineers, utility engineers tend to apply conservative limits to enforce their responsibility for voltage quality. This limits the amount of small PV generators that can be automatically connected to the supply network. When the limit is reached, utilities will need to assess each proposed connection on a case-by-case basis, generally via background measurement and modelling. The lack of an appropriate PV generation model and an accurate LV model again hinders the effectiveness and efficiency of this assessment process.

This research, enabled by the availability of smart meter data, provides recommendations on the establishment of accurate network models and improvements to existing operational practices (voltage control schemes and phase connection of PV generation) so as to increase the capacity of the LV network to host embedded PV generation, before resorting to significant investment in network augmentation and smart grid technologies.

1.5 Original Contribution

Electricity supply utilities worldwide are transforming themselves from an infrastructure provider (“poles and wires” business) to an enabler of various energy services. This transformation is driven by customer preference and is crucial to the future survival of the supply utilities. Pivotal in this transformation process is the development of a customer focused culture.

This research is motivated by the desire to find practical, cost effective solutions that can be adopted by supply utilities to accommodate the increasing penetration of customer roof-top PV systems, and in this way preserve or even increase the value of the supply network to the modern-day customers. Industry research has been mostly focused on the development of smart grid technologies as mitigating measures, which generally require

significant additional grid investment. While transforming the supply grid performance by investing in smart grid technologies is unavoidable, customers are already financially burdened by the transition to a renewable energy future caused by initiatives such as feed-in tariffs¹. A prioritised approach of improving existing operational practices and implementation of smart grid technologies will help to spread the additional investment cost over a longer time horizon, improve customer service and reduce the risk of customer defection (leaving the grid).

The research takes an insider view of the supply utility organisation (enabled by this researcher's many years of experience working for supply utilities), provides insight of network planning and voltage control criteria, identifies the challenges caused by grid connected PV systems, and recommends practical approaches that can be taken to increase the hosting capacity of the supply network. This end-to-end supply utility focus is original, and provides significant value to a supply utility on the path of transformation to a customer-focused energy service provider of the future.

The research is enabled by the availability of residential smart meter data. The mass rollout of smart meters to residential customers is a recent development and is still ongoing in many parts of the world. Insight on smart meter data developed in the research, while specific to the network being studied, will be a useful reference for other distribution networks and demonstrate the value of smart meter data to network service providers.

1.6 Thesis Organisation

This thesis comprises of seven chapters and is organised as follows:

- *Chapter 1:* covers a brief introduction of the key objectives, motivations and methodologies of the research, while providing insight into the research significance in the discipline of electrical engineering.
- *Chapter 2:* presents a comprehensive literature review of smart meter data analytics, impact assessment of grid connected renewable generation systems, PV generation modelling and options for mitigating the impact of grid connected renewable generation systems.

¹ Feed-in tariffs increase the cost of each unit of electricity, resulting in higher electricity prices to customers who have no access to the feed-in tariffs i.e. those who have not installed a PV system

- *Chapter 3*: describes the insight developed by performing exploratory analysis of smart meter voltage quality data. It highlights the usefulness and limitations of existing smart meter data and makes recommendations on how the data can be improved to increase its usefulness.
- *Chapter 4*: develops a PV generation model and demonstrates its use in practical electricity distribution network applications.
- *Chapter 5*: describes the development of a network model for a real distribution circuit that has eight residential customers, two of which have grid connected roof-top PV systems.
- *Chapter 6*: analyses the results of load flow studies performed on the network model under different network scenarios and voltage control strategies, and provides recommendations to supply utilities.
- *Chapter 7*: summarises the work in chapters 1-6 and provides recommendations for future research studies.

1.7 Summary

This chapter has introduced the drivers which lead to the significant development of roof-top residential PV systems. The challenge to supply utilities arising from the development is outlined and the strategic objectives for supply utilities to allow connection of these embedded generation system are described. Attention is brought to the motivation and scope of this research, and the main contributions listed. Finally, the thesis structure and main contents of each chapter are briefly outlined.

Chapter 2 - Literature Review

2.1 Overview

This chapter presents a comprehensive review of the research in voltage quality impact caused by embedded generation, in particular, residential roof-top PV installations connected to the LV networks and the potential mitigating measures that can be applied. Section 2.2 provides some background to the quality of supply in the existing LV networks. Section 2.3 examines the impact of grid connected PV systems. Section 2.4 reviews the use of smart meter data to improve the visibility of the LV networks. Section 2.5 reviews network modelling techniques that are used to quantify the impact of PV systems on LV network performance. Section 2.6 addresses methods which have been used to improve the hosting capacity of LV networks for PV generators. Finally, based on the literature survey, Section 2.7 summarises the key issues identified.

2.2 Quality of Supply in the Low Voltage Networks

There is renewed interest in the quality of supply in the LV networks due to increasing connection of residential PV systems and other emerging customer technologies (such as electric vehicles and energy storage systems). While standards for quality of supply in LV networks have been established (e.g. AS/NZS 61000.3. series), due to the high cost of providing permanent power quality monitoring at every customer connection point compliance measurement is generally carried out on customer complaints or as one-off statistical programs. Since year 2000, the Power Quality Centre of the University of Wollongong, Australia, has been conducting an annual long-term national power quality survey involving many electricity distribution companies [2]. The survey focuses on the power quality data of steady-state voltage, unbalance, harmonics and sags/swells. It is noteworthy that the annual survey has consistently found some 25% to 30% of LV sites record 95th percentile steady-state voltage levels which are above the upper LV limit (230V + 10%), predominately during the light load periods (Figure 2.1). High voltage phenomena during low load periods have also been reported in other countries e.g. the U.K. [3].

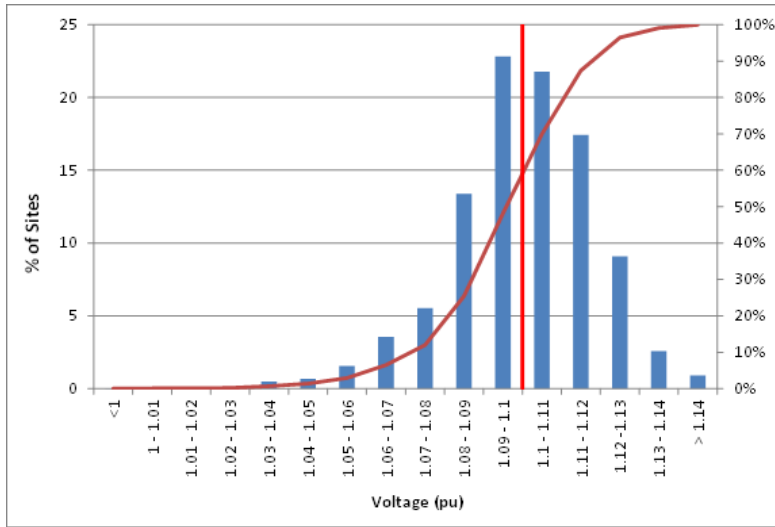


Fig. 2.1. Long-term national power quality survey result for steady state voltages of LV sites (2013-14)

While the annual survey indicates that it is not common for the steady-state voltage levels to drop below the lower LV limit, the situation is less clear at the remote ends of LV feeder runs as the surveyed LV sites are almost all at the sending ends of the LV feeders. This is of particular concern in Australia where LV feeder runs are considerably longer than may be the case in Europe (200 to 300m of overhead line).

2.3 Impact of Grid Connected PV Systems

The impact of grid connected PV systems has been the subject of many recent research projects and government sponsored studies. An example can be found in [4]. Beneficial impacts primarily come from the greenhouse benefits of displacing more carbon intensive generation resources [5, 6]. Grid benefits are more controversial, with loss minimisation [7-9], improved asset utilisation and deferred grid expenditure [10] as the main benefits put forward. Many adverse impacts on the grid have also been put forward, ranging from power system security, asset overloads to localised power quality impacts (such as steady-state voltage deviation, rapid voltage changes, phase unbalance and harmonics) [11-13]. As a result, many countries have developed grid codes for the connection of PV systems to minimise the adverse impacts [14, 15]. It could be said that both sides of the debate have their valid points, depending on the starting assumptions and the particular networks under consideration. One important point that is sometimes missed in the debate is the historic development of the MV and LV supply grids which assumes one-way flows of electricity from a limited number of supply points to the end-use customers. This

assumption is embedded in network planning philosophies, network design criteria, control settings as well as equipment deployed. This situation is particularly acute in the LV networks where the lack of investment means the networks lack observability and incomplete data capture and record keeping means rules of thumbs are used extensively. A complete re-think and re-design of the grid is required to accommodate the increasing level of embedded PV generation.

2.4 Voltage Quality Data from Smart Meters

A recent development which comes to the aid of utility engineers is the deployment of smart meters to residential customers. Smart meters have two important functions:

- Electricity tariff function to capture the demand and energy usage of customers. The electricity tariff function is enhanced by the ability to record usage over pre-defined time intervals (such as every 15 or 30 minutes) allowing customers to be charged based on time-of-use tariffs aligning to the real-time cost for the production and transmission of electricity [16].
- Network monitoring functionality to capture network parameters such as voltages, currents, power factor and supply status.

Equipped with two-way communication capability, smart meters allow customers to make informed decisions on when and how they consume electricity based on real-time price signals. They also allow utilities to monitor the quality of supply they are delivering to their customers at their points of connection, allowing proactive management of compliance.

Smart meter rollout programs to residential and small commercial/industrial customers have been reported in a number of countries. In Europe, smart meter rollout programs have been mandated in fourteen countries [17]. In the state of Victoria, Australia, government mandated a distributor-led rollout of smart meters to 2.8 million customers consuming less than 160MWh per annum. The program, known as Advanced Metering Infrastructure (AMI) program, started in late 2009 and was practically completed by middle of 2014.

A number of research articles have reported the use of smart meter data to aid in the management of supply network and the grid connected PV systems. One of the challenges brought about by smart meters is the sheer volume of data being collected and the time varying nature of the data. Big data analytics is increasingly applied to derive useful

information from the voluminous smart meter data. In [18] data clustering technique is used to derive a set of MV customer load profile. In [19] data clustering technique is used on half-hourly smart meter data to better understand how residential customers use their energy and their effect on the LV networks. In [20] a novel sublinear algorithm uses a small portion of the smart meter load data to characterize the electricity usage distributions of different set of users and allows utilities to offer differentiated user services based on usage patterns.

Ideas on the use of power quality information captured by AMI and smart meters to optimise the operational efficiencies of LV networks are reported in [21]. Implementation of innovative initiatives have been reported in a number of simulations and trials. [22] reports the use of voltages and currents for the calculation of line impedance between supply nodes. [23, 24] propose methodologies to determine the consumer phase connection using voltage information from customer smart meters. [25] uses smart meter instantaneous power measurements to derive phase unbalance on the LV distribution circuit and proposes the use of static transfer switches to dynamically switch houses from the initial connected phase to another, to reduce voltage unbalance. With smart meter recording voltage quality data such as voltage, current and power factor at the customer connection points, visibility of the LV networks has dramatically improved and this paves the way for better management of grid connected PV systems.

2.5 Network Modelling Techniques

A number of studies have attempted to quantify the upper limits of PV penetration before serious network issues arise. In 2007, the US Department of Energy's Renewable System Integration project conducted a literature search and utility engineer survey [11]. The literature survey reveals that a range of limits have been reported for PV penetration on a feeder or system level, between 5% and 40%, depending on the characteristics of the network and the parameters that are found to be limiting. Technical parameters include fast ramp rate requirement of central generators, reverse power swings on cloud transients, excessive load tap changer operations, overvoltage at light load conditions and undervoltage on sudden loss of PV generation. Economic parameters include increased distribution system losses, increased tie-line flows and increased frequency regulation costs. Unacceptable flicker emission caused by cloud transients have also been reported

[26]. Combination of theoretical modelling techniques and experimental results has been used to derive the PV impacts and to infer the penetration limits.

A number of key components are required for an accurate network model incorporating PV systems:

- *PV generation model* - Current research on PV models tends to focus on establishing the electrical representations of the various components that make up a PV installation e.g. solar panels, inverter, associated wirings, etc., and determine PV output based on how these components interact with external factors such as solar irradiance, ambient temperature and wind speed, while taking into account panel orientation, solar cell efficiency and electrical losses [27-29]. These complex models provide accurate output prediction but required extensive data collection effort.
- *Circuit impedance* – in Australia the MV network (typically 11kV or 22kV) is generally 3-phase 3-wire (R, W, B) construction with 3-phase distribution transformer (MV/LV) connected in delta on the MV side and star on the LV side. Single-phase distribution transformers are also used in the rural areas. The MV therefore needs to be modelled as a three-phase 3-conductor unbalanced network. The LV network emulating from the MV/LV distribution transformer is generally 3-phase 4-wire (R, W, B and N), un-transposed, with customers connected between phase and neutral. A Multiple Earthed Neutral (MEN) system is implemented where the neutral conductor is earthed at customer points of connection as well as at the LV star point of the supply distribution transformer. The LV needs to model both the neutral conductor and the earth connection as the loads are inherently unbalanced (due to 1-phase customer connections) so currents will flow in both the neutral conductor and earth, leading to voltages appearing on the neutral conductor [30-32]. Carson's equations can be used to derive the self and mutual impedances of overhead and underground conductors taking into account the return path of current through ground and phase asymmetry (un-transposed phase conductors) [33].
- *Customer phase connectivity* – it is important that phase connection of single-phase LV customers is accurately modelled, as the load/generation balance on each phase plays a significant role on the voltage profile of the LV distribution circuit [34].
- *Customer load profile* – as discussed above, detailed modelling of loads and generation on each phase is required to accurately determine the voltage profile on the LV distribution circuit.

To master the vast amount of network and customer data requires efficient network analysis techniques. [35] describes an advanced analysis tool for the assessment of clustered rooftop solar PV impacts. From the large volume of real-time network data collected from monitoring systems or smart meters, the tool is able to intelligently decide which part of the data would be effective for analysis of solar PV impacts, using data mining techniques to discover hidden patterns and Symbolic Aggregate Approximation (SAX) to reduce the dimensionality of the database. With both loads and PV generations both stochastic in nature, probabilistic load flows are proposed such as Monte Carlo based techniques [36] and analytical method that combines the cumulant method with the Cornish–Fisher expansion [37]. Finally, to reduce the effort of carrying out assessment on a large number of LV networks diverse in characteristics, [38] proposes the development of representative LV feeders from a large number of LV networks using clustering algorithms.

2.6 Methods to Increase the Hosting Capacity of LV Networks for PV Generators

For small grid connected residential PV systems, adverse impacts on the grid are primarily caused by steady-state voltage change and phase voltage unbalance. Many research papers have looked at overcoming localised voltage rise caused by embedded generators. The methods fall into three main categories:

- *Improve existing voltage regulation schemes* – Many electric utilities rely on voltage regulation schemes on the MV network to deliver the appropriate supply voltage to their LV customers. Figure 2.2 shows the typical voltage regulation schemes found in the electricity supply system in Australia.

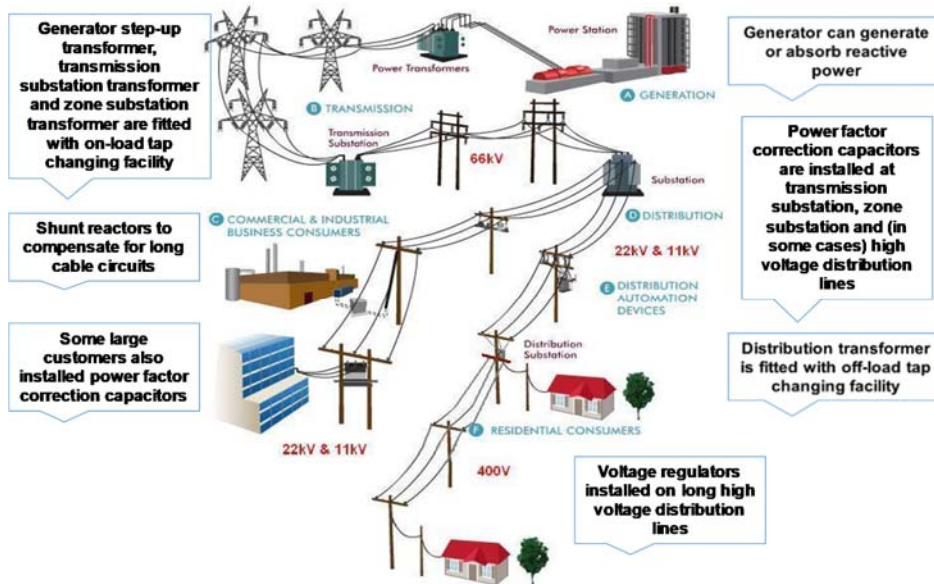


Fig. 2.2. Typical voltage regulation schemes in Australia

The existing voltage control schemes are measuring voltages (and currents) at some distance from the LV customers and are not reflective of what LV customers are experiencing unless the LV generation is significant. [39, 40] look at an innovative approach of applying SuperTAPP n+ relay scheme that is based on locally taken measurements at the substation level combined with a state estimation technique. The scheme applies a voltage generation bias to the traditional line drop compensation (LDC) scheme so the voltage at the MV substation is regulated to allow for voltage rise caused by the embedded generator. [41] presents a risk-based advanced distribution network management system (NMS) aimed at maximizing wind energy harvesting while simultaneously managing congestion and voltages. The NMS allows the adoption of multi-minute control cycles so the volume of actions from on-load tap changers and distributed generation plants can be reduced while effectively catering for the effects of wind power uncertainties. These innovative voltage control schemes will improve the voltage profile on the MV networks, with a flow-on beneficial effect to the voltage profile on the LV networks. They are, however, not sufficient to counteract the voltage rise effect where there are concentrations of PV systems occurring in pockets of the LV network.

- *Improve the siting of new embedded generators* – It is recognised that with appropriate siting of embedded generators, their adverse impacts on the supply network can be minimised and in some cases, may even be beneficial. [42] uses a hybrid approach

combining Generic Algorithms and Optimal Power Flow to determine locations where embedded generator connections will minimise capacity augmentation cost and network losses, based on regulatory incentives in U.K.. However, the methodology is only applicable to embedded generators connected at MV or above, and the assessments are made assuming the traditional worst case scenario of maximum embedded generator output at minimum load. A refined approach using Monte Carlo simulation to acquire solar radiations, ambient temperatures, load demands and substation voltages in Optimal Power Flow is presented in [43]. For small PV systems connected to the LV network, siting of the generators can be improved by switching from one connected phase to another using static transfer switches as proposed in [25].

- *Apply smart grid technologies* – This is the area where significant research activity is occurring. Research directions can be grouped into a number of categories:
 - *Component approach*: Minimise voltage rise and voltage unbalance caused by excessive PV generation using smart control schemes in the grid connected PV inverters (active power and/or reactive power control [44-48]), by installing single-phase switchable LV capacitors [49, 50], by absorbing excess generation (storage battery [51], other household loads such as water heating, electric vehicle charging [52]), by the use of distribution on-load tap changing transformer [53-55], by the use of electronic LV regulator [56], or a combination of the above [57, 58].
 - *System approach*: Minimise voltage rise by coordinated control at the system level. [41, 59] describes a distribution Network Management System (NMS) platform driven by an AC Optimal Power Flow (OPF) engine. The NMS aims to manage network voltages and congestion (thermal overloads) by coordinating the control of on-load tap changers, distributed generation reactive power and curtailment (as last resort). [60] describes an overarching control area solution, called the Grand Unified Scheme (GUS), which coordinates the actions of enhanced automatic voltage control scheme, electrical energy storage, real-time thermal rating and remote terminal units.

2.7 Key Issues Identified

Following the comprehensive literature review performed in this chapter, the following key issues were identified:

- While the adverse impacts of grid connected PV generators are well established, the extent of the problem is only known with certainty for locations where actual measurements have been carried out. Simulations using generalised network models may provide good indications for formulating high level strategy but are found lacking in practical applications.
- We start to see voltage quality data from smart meters being considered for use in voltage control schemes. There are, however, limited discussions on the use of smart meter data to improve the accuracy of LV network data and how the data can be used in setting up accurate network models for simulation studies.
- There is little attention given to the existing voltage quality situation in distribution networks. Many Australian distribution networks are delivering voltages that are biased towards the high side so little headroom is left for voltage rise caused by embedded PV generators. This high voltage bias needs to be fixed and mediated in conjunction with other approaches to increase the hosting capacity of PV generators.
- A lot of attention has been given to the use of smart grid technologies to mitigate the adverse impact of PV generation but not enough attention is given to improving existing network planning standards and operating procedures. The investment in smart grid technologies will generally drive up network costs, at a time when customers are already financially burdened by government initiatives of moving to a renewable energy future.
- Lastly, it is important that a prioritised approach is taken to tackle the impact of PV generation so the most cost effective solutions are selected for implementation to suit the particular characteristics of the distribution network under consideration.

2.8 Summary

This chapter has presented a comprehensive literature review of voltage quality issues caused by PV generation embedded in the distribution network, in particular, the low voltage network. The availability of smart meter data has enabled a new approach where the impact of embedded PV generation can be visualised and modelled in network studies. Various methods to increase the hosting capacity of LV networks for PV generators are reviewed. Finally, key issues pertaining to current research on PV hosting capacity arising from the literature review are highlighted.

Chapter 3 - Exploratory Analysis of Smart Meter Voltage Quality Data

This chapter is based on the following publication:

P.K.C. Wong, R.A. Barr and A. Kalam, “Using smart meter data to improve quality of voltage delivery in public electricity distribution networks”, Saudi Arabia Smart Grid Conference, 2012.

3.1 Overview

This chapter reports on the insight developed from exploratory analysis of smart meter voltage quality data. Section 3.2 describes the smart meter rollout program in the state of Victoria, Australia. Section 3.3 describes the form of the voltage quality data. Results of exploratory analysis of undervoltage and overvoltage events captured by smart meters are given in Section 3.4 and 3.5. Section 3.6 focuses on possible solutions to the voltage issues by analysis that links the smart meter sites to the upstream supply substations. Section 3.7 presents the case that smart meter data is a form of Big Data that will require efficient data analytic tools and platforms. Finally, Section 3.8 summarises the insight developed by performing exploratory analysis of smart meter voltage quality data, highlights the usefulness and limitations of existing smart meter data and makes recommendations on how the data can be improved to increase their usefulness.

3.2 Smart Meter Rollout Program

Since 2009, the five electricity distribution companies in the state of Victoria, Australia, have been rolling out smart meters in a program mandated by the state government. Known as the Advanced Metering Infrastructure (AMI) program, it was completed by middle of 2014. The mandated program covered all customers consuming under 160MWh per annum, essentially all residential customers, small commercial and small industrial enterprises. The smart meters are linked by two-way communication network to a central back office system (Figure 3.1). Apart from 30-minute energy consumption, the meters also monitor steady-state voltage quality.

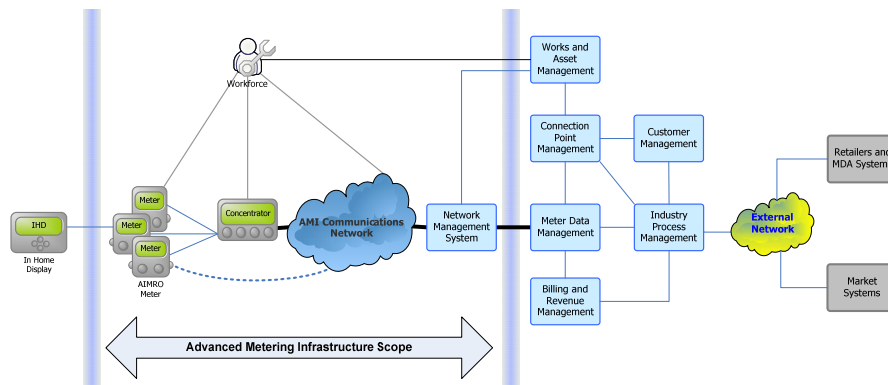


Fig. 3.1. Advanced Metering Infrastructure installed by Jemena Electricity Networks

3.3 Forms of Smart Meter Voltage Quality Data

The AMI communication technology utilised by JEN is a mesh radio network between the AMI meters and the meter access points. The minimum functional specification [61] of the smart meter program requires AMI meters to be capable of monitoring the supply voltage and to generate overvoltage and undervoltage alarms when the set thresholds are exceeded. The function is implemented locally in the smart meters and transmitted to the central Network Management System as events. In essence a "report by exception" methodology has been adopted for voltage quality events to better utilise the limited bandwidth of the mesh radio system.

The events consist of information such as meter identification, event date, start time (for start events), end time (for stop events), average voltage, maximum (minimum) voltage, supply address etc. The events can be downloaded from the Network Management System as Comma-Separated Values (CSV) files. An example of a CSV file containing voltage events is shown in Figure 3.2 below.

event_log_id	event_id	event_name	event_time	event_args	src_name	src_event_count	src_admin_state	src_location_util_id	src_service_pt_util_id
219519705	15569	Voltage variation overvoltage start no specific phase	28/02/2012 23:58:24.000+10:00	{{256.25 volts}{256.25 volts}}	111512	212	Active	6001093653	40109895
219520955	15569	Voltage variation overvoltage start no specific phase	28/02/2012 23:58:23.000+10:00	{{254.57 volts}{255.19 volts}}	86948	3	Active	6001197539	40095125
219519706	15577	Voltage variation overvoltage end no specific phase	28/02/2012 23:58:05.000+10:00	{{255.29 volts}{256.20 volts}}	111512	210	Active	6001093653	40109895
219517269	15569	Voltage variation overvoltage start no specific phase	28/02/2012 23:58:03.000+10:00	{{254.54 volts}{255.19 volts}}	22336	4	Active	6001149836	40031596
219517173	15569	Voltage variation overvoltage start no specific phase	28/02/2012 23:58:00.000+10:00	{{254.64 volts}{255.48 volts}}	50022	3	Active	6001264560	40043616

Fig. 3.2. Example of event list for overvoltage events

The undervoltage and overvoltage thresholds are set in accordance with the Victorian Electricity Distribution Code [62]:

- Undervoltage set point is 216V (230V - 6%);
- Overvoltage set point is 253V (230V + 10%).

To avoid creation of excessive events when the voltage hovers around the threshold values, a hysteresis setting of 2% (4.8V) is applied. A persistence time is also applied to avoid reporting on momentary excursions outside limits and is set at 180 seconds. A diagrammatic representation of the parameters associated with a voltage quality event is shown in Figure 3.3.

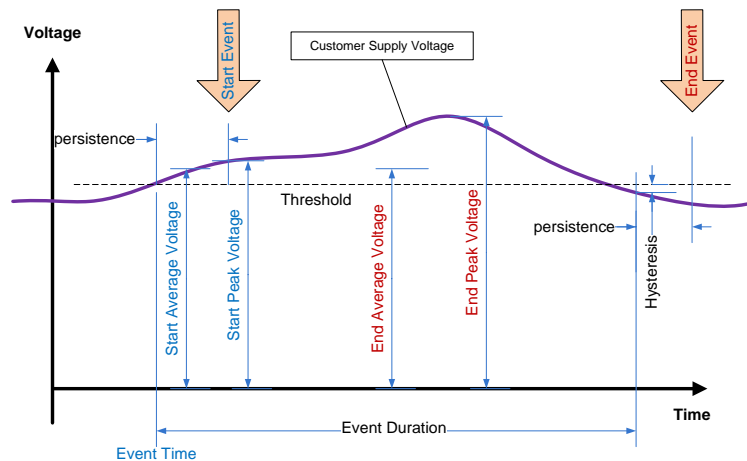


Fig. 3.3. Parameters associated with a voltage quality event

The analysis of smart meter voltage quality events presents a number of challenges. Firstly, the large volume of data requires efficient data analysis techniques. Secondly, the events are "snapshots" of voltage delivered to customers (when the supply thresholds are exceeded) and do not explicitly provide a time series data of voltage delivery. Thirdly, as the smart meters are not power quality meters designed to AS/NZS61000.4.30 [63], the events captured can only be treated as indicative and not be used for strict compliance purpose.

3.4 Exploratory Analysis of Smart Meter Voltage Quality Data

3.4.1 Data Set

Overvoltage and undervoltage events reported by 100,000 smart meters, over a 6-day period in summer 2012, were downloaded from the Network Management System as

CSV files. A total of 15,180 undervoltage events and 38,238 overvoltage events were captured over the 6-day period. Other database extracts include network loading data from Supervisory Control and Data Acquisition (SCADA) system, network topology snapshots from Geographical Information System (GIS), residential PV installation data from GIS, meter reference data from SAP, and ambient temperature information from the Bureau of Meteorology. Microsoft Excel is used as the software tool to ‘slice and dice’ the data in a number of ways to answer questions such as

- How many overvoltage and undervoltage events occur in the 6-day period?
- Is there any relationship between the number of voltage events and
 - ambient temperature?
 - electricity usage?
- How many customer sites are affected?
- Are the sites consistently producing overvoltage and undervoltage events over the 6-day period?
- Are there sites that produce both overvoltage and undervoltage events?
- At what times of day do the voltage events occur?
- How long do these voltage events last?
- What are the trigger voltages for these events?
- What are the extreme voltages experienced during these events?
- From an electrical connectivity perspective, are these customers supplied from the same distribution circuits, same distribution substations or same zone (primary) substations?

Results of the exploratory data analysis are detailed in the next section.

3.4.2 Analysis of Undervoltage Events

Before analysis is carried out, the undervoltage event data is cleansed to remove outliers caused by network faults such as supply interruptions and brown-outs (where voltage goes down to abnormally low level due to the loss of one phase of the high voltage supply), and short duration undervoltages that have marginal effect on equipment thermal performance. After data cleansing, a total of 15,180 undervoltage events were captured

over the 6-day period. These events were generated from 6,131 smart meters, or 6.1% of the total smart meter population (Table 3.1).

Table 3.1 Undervoltage events

Date	23/2/12 (Thurs.)	24/2/12 (Fri.)	25/2/12 (Sat.)	26/2/12 (Sun.)	27/2/12 (Mon.)	28/2/12 (Tue.)
Maximum ambient temperature (°C)	25.8	37.1	37.1	33.2	25.1	21.1
Number of undervoltage events	80	2,664	6,590	5,545	267	34
Number of sites (%) detecting undervoltage	68 (0.07%)	2,219 (2.22%)	5,199 (5.2%)	4,446 (4.45%)	121 (0.12%)	24 (0.02%)
Total number of sites generating undervoltage events over the 6-day period					6,131 (6.13%)	

It is clear from Table 3.1 that not all 6,131 sites experience undervoltage throughout the 6-day period. In fact, very few sites experience undervoltage for more than 3 days, as shown in Table 3.2.

Table 3.2 Analysis of the 6,131 undervoltage sites

Number of sites experiencing undervoltage in the 6-day period					
One day of the 6-day period	Two days of the 6-day period	Three days of the 6-day period	Four days of the 6-day period	Five days of the 6-day period	Six days of the 6-day period
2,195	2,033	1,828	55	7	13

Another way to look at the severity of the undervoltage problem is to determine the number of "active" undervoltage sites on a time series basis, as shown in Figure 3.4:

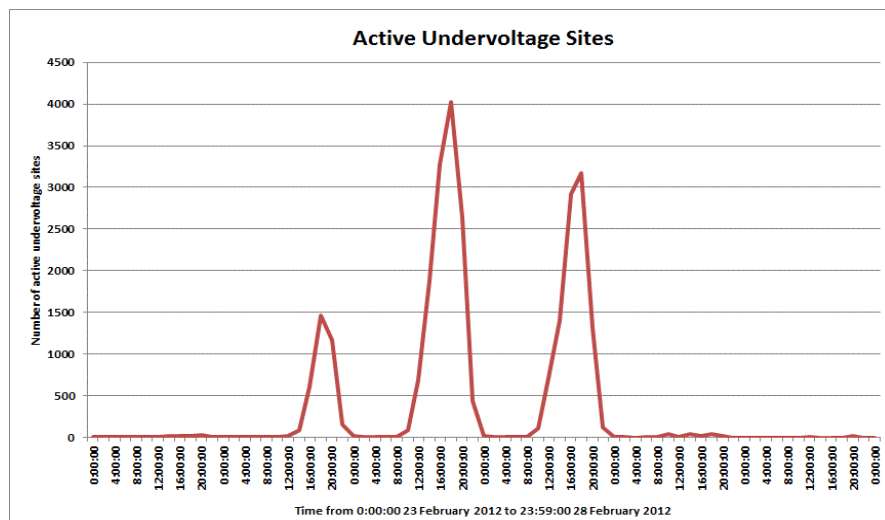


Fig. 3.4. Number of active undervoltage sites during the 6-day period

3.4.2.1 Correlation of undervoltage events with ambient temperature

It is observed that the number of undervoltage events exhibits strong correlation with ambient temperature (Figure 3.5). Undervoltage events are virtually non-existent when daily maximum ambient temperature is below mid 20s, but the number of events rises rapidly when the maximum ambient temperature reaches the mid 30s. This indicates that undervoltage events are triggered by the use of space cooling equipment during high ambient temperature, primarily refrigerated air conditioning. The increase in loading on the distribution equipment and circuits causes increases in voltage drop, with resultant undervoltage experienced by customers especially near the end of low voltage distribution circuits. The data indicates that a significant number of customers (6%) have experienced some instances of undervoltage during the three consecutive hot days, peaking at 5.2% of customers on 25th February.

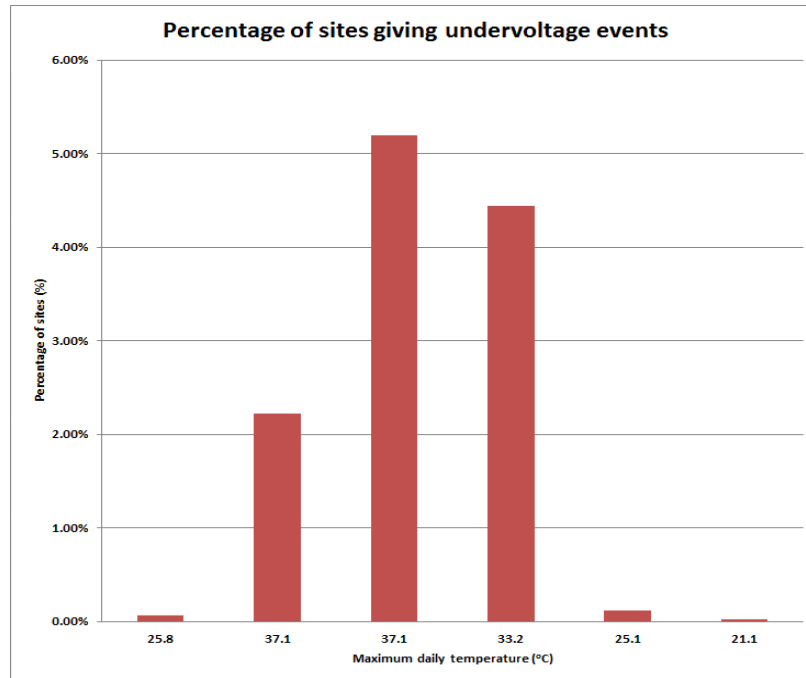


Fig. 3.5. Number of undervoltage events versus maximum daily ambient temperature

3.4.2.2 Start Times of Undervoltage Events

The majority of undervoltage events commenced between noon to 8pm at night, generally coinciding with heavy electricity usage (Figure 3.6).

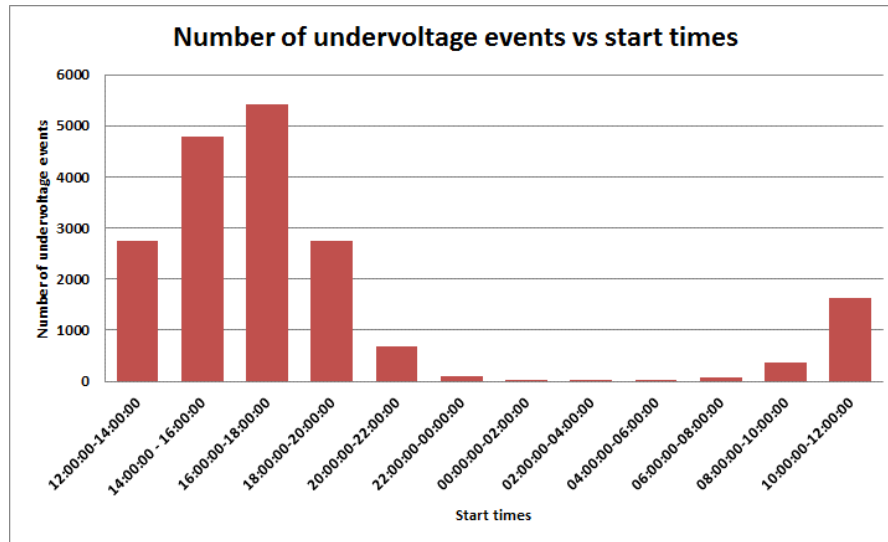


Fig. 3.6. Number of undervoltage events versus start times

3.4.2.3 Duration of Undervoltage Events

One key indicator of the severity of an undervoltage event is its duration. Figure 3.7 shows the number of undervoltage events and their duration. It is observed that the longest undervoltage event lasted nearly 15 hours. Most of the undervoltage events, however, lasted between half an hour to 8 hours.

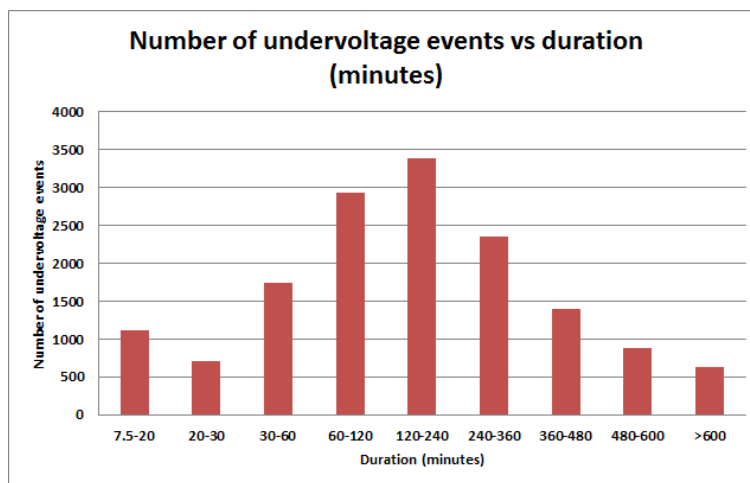


Fig. 3.7. Number of undervoltage events versus duration (minutes)

3.4.2.4 Residual Voltage

The event records the lowest voltage during the duration of the undervoltage event. It does not mean the voltage stays at this low level during the whole event. The lowest voltage recorded varied from 161V to 216V. It can be seen from Figure 3.8 below that majority of the undervoltage events are just marginally below the regulatory threshold (230V-6% or 216V). From a detailed investigative work perspective, the events with much lower residual voltage should be given priority.

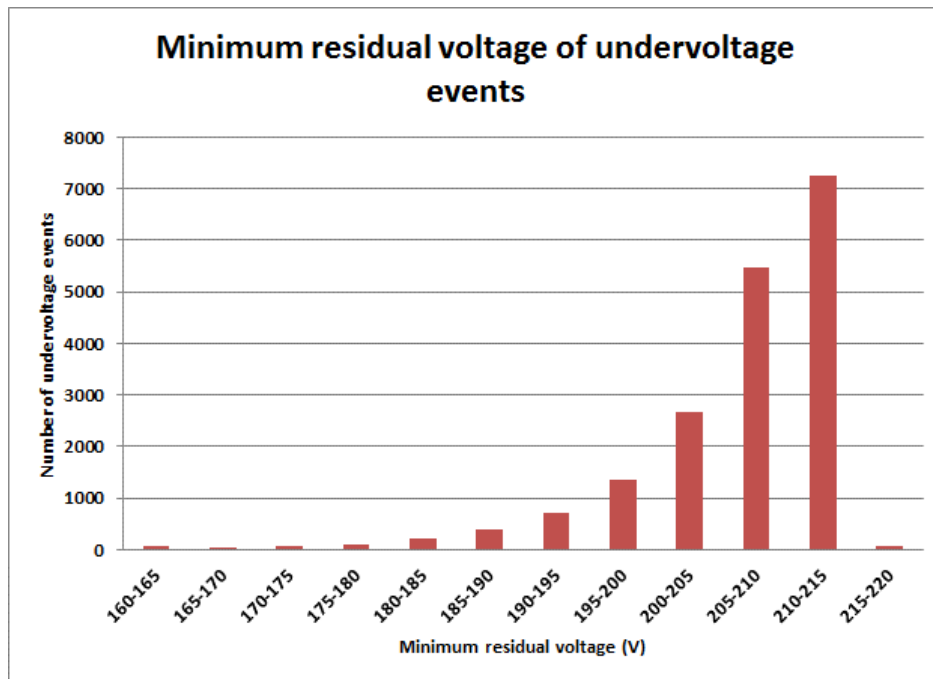


Fig. 3.8. Minimum voltage of undervoltage events

3.4.3 Analysis of Overvoltage Events

It is observed that there are a lot more overvoltage events generated in a day compared with undervoltage events. To explore the relationship between undervoltage and overvoltage events, the same 6-day period is analysed. A total of 38,238 overvoltage events were generated over the 6-day period. These events were generated from 12,251 smart meters, or 12.3% of the total smart meter population. While a site could experience multiple overvoltage events in the same 24-hour period, most sites experienced only one overvoltage event in each 24-hour period (Table 3.3).

Table 3.3 Overvoltage events

Date	23/2/12 (Thurs.)	24/2/12 (Fri.)	25/2/12 (Sat.)	26/2/12 (Sun.)	27/2/12 (Mon.)	28/2/12 (Tue.)
Number of overvoltage events	8,407	6,129	4,942	6,249	6,733	5,778
Number (%) of sites giving overvoltage events	6,294 (6.29%)	4,724 (4.72%)	3,957 (3.96%)	4,620 (4.62%)	4,733 (4.73%)	3,378 (3.38%)
Total number of sites giving overvoltage events over the 6-day period						12,251 (12.3%)

It is clear from Table 3.3 that the 12,251 sites only give rise to overvoltage events occasionally during the 6-day period. In fact, very few sites give rise to overvoltage event throughout the period, as show in Table 3.4.

Table 3.4 Analysis of the 6,131 overvoltage sites

Number of sites experiencing overvoltage in the 6-day period					
One day of the 6-day period	Two days of the 6-day period	Three days of the 6-day period	Four days of the 6-day period	Five days of the 6-day period	Six days of the 6-day period
5,192	2,803	2,465	1,242	549	300

Another way to look at the severity of the overvoltage problem is to determine the number of "active" overvoltage sites on a time series basis, as shown in Figure 3.9.

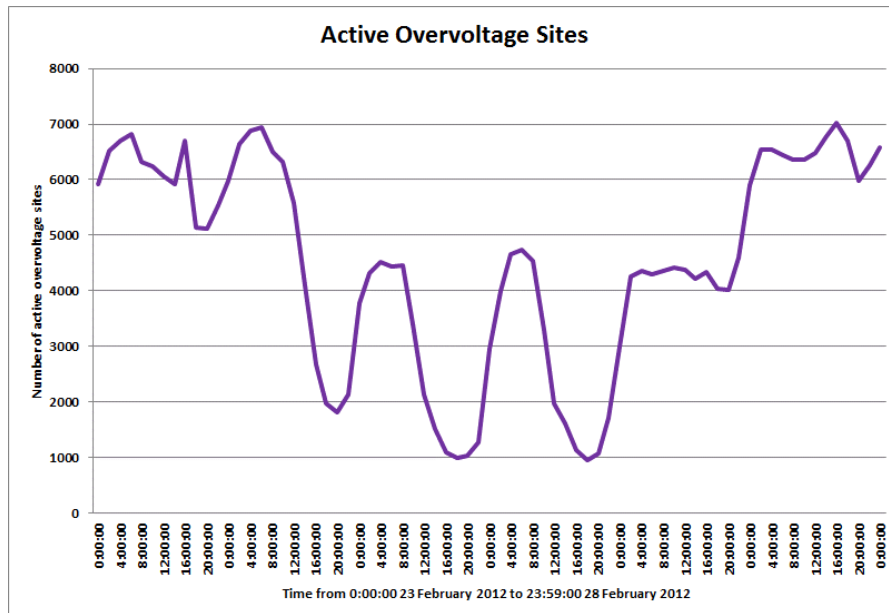


Fig. 3.9. Number of active overvoltage sites during the 6-day period

Figure 3.9 indicates that there are significant overvoltage problems within the electricity network, with the number of active overvoltage sites in the range of 6,000 or more during a normal temperature day. Even during high ambient temperature days when electricity usage has increased, there are still a minimum of 1,000 sites experiencing overvoltage at any time of the day.

3.4.3.1 Correlation of overvoltage events with ambient temperature

Unlike undervoltage events, it is observed that the number of overvoltage events do not show strong correlation with ambient temperature (Figure 3.10).

This is expected as overvoltage generally occurs at light load periods when the voltage drop across the distribution circuit is at its minimum. As Melbourne summers tend to have high temperatures during the day and cooler temperatures at night, use of air conditioners during the light load period (i.e. at night) is infrequent unless there are consecutive hot days. One would therefore expect that overvoltage would still be prevalent at light load period even during hot days.

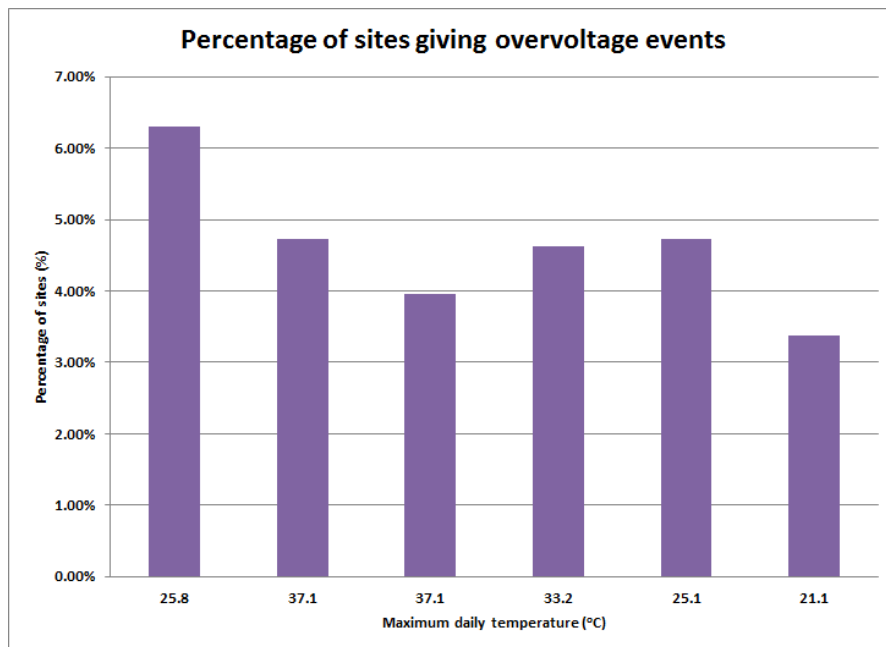


Fig. 3.10. Percentage of sites giving overvoltage events versus maximum daily ambient temperature

3.4.3.2 Start times of overvoltage events

By far the most common start times for overvoltage events are 10pm to 2am (Figure 3.11).

This coincides with lower electricity usage.

However, some overvoltage events also occur at times which are quite unexpected. There is a possibility that these overvoltages could have been generated by solar panels installed at these customer premises. This is further explored in section 3.4.4.

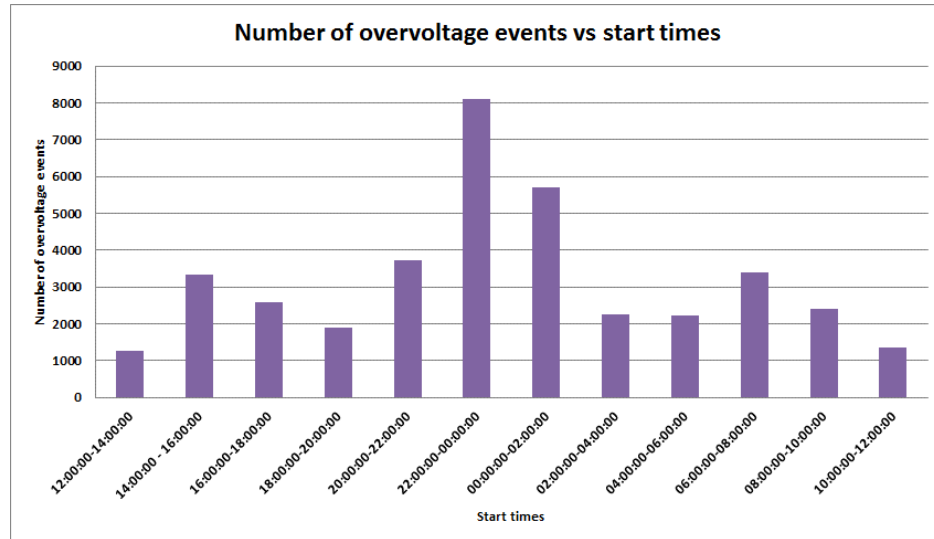


Fig. 3.11. Number of overvoltage events versus start times

3.4.3.3 Duration of Overvoltage Events

One key indicator of the severity of an overvoltage event is its duration. Figure 3.12 shows the number of overvoltage events and their duration. The longest overvoltage event lasted nearly 45 hours! However, most of the overvoltage events lasted between 2 to 15 hours.

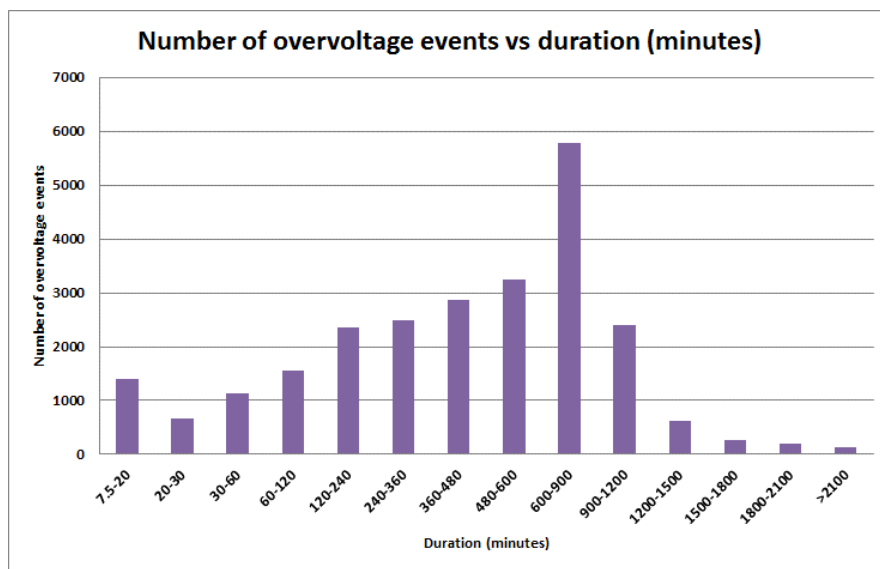


Fig. 3.12. Number of overvoltage events versus duration (minutes)

3.4.3.4 Highest Overvoltage

The event records the highest voltage during the duration of the overvoltage event. It does not mean the voltage stays at this high level during the whole event. It can be seen from Figure 3.13 that majority of the overvoltage events are just above the regulatory threshold (230V+10% or 253V).

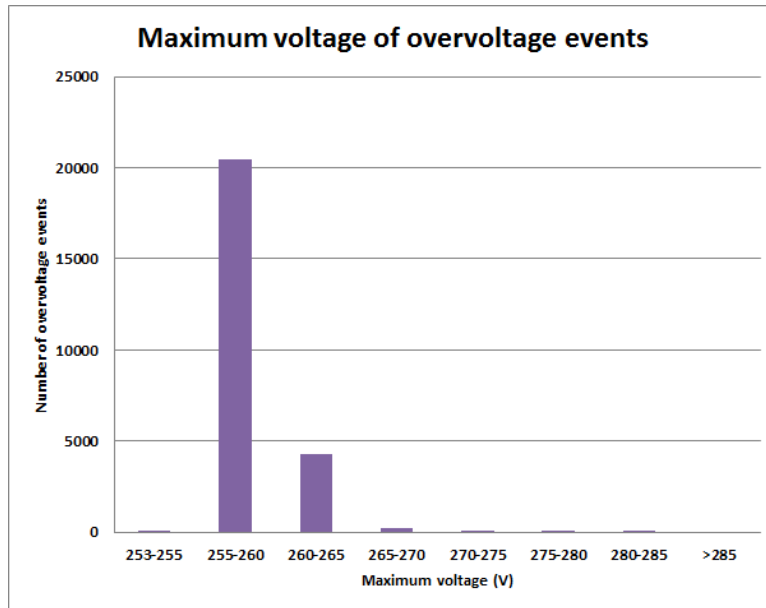


Fig. 3.13. Maximum voltage of overvoltage events

So while Figure 3.9 indicates that there are a significant number of overvoltage events occurring on the network at any instant in time, Figure 3.13 indicates that most of these are moderate overvoltages.

3.4.4 Relationship Between Overvoltage and Embedded Photovoltaic Generation

In recent years there is an increasing trend of residential PV systems installed on customers' rooftop. The trend is encouraged by the various feed-in tariffs established by the state government and the significant reduction in PV system cost. The number of residential PV installations in JEN was about 12,000 (4% of the customer base) at the time when these voltage events were analysed. It has since grown to about 8% by June 2016 (Figure 3.14).

It is well known that these PV installations can cause local voltage rise when the excess generation is fed back into the supply network. Figure 3.11 shows the start times of overvoltage events. By far the most common start times of overvoltage events are

between 10pm to 2am which coincide with periods of light load. There are, however, also a considerable number of overvoltage events that start between 8am to 4pm which is unusual as these tend to be higher electricity usage periods. Table 3.5 shows the proportion of overvoltage sites that have known PV installations compared with the total number of overvoltage sites. It can be seen that higher proportion of PV sites are generating overvoltage events between the period of 8am to 2pm. This suggests that PV installations do contribute to overvoltage problem but their effect is not significant at this point in time due to the modest penetration.

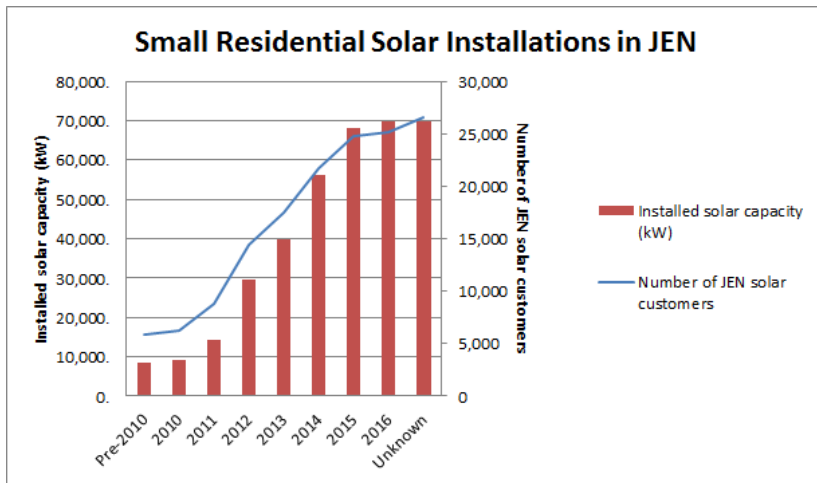


Fig. 3.14. Growth of residential PV systems in JEN

Table 3.5 Proportion of overvoltage events generated by sites with PV installation

Start Time	Total number of OV events generated by PV sites	Total number of OV events	% of PV sites OV events to total number of OV events
00:00:00-02:00:00	228	5718	4.0
02:00:00-04:00:00	63	2246	2.8
04:00:00-06:00:00	57	2223	2.6
06:00:00-08:00:00	116	3399	3.4
08:00:00-10:00:00	122	2415	5.1
10:00:00-12:00:00	92	1356	6.8
12:00:00-14:00:00	59	1270	4.6
14:00:00 - 16:00:00	138	3343	4.1
16:00:00-18:00:00	70	2570	2.7
18:00:00-20:00:00	48	1887	2.5
20:00:00-22:00:00	113	3718	3.0
22:00:00-00:00:00	283	8092	3.5

3.4.5 Relationship Between Voltage Non-compliance and Customer Complaints

Before the era of smart meters, utilities could not continually monitor the quality of the voltage they deliver to customers due to the high monitoring costs. Most utilities relied on customer complaints as a trigger to undertake more detailed measurements. For JEN there were about 120 cases of confirmed voltage complaints in year 2011 attributed to a number of causes as shown in Figure 3.15. This number of voltage complaints is just not comparable with what has been revealed by smart meters (15,180 undervoltage and 38,238 overvoltage events in a 6-day period). This indicates that the effect of undervoltages and overvoltages is generally not apparent to most customers as their appliances often continue to work under these conditions. The life and performance of these appliances, however, are affected and this represents the ‘hidden’ cost of voltage quality non-compliance.

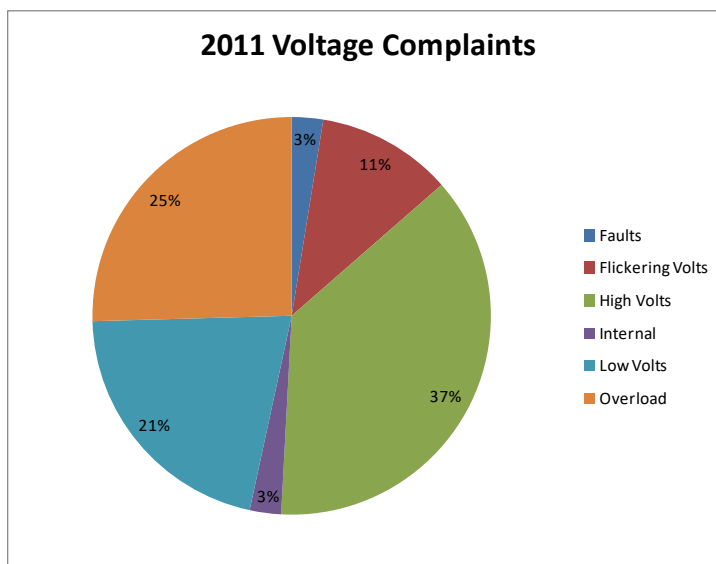


Fig. 3.15. Analysis of customer voltage complaints

3.5 Linking Voltage Quality Events to Supply Substations

For the purpose of voltage regulation, distribution substations are fitted with off-load transformer tap changing facility. Zone substations are generally fitted with transformer on-load tap changer controlled by voltage regulating relays. In JEN some zone substations are regulated at a flat supply voltage while some others have Line Drop Compensation (LDC) applied.

The most common causes of undervoltage and overvoltage problems are:

- Inappropriate tap setting of the distribution transformer;
- Inappropriate voltage regulation setting of the zone substation;
- For undervoltage - distribution substation and/or circuit overload; and
- 3-phase load unbalance, especially in the low voltage circuits.

It is therefore imperative to link the overvoltage and undervoltage sites to the upstream distribution and zone substations, and look for clues that may indicate where the problem lies (Figure 3.16). The relationship between sites and upstream supply substations is provided in JEN's GIS.

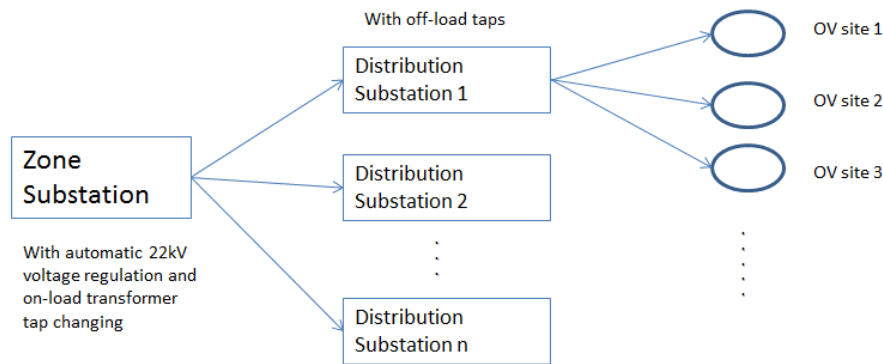


Fig. 3.16. Linking OV sites to upstream supply substations

3.5.1 Undervoltage Sites

GIS data allows the linking of undervoltage sites to upstream distribution substations. Percentage of undervoltage sites to the total number of sites for each distribution substation is established and the distribution substations ranked in decreasing order of percentage.

There were 760 distribution substations upstream of undervoltage sites in the 6-day period. The percentage of undervoltage sites supplied by each distribution substation varies from 100% (i.e. all customers supplied from that distribution substation have experienced undervoltage during the 6-day period) to nearly 0% (very few customers supplied from that distribution substation have experienced undervoltage during the 6-day period). The 20 distribution substations with the highest percentage of undervoltage sites are listed in Table 3.6.

Table 3.6 20 distribution substations with the highest percentage of undervoltage sites in the 6-day period

Distribution substation	Undervoltage sites	Total number of sites	% of sites with UV events
ST GEORGES 102-MURRAY	62	100	62.0%
STUDLEY-BANKSIA	26	65	40.0%
VALLEY-AUGUSTINE	59	170	34.7%
SEXTON-HALSEY	97	288	33.7%
GOURLAY-SUGAR GUM	21	64	32.8%
LAURIE-PURINUAN	51	165	30.9%
YALLAMBIE-JANICE	36	120	30.0%
BLACK-MC MAHON	31	111	27.9%
PASCOE VALE-SHANKLAND	43	157	27.4%
HART-BOWES	77	282	27.3%
DUFFY-BARRY	64	240	26.7%
FULLARTON-WALTERS	20	78	25.6%
CUDGEWA-BORVA	33	129	25.6%
WARANGA-BLAIR	46	180	25.6%
VICTORY-FOSTERS	51	203	25.1%
MOUSHALL-NOLAN	50	205	24.4%
GRAHAM 138-SYLVA	48	201	23.9%
BLIBURG-SUNSET	33	141	23.4%
MULBERRY-GONA	45	209	21.5%
GREEN-SPARKFORD	41	193	21.2%

Before taking the decision to change the taps on these distribution transformers, it is important to check if these distribution substations are affected by inappropriate voltage regulation settings at the upstream zone substation. One method to establish this relationship for each zone substation is to determine the percentage of downstream distribution substations that have experienced undervoltage events. The result for the ten worst zone substation is tabulated in Table 3.7.

Table 3.7 Ten worst zone substations which supply distribution substations with undervoltage events

Zone Sub	Number of distribution substations with undervoltage events	Total number of distribution substations	% of distribution substations with undervoltage events
TT	72	137	52.6%
HB	45	105	42.9%
PV	59	159	37.1%
ES	42	136	30.9%
CS	63	216	29.2%
NH	73	255	28.6%
NT	41	145	28.3%
BY	34	129	26.4%
NS	26	108	24.1%
CN	70	299	23.4%

3.5.2 Overvoltage Sites

GIS data allows the linking of overvoltage sites to upstream distribution substations. Percentage of overvoltage sites to the total number of sites for each distribution substation is established and the distribution substations ranked in decreasing order of percentage. There were 922 distribution substations upstream of overvoltage sites in the 6-day period. The percentage of overvoltage sites supplied by each distribution substation varies from 100% (i.e. all customers supplied from that distribution substation have experienced overvoltage during the 6-day period) to nearly 0% (very few customers supplied from that distribution substation have experienced overvoltage during the 6-day period). The 20 distribution substations with the highest percentage of overvoltage sites are listed in Table 3.8.

Table 3.8 20 distribution substations with the highest percentage of overvoltage sites in the 6-day period

Distribution substation	Overvoltage sites	Total Number of Sites	% of sites with OV events
BARRINGTON LA-P6A	1	1	100.0%
WOOD-NORTHLAND	46	53	86.8%
LOVAT-LONGFORD	41	50	82.0%
BARRY-PASCOE VALE	22	27	81.5%
GRAHAM-ULRICH	123	152	80.9%
AUGUSTA-HUME	23	29	79.3%
STAWELL-CLUNES	54	73	74.0%
TATE-LIVINGSTONE	93	127	73.2%
PAVLEKA-ALLENBY	101	138	73.2%
BLAKE-SESTON	77	113	68.1%
DARLING-WHITE	127	189	67.2%
IRONBARK- RUTHERFORD	88	131	67.2%
WATTLEVALLEY- GOLDEN	80	121	66.1%
LONDON-CUTHBERT	103	156	66.0%
BUSHFIELD-LONGFORD	17	26	65.4%
HUME-PARAMOUNT CO	20	31	64.5%
MOROBE-ALAMEIN	28	44	63.6%
THORPDALE-KYABRAM	40	63	63.5%
CHURCHILL- COONAMAR	40	64	62.5%
JOHNSON-BENAUD	82	135	60.7%

Before taking the decision to change the taps on these distribution transformers, it is important to check if these distribution substations are affected by inappropriate voltage regulation settings at the upstream zone substation. One method to establish this relationship for each zone substation is to determine the percentage of downstream distribution substations that have experienced overvoltage events. The result for the ten worst zone substations is tabulated in Table 3.9.

Table 3.9 Ten worst zone substations which supply distribution substations with overvoltage events

Zone Sub	Number of distribution substations with overvoltage events	Total number of distribution substations	% of distribution substations with overvoltage events
FF	38	70	54.3%
PV	66	159	41.5%
NS	37	108	34.3%
ES	46	136	33.8%
YTS	34	124	27.4%
P	13	48	27.1%
CN	80	299	26.8%
NH	67	255	26.3%
TT	28	137	20.4%
BD	99	489	20.2%

3.5.3 Sites Experiencing both Overvoltage and Undervoltage

During the 6-day period, 12,251 sites and 6,131 sites experienced overvoltage and undervoltage events respectively.

There were 88 sites that have experienced both undervoltages and overvoltages. These sites present a unique problem in that the voltage issues cannot be fixed simply by raising or lowering the voltage regulation. There are only 4 sites with PV installation in this group so it appears PV does not contribute to the overvoltage issue.

These 88 sites are linked to 31 distribution substations. The seven worst distribution substations are shown in Table 3.10.

Table 3.10 Seven worst distribution substations whose customers have experienced both overvoltage and undervoltage events in the 6-day period

Distribution substation	Number of sites with both overvoltage and undervoltage
MCCOLL-MALPAS	11
SEPARATION-FULHAM	10
ARTHUR-SEPARATION	9
BLOOMFIELD-ROSAMOND	8
DARLING-WHITE	7
DELAWARE-MENDIP	5
MITCHELL-GILLIES	4

Of these 7 distribution substations, Arthur-Separation and Mitchell-Gillies are already earmarked for capacity upgrade due to confirmed substation overload.

3.6 A Big Data Problem

Gartner, a leading information technology research and advisory company, defines "big data" as having characteristics that can be denoted by three "Vs": *Volume*, *Velocity* and *Variety*. Voltage quality data is a form of "big data" as it possesses the following characteristics:

- *Volume* – Voltage quality events generated from smart meters are voluminous. In the 6-day period, there are 15,180 undervoltage and 38,238 overvoltage events.
- *Velocity* - Velocity refers to the speed of data generation and disappearance. A total of 6,131 customer sites have experienced undervoltage in the 6-day period. However, not all 6,131 sites experienced undervoltage throughout the six days. Similarly, 12,251 customer sites experienced overvoltage in the 6-day period but few sites gave rise to overvoltage events throughout the period. In other words, under and overvoltage conditions are transient in nature and do not form an easily recognisable pattern.
- *Variety* - Variety refers to the number of disparate databases containing data that must be processed for enhanced insight and decision making. To allow corrective action to be taken, the smart meter voltage quality data must be analysed in conjunction with network connectivity data (stored in spatial database such as GIS), network asset data (in GIS and/or SAP) and real-time voltage data (in SCADA).

The exploratory data analysis conducted in 3.4 and 3.5 is valuable as it allows insight to be gained on the specification for the ultimate data analytic tools, the ancillary data requirement as well as the types of queries to be run on the data sets. Efficient data analytic tools including in-memory processing databases are required to handle the big data generated by smart meters.

3.7 Summary

The exploratory data analysis reveals the following useful insights:

- Strong correlation of undervoltage events with ambient temperature – undervoltage events are virtually non-existent at ambient temperature below mid 20s, and rising

rapidly when ambient temperature reaches the mid 30s. Overvoltage events, on the other hand, do not show strong correlation with ambient temperature.

- The majority of overvoltage events are caused by the existing voltage regulation being set marginally too high. This existing practice is likely to limit the amount of embedded generation (such as PV) that can be connected to the supply network. Care needs to be exercised, however, to ensure that dropping the voltage regulation setting will not lead to worsening of the undervoltage situation on hot days.
- The appropriateness of conventional Line Drop Compensation voltage regulation schemes. These schemes may need to be reviewed.
- Definitive patterns of start times can be observed for undervoltage events. Coupled with the insight gained from ambient temperature relationship, adaptive voltage control schemes based on ambient temperature and time of day could be explored to improve on the undervoltage situation.
- Residential photovoltaic installations, modest in its penetration at the time of analysis (about 4%), is already observed to have a discernible impact on overvoltage occurrence. The effect will become more significant as the penetration of PV increases further.
- Priority for voltage non-compliance investigation and rectification can be set based on the level of voltage deviation and time duration as revealed by the smart meter voltage events.
- Clusters of voltage events around particular distribution substations may indicate inappropriate off-load transformer tap setting.
- Clusters of distribution substations around particular zone substations may indicate inappropriate on-load tap change voltage regulating relay settings.
- Customers who experience both overvoltage and undervoltage events may indicate an upstream asset overload condition.

The exploratory data analysis also exposes the limitation of the existing voltage quality data from JEN:

- Due to the use of hysteresis, an event does not end until the voltage has restored back to well within the allowable range. The event duration, obtained by the difference between the start and stop times, is likely to be longer than duration of the voltage non-compliance.

- The lack of accurate phase information of customer connection limits the usefulness of the data analysis.
- Voltage profile along the LV distribution circuit cannot be established due to the lack of time series data of voltage measurements.
- Voltage measurements alone are not sufficient to reveal what is occurring in the supply network that leads to the voltage non-compliance, e.g. phase current unbalance could be the cause of overvoltages or undervoltages. Time synchronised current and power factor measurements, at adequate time resolution, will be required to complete the picture.

Moreover, due to the limitations posed by Microsoft Excel in the size of CSV files that it can handle and the computational speed, only 6-day of voltage events can be analysed at one time. Excel is clearly not suitable for big data analytics.

JEN is currently implementing an enhancement to its AMI to enable the collection of time synchronised voltage, current and power factor measurements at 5-minute intervals. It is also implementing an in-memory computing platform for data analytics applications based on SAP® HANA®. A number of applications are planned with the 5-minute AMI data, including customer connection phase identification and supply impedance measurements.

Chapter 4 - A PV Generator Model Suitable for Practical Utility Applications

This chapter is based on the following publication:

Peter K.C. Wong, Robert A. Barr & Akhtar Kalam (2015), “Generation modelling of residential rooftop photovoltaic systems and its applications in practical electricity distribution networks”, Australian Journal of Electrical and Electronics Engineering, 12:4, 332-341.

4.1 Overview

Utilities have an obligation to supply voltage to customers that meet quality standards as defined in various codes, regulations and standards. This obligation can only be met by collaboration between utilities and customers as customer equipment connected to the supply network can cause disruption to the power supply. This is particularly important in this modern age where most customer electrical equipment are based on digital electronics susceptible to electromagnetic interferences. Renewable energy resources are increasingly connected to the grid due to their greenhouse gas reduction benefits but have potential impacts on supply quality. In order to make sure that integrating these resources into the power system does not jeopardize its reliability, security and quality, comprehensive studies and simulations are needed based on appropriate and credible component models. Developing precise, realistic and yet simple to implement models for these new electric power sources is of vital importance to facilitate their integration into the system.

In Chapter 3 we discussed the opportunity brought about by smart meters installed at LV customer premises whereby power quality monitoring is now possible through the network sensing functions implemented in these smart meters. In addition, advanced data analytics applied to smart meter data can reveal network characteristics such as supply impedance and customer phase connection. The additional information allows utilities to study the impact of renewable energy resources by establishing computer models that

accurately simulate the electricity supply network. To understand the power quality impact of grid connected residential roof-top PV systems, utilities require PV generator models that are easy to apply.

Section 4.2 provides a literature survey of PV generator models and identifies the limitations of these models for supply utility applications. Section 4.3 provides the theoretical background to a utility PV generator model. Practical applications of the utility PV generator model are presented in Section 4.4 and its accuracy demonstrated using smart meter data. Section 4.5 summarises the chapter and discusses potential future applications of the model.

4.2 Survey of Existing PV Generator Models

4.2.1 Solar Cell Modelling [28, 29, 64-69]

For silicon based PV systems, the majority of models developed are based on the fundamental construct of a p-n junction solar cell. A typical equivalent circuit of a PV cell is shown in Figure 4.1.

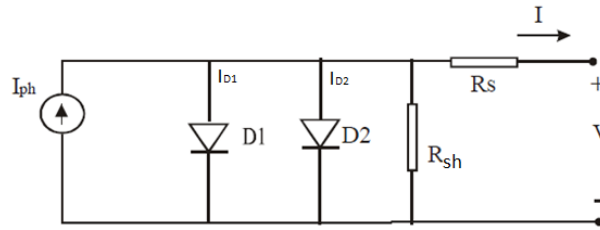


Fig. 4.1. Equivalent circuit of a PV cell (5-parameter model)

In this equivalent circuit, the constant current source I_{ph} represents the photo-generated current, R_{sh} the shunt resistance to account for the leakage current due to the surface stain and crystal defects, and R_s the series resistance representing the surface diffusion resistance of diffusion top area, the body resistance of the cell and the metal conductor resistance. The output characteristics of the PV cell is represented by Equation 4.1.

$$I = I_{ph} - I_{D1} - I_{D2} - \frac{V + IR_s}{R_{sh}} \quad (4.1)$$

The photo-generated current depends on both irradiance and temperature.

The diode currents I_{D1} and I_{D2} are given by the Shockley equation:

$$I_{D1} = I_{01} \left\{ \text{Exp} \left[\frac{q(V + IR_s)}{k_B T_c} \right] - 1 \right\} \quad (4.2)$$

$$I_{D2} = I_{02} \left\{ \text{Exp} \left[\frac{q(V + IR_s)}{2k_B T_c} \right] - 1 \right\} \quad (4.3)$$

where q is charge of electron, $1.602 \times 10^{-19} \text{C}$; k_B is Boltzmann constant, $1.38 \times 10^{-23} \text{J/K}$; I_{01} is the dark saturation current; I_{02} is dark saturation current caused by recombination; T_c is the junction/cell temperature.

The 2-diode equivalent circuit shown in Figure 4.1 can be simplified into the 4-parameter model shown in Figure 4.2, by neglecting the recombination current as it is relevant only at low voltage bias, and incorporating the effect of the shunt resistance in a nonideality factor γ .

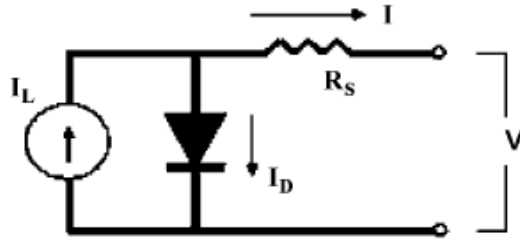


Fig. 4.2. Simplified 4-parameter model of a PV cell

$$I = I_{ph} - I_D \quad (4.4)$$

$$I_D = I_0 \left\{ \text{Exp} \left[\frac{q(V + IR_s)}{\gamma k_B T_c} \right] - 1 \right\} \quad (4.5)$$

γ is an empirical nonideality factor that takes into account the effect of the shunt resistance and normally has a value between 1 and 2; I_0 is the dark saturation current and is a function of temperature.

Combining Equations 4.4 and 4.5

$$I = I_{ph} - I_0 \left\{ \text{Exp} \left[\frac{q(V + IR_s)}{\gamma k_B T_c} \right] - 1 \right\} \quad (4.6)$$

Generally the manufacturer's available information is set at three points at the reference conditions known as Standard Test Conditions (STC) of AM1.5 spectrum, solar irradiance G_{ref} (1000W/m^2) and a cell temperature $T_{c,ref}$ (298°K). These parameters are

the voltage at open circuit $V_{oc,ref}$, the current at short circuit $I_{sc,ref}$ and the voltage and current at maximum power $V_{mp,ref}$ and $I_{mp,ref}$. The relationships for these points are: $I = I_{sc}$ and $V = 0$ at short circuit, $I = 0$ and $V = V_{oc}$ at open circuit, $I = I_{mp}$ and $V = V_{mp}$ at maximum power.

$$I_{sc,ref} = I_{ph,ref} - I_{0,ref} \left\{ \text{Exp} \left[\frac{qI_{sc,ref}R_s}{\gamma k_B T_{c,ref}} \right] - 1 \right\} \quad (4.7)$$

$$0 = I_{ph,ref} - I_{0,ref} \left\{ \text{Exp} \left[\frac{qV_{oc,ref}}{\gamma k_B T_{c,ref}} \right] - 1 \right\} \quad (4.8)$$

$$I_{mp,ref} = I_{ph,ref} - I_{0,ref} \left\{ \text{Exp} \left[\frac{q(V_{mp,ref} + I_{mp,ref}R_s)}{\gamma k_B T_{c,ref}} \right] - 1 \right\} \quad (4.9)$$

The reverse saturation current I_0 for any diode is a very small quantity, in the order of 10^{-5} or 10^{-6} A. This minimizes the impact of the exponential term in Equation 4.7, so it is safe to assume that the photo-generated current equals the short-circuit current, that is, $I_{sc,ref} = I_{ph,ref}$.

In addition, to further simplify the estimation process, the term “-1” in Equations 4.8 and 4.9 can be neglected, as the exponential term is large compared to 1.

Equation 4.8 can be re-written as

$$I_{0,ref} = I_{sc,ref} \left\{ \text{Exp} \left[\frac{-qV_{oc,ref}}{\gamma k_B T_{c,ref}} \right] \right\} \quad (4.10)$$

R_s can be determined from Equation 4.9

$$R_s = \frac{V_{oc,ref} - V_{mp,ref} + [\log(1 - \frac{I_{mp,ref}}{I_{sc,ref}})] \frac{\gamma k_B T_{c,ref}}{q}}{I_{mp,ref}} \quad (4.11)$$

The non-ideality factor γ takes a value between 1 and 2, being near one at high currents, rising towards two at low currents. We can estimate the value of γ to be 1.3. Alternatively, an average value of γ can also be determined by the derivative of voltage with respect to temperature at the reference open circuit condition:

$$\left. \frac{\partial V}{\partial T} \right|_{V=V_{oc}} = \mu_{v,oc} = \frac{\gamma k_B}{q} \left[\log \left(\frac{I_{sc,ref}}{I_{0,ref}} \right) + \frac{T_{c,ref} \mu_{I,sc}}{I_{sc,ref}} - \left(3 + \frac{q E_g}{\gamma k_B T_{c,ref}} \right) \right] \quad (4.12)$$

where $\mu_{v,oc}$ is the temperature coefficient of the open circuit voltage and $\mu_{I,sc}$ is the temperature coefficient of the short circuit current. The data is generally available from manufacturer's data sheet.

Values of I_{ph} and I_0 at other conditions of irradiance and cell temperature can be determined from the following equations

$$I_{ph} = \frac{G}{G_{ref}} [I_{ph,ref} + \mu_{I,sc} * (T_c - T_{c,ref})] \quad (4.13)$$

$$I_0 = I_{0,ref} \left(\frac{T_c}{T_{c,ref}} \right)^3 \left\{ \text{Exp} \left[\frac{q E_g}{k_B} \left(\frac{1}{T_{c,ref}} - \frac{1}{T_c} \right) \right] \right\} \quad (4.14)$$

where G , T_c is the actual amount of solar radiation and cell temperature in degrees K, $\mu_{I,sc}$ is the temperature coefficient of the short circuit current and is usually 2.3mA/K, and E_g is the energy band, with a typical value of 1.12eV in silicon.

The cell temperature T_c can be estimated from the ambient temperature T_a and the irradiance G with the use of a parameter called the Nominal Operating Cell Temperature (NOCT):

$$T_c = T_a + \frac{(NOCT - 20)G}{800} \quad (4.15)$$

NOCT is taken to be 48°C if not known.

A PV array is made up of series and parallel combinations of PV cells that give the desired I-V characteristics. The whole assembly has a circuit model that is analogous to a 4-parameter model but its parameters are scaled. Consider N_P cells in parallel and N_S cells in series, and assume uniform irradiance and temperature for all the PV cells:

$$\begin{aligned} I_{ph,total} &= I_{ph} * N_p \\ I_{D,total} &= I_D * N_p \\ R_{S,total} &= R_S * N_S / N_P \\ I_{total} &= I * N_p \\ V_{total} &= V * N_S \end{aligned} \quad (4.16)$$

Once $I_{ph,ref}$, $I_{0,ref}$ and R_S are determined using manufacturer's supplied data ($V_{oc,ref}$, $I_{sc,ref}$, $V_{mp,ref}$, $I_{mp,ref}$, $\mu_{v,oc}$, $\mu_{I,sc}$), Equations 4.6, 4.12 – 4.15 can be used in an interactive computer

program to determine the output characteristics of the PV array under different conditions of irradiance and ambient temperature conditions. Figure 4.3 shows data required to set up a PV output model in a commonly used engineering software package, and an example of I-V and P-V characteristics of a PV array for three irradiance levels is shown in Figure 4.4.

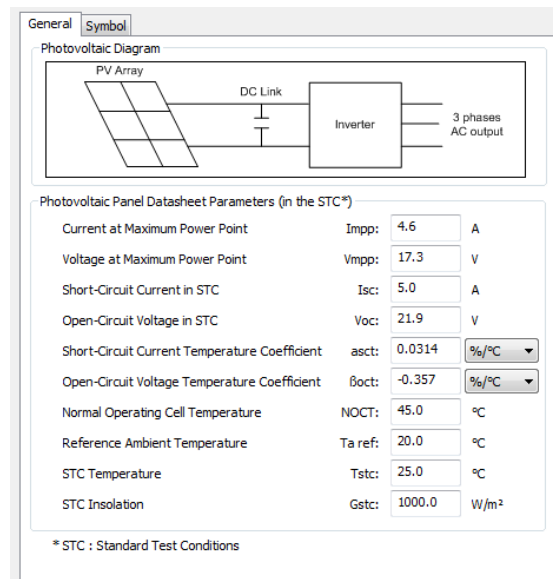


Fig. 4.3. Example of data required to set up a PV output model in a commonly used engineering software package

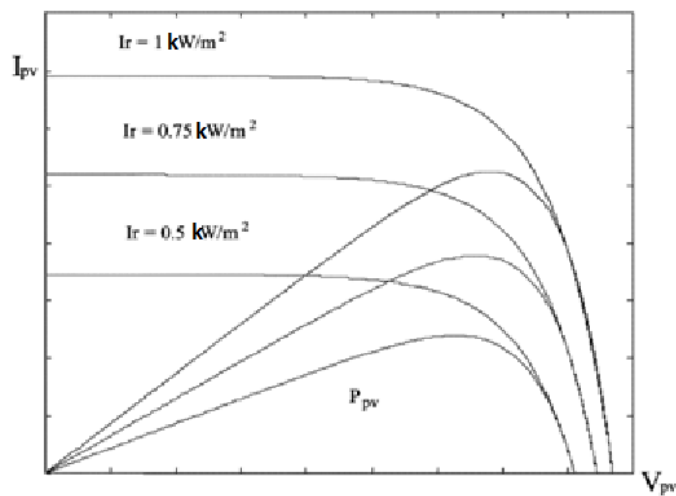


Fig. 4.4. I-V and P-V characteristics of a PV array at different irradiance levels

4.2.2 Inverter Modelling [69-72]

PV systems are connected to the grid via DC/AC inverters. Apart from performing voltage conversion function from the DC output of the PV array to the AC voltage of the grid and the associated grid interface functions such as power factor and anti-islanding control, the inverters also incorporate Maximum Power Point Tracking (MPPT) algorithm to ensure the maximum amount of power is extracted from the PV array. A number of MPPT algorithms are in use such as open circuit voltage method, the incremental conductance method, the ripple-based method, the parasitic capacitance method and the perturbation and observation (P&O) technique. The MPPT algorithm chosen will affect the conversion efficiency of the inverter and its response to transient disturbances in the PV array output (such as those caused by passing clouds). For transient studies the behaviour of the MPPT algorithm needs to be modelled.

Although the inverter topology structure can be complex, it has less impact on output power calculation, which mainly depends on the relationship between its input and output power, namely conversion efficiency. The conversion efficiency is made up of two main components: MPPT efficiency which depends on the implementation of the MPPT algorithm, and energy losses in the inverter. The latter is a function of input power to the inverter:

$$P_{losses} = k_0 + k_1 P_{pv,n} + k_2 P_{pv,n}^2 \quad (4.17)$$

where $P_{pv,n}$ and P_{losses} are the inverter input power and losses normalised to the inverter rating, with $P_{pv,n} = \frac{P_{pv}}{P_{inv,rated}}$ and $P_{losses} = \frac{\text{Inverter power losses}}{P_{inv,rated}}$.

The constants k_0 , k_1 and k_2 are specific to the inverter type being used and are generally obtained via experimentation.

It is important to note that an undersized inverter will affect the inverter output, as the inverter goes into power limiting mode when the input power (from the PV array output) is higher than the rating of the inverter. An oversized inverter, on the other hand, suffers from cost penalty and an inferior MPPT efficiency at lower PV array output due to the difficulty in locating the maximum power point.

4.2.3 Solar Irradiance Modelling [69, 73, 74]

The photo-generated current (and hence output power) of the PV array is dependent on the solar irradiance incident on the array surface – the plane-of-array (POA) solar

irradiance. Unless the PV array is mounted on a tracker that tracks the sunlight direction and adjusts the position of the array to suit, the plane-of-array solar irradiance is expected to vary in accordance with the solar zenith angle, leading to a corresponding variation in the daily and seasonal output of the PV system.

Apart from the solar zenith angle, cloud cover (or the concentration of aerosols in the atmosphere) will have an impact on the amount of POA solar irradiance received by the PV array. Sky clearness index has been created to allow the modelling of solar irradiance under different sky conditions.

As direct measurement of solar irradiance at the PV array is not practical for most installations, extrapolation of measurement results from nearby weather stations is generally required. These weather stations measure solar irradiance falling on a horizontal plane whereas PV arrays are generally mounted at an angle (tilted) to suit the roof pitch and to maximise the amount of energy production. The total radiation on a tilted surface consists of three components: beam, reflected radiation from the ground and diffuse from all parts of the sky. The direct and reflected components can be computed with good accuracy by using simple algorithms but the nature of diffuse part is more complicated. Fairly elaborate models are developed to determine the diffuse irradiance on a tilted PV array, the isotropic and anisotropic models. The isotropic models assume that the intensity of diffuse sky radiation is uniform over the sky dome. Hence, the diffuse radiation incident on a tilted surface depends on a fraction of the sky dome seen by it. The anisotropic models, on the other hand, assume that the diffuse radiation is made up by the anisotropy of the diffuse sky radiation in the circumsolar region (sky near the PV array) plus the isotropically distributed diffuse component from the rest of the sky dome (horizon brightening fraction).

4.2.4 Overall PV generator model

The PV cell model and the inverter model are combined to provide a PV generator model. Model inputs of solar irradiance, ambient or cell temperature are then used to derive PV generator output.

4.2.5 Need for a Simplified Generator Model for Residential Roof-top PV Systems

Current PV generator models provide accurate output prediction but required extensive data collection effort. In public electricity distribution networks, the parameters required

to determine these electrical models are not generally known as the PV panels are part of private customer installations. A simplified, yet reasonably accurate PV generator model is highly desirable.

4.3 Simplified Generator Model for Residential Roof-top PV Systems

4.3.1 Insight from Smart Meter Data

Residential PV installations in Australia are metered in two ways: gross metering where separate channels are used to record load consumption and PV generation, and net metering where a single channel (with separate export and import registers) is used to record the aggregate load consumption and PV generation. An integrating time interval of 30 minutes is commonly used. An example of a gross metering site with a 1kW PV system is shown in Figure 4.5 where “GEN” is solar generation, “CON” is consumption and “NET” is net consumption (derived using GEN and CON data). Negative values of net consumption indicate net generation export from the customer premises.

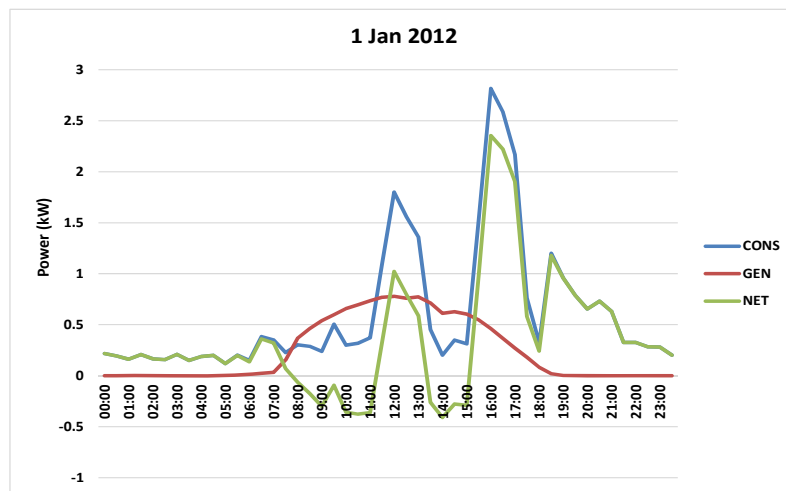


Fig. 4.5. Energy demand data of a customer with a 1kW PV system

A number of observations can be made from Figure 4.5:

- The maximum output (averaged over 30 minutes) of the 1kW PV system is about 0.8kW on this day and this occurs between 12 to 1pm;
- Where PV generation is higher than the consumption, the customer is exporting energy back into the electricity network;
- The customer has a peak usage at 4pm. As the PV is still generating at that time it is able to contribute to peak reduction.

To show the daily variation of generation and load consumption, consumption and generation data for the whole month of January are shown in Figure 4.6 and Figure 4.7 for the same customer.

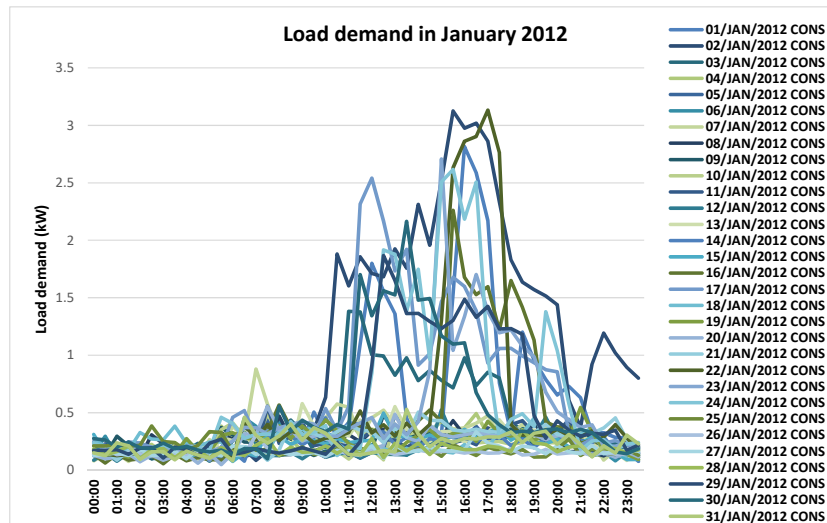


Fig. 4.6. Consumption data for a customer

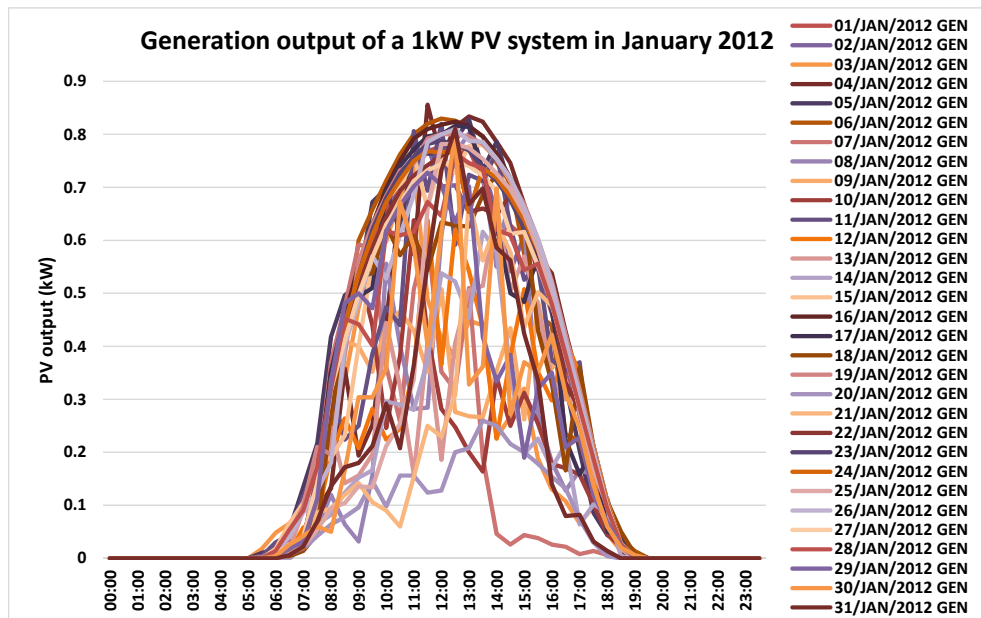


Fig. 4.7. PV generation data for a customer

Energy consumption is generally recognized as a stochastic process and this is seen in Figure 4.6 where the consumption data varies daily. Generation from the 1kW PV system also exhibits significant variation from day to day as show in Figure 4.7. The peak output of the PV system never reaches its nameplate rating of 1kW. This poses a challenge to utility engineers to translate PV panel rating into capacity that can be used to support network operation.

The variation in PV generation at the same site is due to a number of factors:

- Solar irradiance falling on the PV panel surface exhibits seasonal variation due to the changing angle of the sun’s ray.
- Solar cell output exhibits a negative temperature coefficient with respect to cell temperature. The process where sunlight is converted into electricity is therefore less efficient on a hot day than a cold day.
- Cloud cover affects the amount of solar irradiance that reaches the PV panel surface. This is the primary factor that accounts for the randomness of solar generation.

Figure 4.8 shows the maximum monthly generation output (kW) of a number of PV sites over a one-year period. The outputs are averages over 30-minute intervals (not instantaneous output). Seasonal variation of the maximum power output of the PV panels

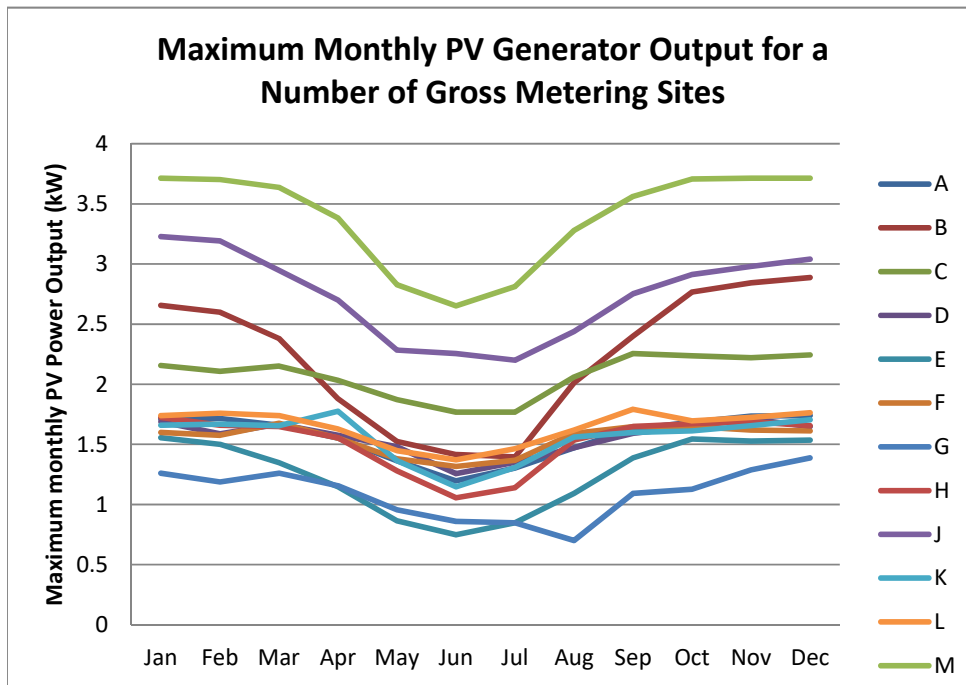


Fig. 4.8. Maximum power output of a number of PV sites over the course of one year

can be readily visualised. The lowest output occurs between June to August which coincides with wet winter months in Victoria, Australia.

4.3.2 Derivation of a Simplified PV Generator Model

Cell temperature of a solar installation is not a parameter that can be easily measured. A simplified empirical formula linking cell temperature to ambient temperature [64] is given in Equation 4.15 and repeated here:

$$T_c(t) = T_a(t) + [\text{NOCT} - 20] * \frac{G_{POA}(t)}{800} \quad (4.18)$$

where T_c is the cell temperature, NOCT is the nominal operating cell temperature (taken to be 48°C), and G_{POA} is the plane-of-array solar irradiance in Wm^{-2} .

According to [75] the AC output of a PV system is given by

$$P_{AC} = P_{DC} \eta \quad (4.19)$$

$$P_{DC}(t) = \frac{P_{STC} \cdot G_{POA}(t)}{1000} \{1 + [T_c(t) - 25]C_T\} \quad (4.20)$$

where P_{AC} is the AC output of the PV inverter, P_{DC} is the DC output of the PV array, η is the dc/ac conversion efficiency (which includes the inverter MPPT and energy efficiency, soiling and ageing of the PV array), P_{STC} is the PV panel dc rating specified at STC, and C_T is the temperature coefficient of PV cell (taken to be -0.5%/°C).

Combining Equations 4.18 - 4.20 gives

$$P_{AC}(t) = \frac{P_{STC} \cdot \eta \cdot G_{POA}(t)}{1000} [1.125 - 0.005T_a(t) - 0.000175G_{POA}(t)] \quad (4.21)$$

Equation 4.21 can be used to model the AC output of a PV system using only ambient temperature, solar irradiance and DC/AC conversion efficiency. There are a few conditions for its use:

- It is a quasi steady-state equation and cannot be used to determine the transient response of a PV system to sudden changes in solar irradiance. The Maximum Power Point Tracking (MPPT) algorithm incorporated in the inverter dominates the dynamic behaviour of the PV system and has not been taken into account in the equation [71, 76]
- DC/AC conversion efficiency is dependent on the amount of solar irradiance, soiling and ageing of the PV panels, DC losses, inverter design and the amount of input power

relative to the inverter rating. The maximum AC output of a PV system normally occurs at maximum solar irradiance where inverter efficiency is at its highest and a nominal DC/AC conversion efficiency of 0.85 to 0.9 can be assumed [70]. For energy yield calculation, [77] recommends an overall system derate factor (or efficiency) of 0.77.

Further simplification of Equation 4.21 is possible to improve its ease of use.

The plane-of-array solar radiation is made up of two components: a direct component resulting from the sun's direct beam, and a diffuse component resulting from scattering of the sun's beam due to atmospheric constituents and reflection from surrounding objects (the diffuse component is sometimes further split up into a diffuse component and a reflected component). It can be expressed as below:

$$G_{POA}(t) = G_{Dir}(t)\cos Y(t) + G_{Dif}(t)\frac{(1 + \cos(\alpha))}{2} \quad (4.22)$$

where G_{Dir} is the direct irradiance measured in a plane normal to the sun, G_{Dif} is the diffuse irradiance measured in the horizontal plane, α the inclination of the array from the horizontal, and Y is the angle of incidence, between the direction of the sun's ray and the array normal, and is also known as the sun's zenith distance.

Equation 4.22 can also be expressed using global irradiance G_{Glo} , defined as the total solar irradiance (both direct and diffuse) measured on the horizontal plane:

$$G_{Glo}(t) = G_{Dir}(t)\cos Y(t) + G_{Dif}(t) \quad (4.23)$$

Combining Equations 4.22 and 4.23 gives

$$G_{POA}(t) = G_{Glo}(t) + G_{Dif}(t)\frac{(\cos(\alpha) - 1)}{2} \quad (4.24)$$

The inclination angle of the array (α) normally follows the pitch of the roof, with a typical value of 22.5°. With G_{Dif} always smaller than G_{Glo} (the two only become equal in a totally overcast day where there is no direct ray from the sun), the second term in Equation 4.24 is less than 4% of the first term. We can therefore assume that G_{POA} is equal to G_{Glo} .

Equation 4.21, which gives the output of a PV system, can now be further simplified using G_{Glo} :

$$P_{AC}(t) = \frac{P_{STC}\eta G_{GLO}(t)}{1000} [1.125 - 0.005T_a(t) - 0.000175G_{GLO}(t)] \quad (4.25)$$

The maximum error introduced by this simplification is less than 1% when Equation 4.25 is used where the diffuse solar component is less than 20% of the global component, as discussed in 4.4.1 below.

4.4 Applications of the Simplified PV Generator Model

4.4.1 Solar Irradiance Data at PV Locations

Unless local weather station has been installed, data for the solar irradiance falling on a residential PV array is not readily available. To get around this limitation, tools developed to determine the sizing of PV arrays and payback period generally use historic solar statistics by establishing metrics such as Typical Meteorological Year (TMY) for a particular region/country [77]. These solar irradiance data are useful for benchmarking the annual energy yield of various PV systems. They are, however, not suitable for predicting solar irradiance on shorter time horizons.

The Australian Bureau of Meteorology has a number of weather stations that measure solar irradiance in time intervals of one second (averaged over a minute). The weather station located at Tullamarine International Airport, in north-west of Melbourne, is in the

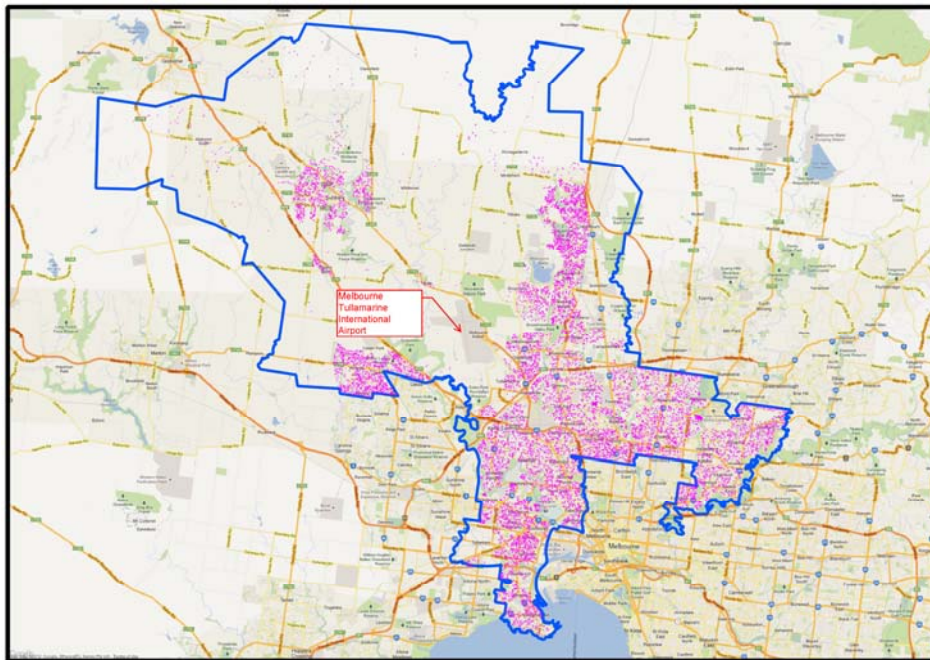


Fig. 4.9. Map of Jemena Electricity Networks

The area bounded by the blue contour is the electricity distribution network. The pink dots represent locations of PV systems. Location of the Tullamarine International Airport is shown by the call-out text box.

geographical centre of the Jemena Electricity Networks where these PV systems are installed (Figure 4.9). The solar irradiance recorded at this weather station [78] is used as the ‘proxy’ for the solar irradiance received by PV arrays located in any part of the electricity distribution network.

To test the validity of this assumption, a linear correlation study is performed between the global solar irradiance daily dataset and the generation daily dataset of a 1kW PV system over a one-year period (2012). As the generation dataset is only available in 30-minute aggregate values, the 1-second solar irradiance data (Wm^{-2}) are firstly aggregated to form 30-minute solar irradiance energy (Jm^{-2}).

The MATLAB function *corrcoef* is then run for the data matrix (where each column represents a separate quantity). A positive linear relationship between the data columns will return a matrix of correlation coefficients with values close to 1. The correlation coefficients are plotted in Figure 4.10 and also summarized in Table 4.1.

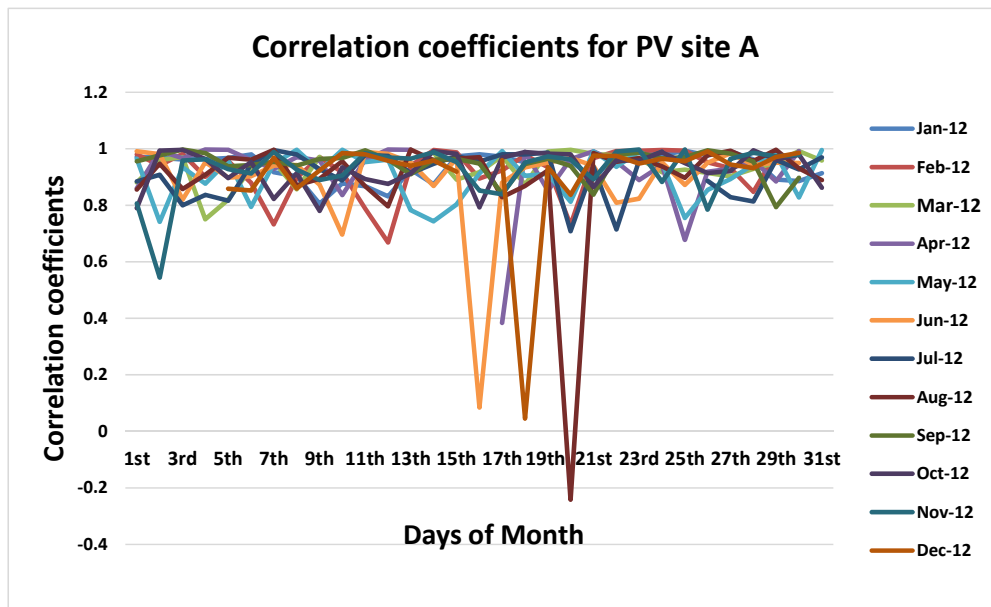


Fig. 4.10. Daily correlation coefficients for the 1kW PV customer site

Table 4.1 Summary of correlation coefficients

Value of correlation coefficient	Days	Percentage of days in 2012
≥ 0.95	183	51.50%
≥ 0.90	257	72.40%
≥ 0.85	306	86.20%

It is clear from Figure 4.10 and Table 4.1 that strong linear correlation exists on most days of the year. Very low values of correlation coefficients are caused by missing solar data. Lower values of correlation coefficients (e.g. ≤ 0.8) are found to be days where there is significant cloud coverage (indicated by significant diffuse solar component relative to global solar component). Two examples are shown in Figures 4.11 and 4.12.

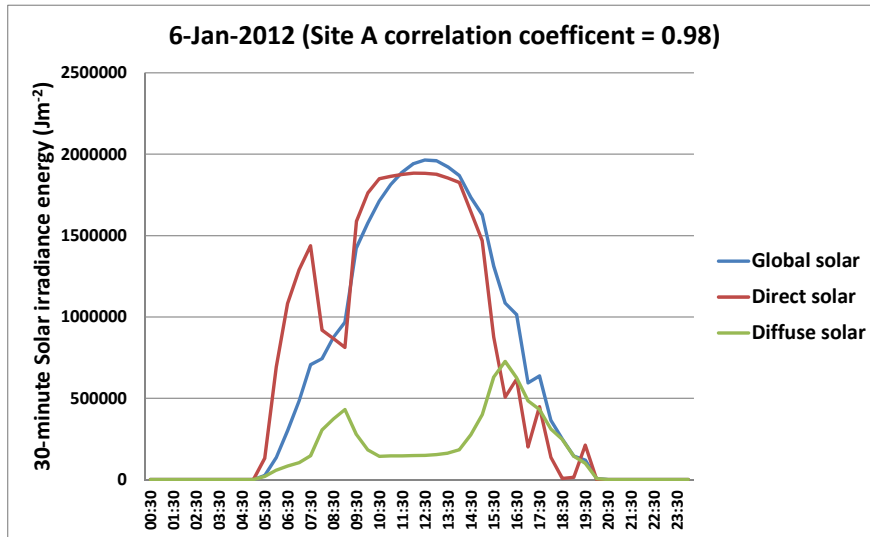


Fig. 4.11. Components of solar irradiance on a day where strong correlation is found between solar irradiance and PV generation

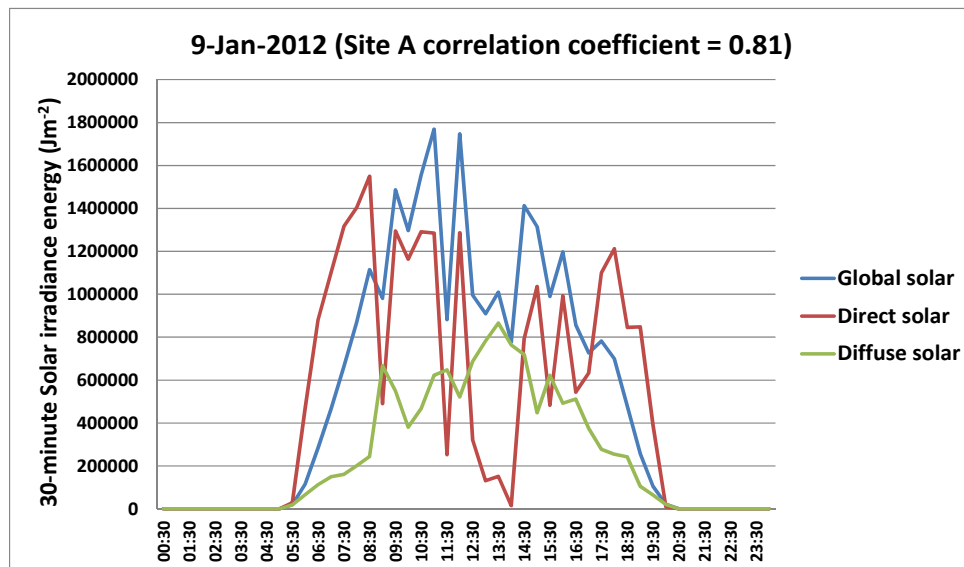


Fig. 4.12. Components of solar irradiance on a day where weak correlation is found between solar irradiance and PV generation

Solar irradiance on a clear-sky day is dominated by the direct solar irradiance component and one would expect that this direct component will be experienced by PV panels installed in relative close proximity to the weather station. On a cloudy day, however, solar irradiance has a significant diffuse component. This diffuse component is caused by scattering of the sun's ray by cloud and surrounding objects, including reflection from the ground. The diffuse component can show significant variation depending on the local site condition and the measurements taken at Tullamarine weather station may not be representative.

Similar observation is obtained from analysis of other PV sites. It is therefore concluded that the aggregate (30-minute) solar irradiance data at the Tullamarine weather station is a reasonable 'proxy' to model the solar irradiance received by a local PV system on a clear sky day, when the diffuse solar irradiance contributes less than 20% to the global solar irradiance.

As shown later in Section 4.4.3, the proposed PV output model has also been used in predicting the one-minute output profile of PV system in a power quality investigation, using one-minute solar and 30-minute ambient temperature data from the Tullamarine weather station. It looks promising that the proposed approach to the solar irradiance data will be accurate enough to simulate the steady-state output of a PV system down to 1-minute time horizon.

Solar forecasting is under active research currently. It is possible that accurate solar forecast data will become available soon [79] which can then be used as 'proxy' to forecast the output of PV systems in day-ahead planning studies.

4.4.2 Modelled and Actual Output of a PV System

Equation 4.25 provides the quasi steady-state output of a PV system at any time t , provided the global solar irradiance and ambient temperature at that instance in time are known. While instantaneous value of the PV system output is useful for power quality impact assessment, utility planning engineers are more interested in 'average' PV output over a time interval, typically 30-minute, as this aligns with the thermal inertia of equipment commonly found in electrical power networks. This can be achieved by summing the calculated PV output, at every second, over a 30-minute interval, then dividing the summation by the time interval (1800 seconds), as per Equation 4.26:

$$\begin{aligned}
& \frac{1}{1800} \sum_{t=t_1}^{t=t_1+1800} P_{AC}(t) \\
& = P_{STC} \\
& \cdot \eta \frac{0.001}{1800} \left[1.125 \sum_{t=t_1}^{t=t_1+1800} G_{GLO}(t) - 0.005 \sum_{t=t_1}^{t=t_1+1800} [T_a(t) \cdot G_{GLO}(t)] \right. \\
& \quad \left. - 0.000175 \sum_{t=t_1}^{t=t_1+1800} G_{GLO}(t)^2 \right] \tag{4.26}
\end{aligned}$$

For the time varying quantities on the right-hand side of Equation 4.26, global solar irradiance G_{Glo} is available from the Bureau of Meteorology weather station while ambient temperature measurements are only available as 30-minute snapshots which are considered acceptable as ambient temperature does not exhibit rapid variation. Finally for maximum output determination, the efficiency η is taken as 0.9.

The 30-minute generation output of the 1kW PV site is determined using Equation 4.26, and compared with the measured generation output by smart meter. The results for 2 days in January 2012 are shown in Figures 4.13 and 4.14. On 2 January the sky was overcast (shown by the high diffuse to global solar irradiance ratio) whereas the sky was relatively clear on 6 January. It can be seen that Equation 4.26 gives an accurate estimate of 30-minute generation output when cloud cover is minimal, reinforcing the observation made in Section 4.4.1 above.

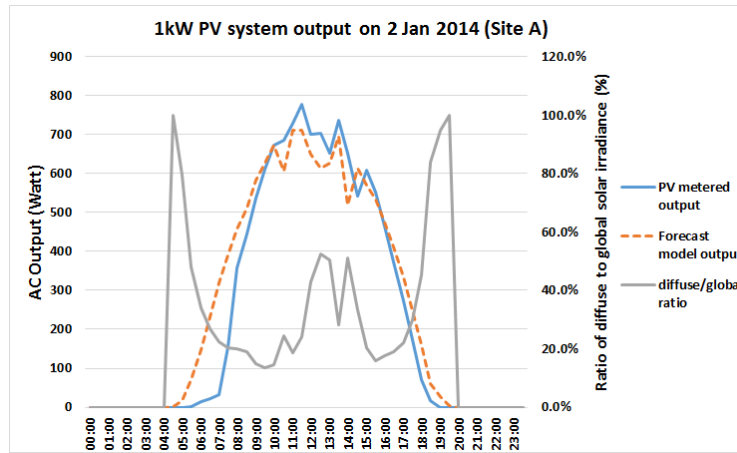


Fig. 4.13. Actual and estimated output of a 1kW PV system on a relatively cloudy day

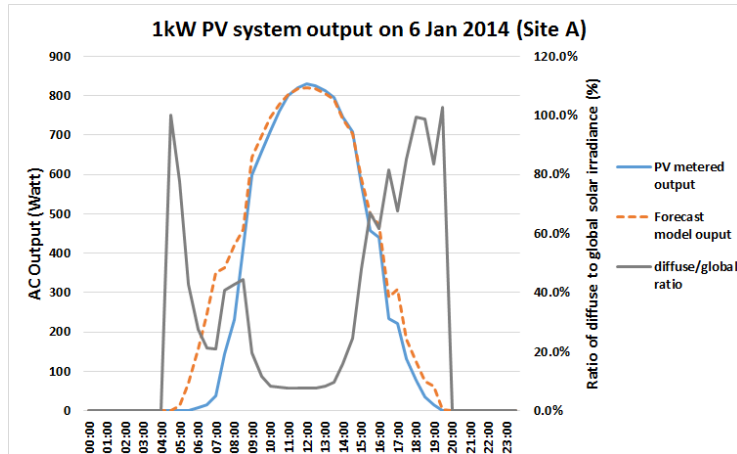


Fig. 4.14. Actual and estimated output of a 1kW PV system on a relatively clear sky day

It should be noted that the error of Equation 4.26 is larger at low PV output. This is due to the fact that the PV inverter is generally less efficient at low power (corresponding to low solar irradiance level early in the morning or late in the afternoon) [70]. This is not considered a limitation when Equation 4.26 is used for the purpose of determining the maximum output of a PV system.

While the accuracy of the approach cannot be determined analytically, the error of peak power prediction in the sample of the PV systems modelled varies from -0.2% to 7.8%.

It can be concluded that the output of a PV system can be estimated reasonably accurately by the proposed method, provided the solar irradiance data used in the calculation (and measured at a nearby weather station) has only a small diffuse component, and that the solar system is operating at high output level relative to its rating.

4.4.3 Power Quality Investigations

Jemena Electricity Networks, who contributes data to this research project, has been experiencing increasing level of overvoltage complaints from its customers who have installed PV systems. Complaints are generally related to the loss of revenue caused by the inability to export surplus PV power when the PV inverters trip on overvoltage occurrences. On receiving the complaint, the company initiates power quality investigation by installing portable power quality meters at the supply substation and the customer supply point, recording voltages, currents and other related quantities (such as power factor and harmonics) over a one-week period. The results are then analysed and remedial action taken if the supply voltages are found to be outside the regulatory limits.

The result of a case study involving a three-phase customer with a single-phase 5kW PV installation is shown (Figure 4.15). The 1-minute power output of the PV system is calculated using Equation 4.25, with 1-minute global solar irradiance and 30-minute ambient temperature data from the Tullamarine weather station, and compared with 1-minute voltages recorded by a power quality meter. The voltage rise calculation is based on a simple model of constant grid voltage at the point of common coupling. It can be seen that the calculated voltage from the PV model follows closely the voltage profile recorded by the power quality meter during daylight hours. More elaborate network modelling work is reported in Chapters 5 and 6.

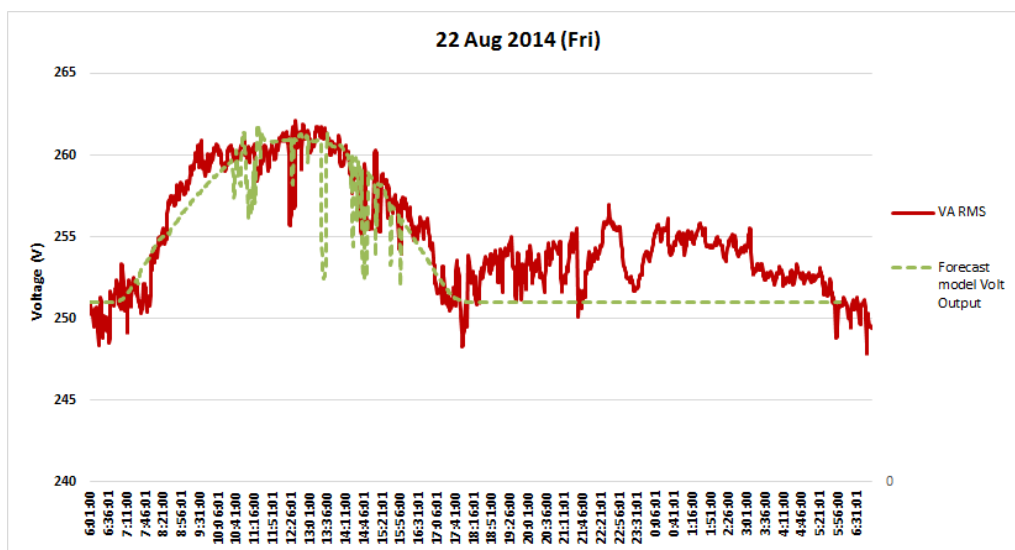


Fig. 4.15. Model voltage output of a 5 kW PV system in a power quality investigation

4.4.4 Gross and Net Load Profiles

It is well known that generation systems embedded in the distribution network can cause overvoltage issues. The connection rules and network impact assessment are generally based on a deterministic steady-state analysis. Due to the randomness of load and generation, however, deterministic load flow analysis is of little value in predicting how often or to specify the location where overvoltages are likely to occur in the network over a given time period. It is generally based on worst case scenario (maximum generation and minimum load) which could place unnecessary limit on the amount of embedded generation that can be connected. Probabilistic load flow study based on analytical techniques or the Monte Carlo method [37] is the emerging network planning approach

that takes into account the stochastic nature of intermittent renewable generation (such as PV) and load.

An inherent requirement for any probabilistic load flow technique is the determination of Probability Density Functions (PDFs) of the loads based on historic load profiles. With the increasing penetration of PV generation in the electricity distribution network, the historic load profiles measured at various network assets (such as distribution transformers, distribution lines) are net profiles combining the effect of electricity usage and PV generation. As PV generation and load consumptions are affected by different external factors, their PDFs do not follow the same probability distribution curve. To use probabilistic load flow technique, the net load profiles should be disaggregated into load and generation profiles before PDFs are determined. This can be achieved by using the PV model established in Section 4.4.2.

Let $X(t)$ be a random variable representing 30-minute energy data measured by the smart meter, $Y(t)$ be the corresponding random variable of 30-minute solar generation, and $Z(t)$ the random variable of energy consumption within the premise. The three random variables have the following relationship at time instant t :

$$X(t) = -Y(t) + Z(t) \quad (4.27)$$

As $X(t)$ is known and $Y(t)$ can be estimated by Equation 4.26, $Z(t)$ can be determined.

To illustrate the concept, load and generation data from the gross metering PV site are aggregated together to form net load profile. Generation output is then calculated using Equation 4.26, after which the load profile is derived using Equation 4.27, and compared with the metered load data. The results are shown in Figure 4.16. The estimation error at low PV output can be improved by fitting a curve for the PV efficiency η at different output power levels, rather than the use of a single (high) value.

Many PV sites in Australia have net metering applied where a single meter (with separate export and import registers/channels) is used to record the aggregate energy flow into or out of the point of connection. In other words, the energy recorded by the meter represents the net consumption/generation of the site. The above approach can be used to disaggregate the net metering data into load and generation data.

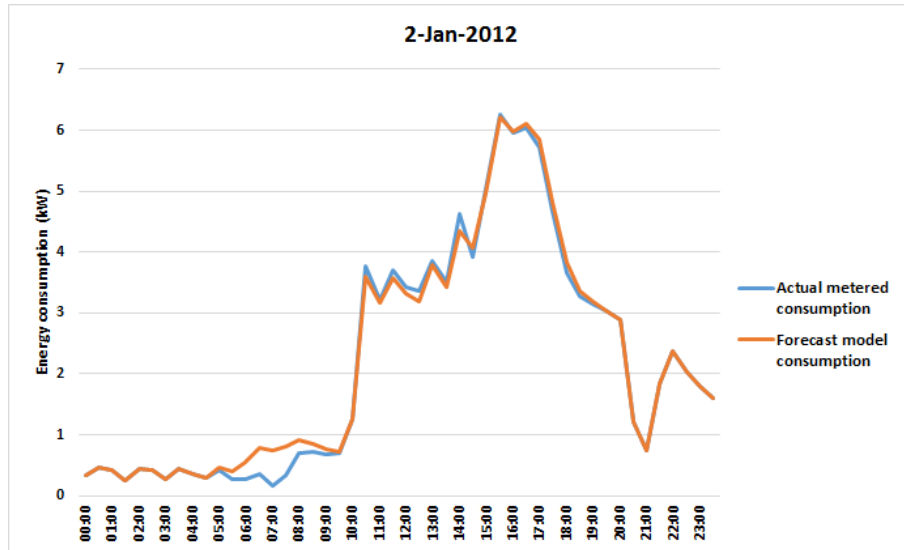


Fig. 4.16. Estimated and measured load profile for the 1kW PV site

4.5 Summary

One of the major challenges faced by the electrical supply industry in accommodating customer PV installations today is delivering secure, reliable and high quality power while managing voltage rise, fluctuations and intermittency of the energy source. Meeting the challenge requires knowledge about real-life output of the installed PV systems.

Significant work has been carried out by the international research community to develop mathematical models of PV arrays for applications including energy forecasting, economic payback assessment, electricity network impact assessment and transient stability. Simplification of these models, however, is required for practical applications in electricity distribution networks, particularly for small roof-top PV installations. This chapter provides utility engineers a tool to efficiently determine the in-situ output of roof-top PV systems installed on customer premises, without the need for extensive data collection. The methodology is based on DC rating of the PV system, ambient temperature and solar irradiance data. To overcome the challenge posed by the lack of local measurements of solar irradiance data, covariance analysis has confirmed that data captured in a nearby weather station can be used provided the sky is relatively clear. While this constraint may seem to be limiting, the methodology is applicable to electricity network studies which have the focus on extremes (such as maximum solar irradiance and clear sky) rather than averages.

As penetration of PV system increases in electricity distribution network, it would become necessary to disaggregate load measurements captured by monitoring systems (such as smart meters and SCADA) into solar generation and load consumption. This will allow the appropriate drivers to be incorporated into the analysis of historic data and future forecast. In this regard, it is important to point out that load demand in Australia is generally driven by air conditioning use during hot summer days, many of which are coincident with dense cloud cover. As solar output is reduced at high ambient temperature and cloud coverage, it is important to extract generation output from load data to allow separate forecasting methodology to be applied.

The use of the PV generator model is further explored in Chapters 5 and 6.

Chapter 5 - LV Network Model for Simulation Studies

This chapter is based on the following publication:

Peter K.C. Wong, Akhtar Kalam and Robert Barr, “Modelling and Analysis of Practical Options to Improve the Hosting Capacity of Low Voltage Networks for Embedded Photo-Voltaic Generation”, accepted for publication in the IET (Institution of Engineering & Technology) Journal of Renewable Power Generation. Doi: 10.1049/iet-rpg.2016.0770.

5.1 Overview

Australian electricity supply utilities run extensive 4-wire LV (230/400V) reticulations along the streetscape. The LV distribution network employs a Multiple Earthed Neutral (MEN) design where the neutral conductor is earthed at the LV star point of the distribution transformer and at points of connection into customer premises.

Due to the lack of data and real-time monitoring by utilities, it has been difficult to establish accurate LV network models to perform simulation studies incorporating the impact of customers’ embedded PV generators. Network models based on generalised network characteristics have been used in the past for planning studies but they either produce conservative results or are used conservatively by utility engineers.

The mass rollout of smart meters to residential customers in Victoria, Australia, has opened up an opportunity. In Chapter 4 we established a reasonably accurate PV generator model which can be incorporated in a LV network model. Smart meter consumption data allows load models of individual customers or customer groups to be established. In addition, it is now possible, through advanced data analytics performed on smart meter voltage and current data [[22](#), [80](#)], to accurately identify the phase and circuit connection of individual customers and derive line impedance between supply nodes. The key components for a LV network model are therefore available.

In this chapter we present the case study for the establishment of a LV network model that is designed for performing simulation studies of the effect of embedded PV generators and mitigating technologies, based on data collected on a real LV network.

5.2 Network Asset Data

The network model is set up from the source MV zone substation. This approach is taken so that the voltage regulating devices on the MV network are included in the modelling and simulation. The distribution circuit used in the case study is a 22kV/433V distribution substation (Cypress-Stillia) supplied by 22kV feeder (SHM14) from SHM 66/22kV Zone Substation. The circuit forms part of the electricity distribution network operated by Jemena, an electricity distribution company in the state of Victoria, Australia.

The MV supply network and the LV distribution circuit have the characteristics shown in Table 5.1. Figures 5.1 and 5.2 provide geographic view of the LV distribution circuits and the details of LV distribution circuit #4.

Table 5.1 Network Characteristics (provided by Jemena Electricity Networks)

Circuit Element	Characteristics			
Supply source (SHM 66kV side)	3-phase fault level = 7.1kA, 1-phase fault level = 4.0kA, voltage regulated at 67kV.			
SHM 66/22kV transformers	40MVA, 66/22kV, delta/star, tap winding = 66kV, tapping range = 0.95 to 1.05, tap number = 16, impedance = 10% on 40MVA.			
22kV feeder SHM14	Six overhead circuit segments, with a distribution substation at the end of each circuit segment. The overhead lines are 3-wire 19/3.25AAC. Note the MV feeder characteristics has been simplified to reduce the complexity of modelling work.			
Cypress-Stillia distribution substation	Connected to the end of the fifth 22kV circuit segment. Comprises of a transformer: 300kVA, 22/0.433kV, delta/star, tap winding = 22kV, tapping range = 0.925 to 1.025, tap number = 4, impedance = 4% on 300kVA. There are 38 customers supplied from this substation arranged in three LV distribution circuits.			
LV Distribution Circuit #4 (coloured brown in Figure 1) ex Cypress-Stillia distribution substation	Underground cables supplying eight customers. The cable forming the LV backbone is 185mm ² Al 4/C while the branch cable is 16mm ² Cu 4/C.			
Customer details on LV Distribution Circuit #4	Customer	Supply	Max Load	PV
	Cus 1	3-phase	5kVA	
	Cus 2	B-phase	5kVA	
	Cus 3	3-phase	15kVA	
	Cus 4	3-phase	7.8kVA	
	Cus 5	3-phase	7kVA	4kW
	Cus 6	W-phase	5kVA	
	Cus 7	3-phase	9kVA	5kW
	Cus 8	3-phase	9KVA	



Fig. 5.1. LV Distribution Circuits from Cypress Stillia Distribution Substation



Fig. 5.2. Details of LV Distribution Circuit #4

5.3 Derivation of Line Impedances

5.3.1 The Need to Model Neutral Conductor and Earth

The 22kV feeder backbone of SHM14 comprises of 3-phase, 3-wire overhead conductors, single-point earthed on the 22kV neutral of the 66/22kV transformer. We have simplified the backbone structure to six overhead line segments and lumped loads at each segment node. The three LV distribution circuits of Cypress-Stillia supply 38 customers via 3-phase, 4-wire underground cables (backbone & 3-phase customers) and 1-phase, 2-wire underground cables for 1-phase customers. A Multiple Earthed Neutral (MEN) system is implemented where the neutral conductors are earthed at customer points of connection (POC) as well as at the LV star point of the supply distribution transformer. The neutral to earth impedance is taken to be 10 ohms at the supply distribution substation and 100 ohms at the customer POC based on design standard and empirical measurements. For LV network modelling it is more accurate to model both the neutral conductor and the earth connections as the loads are inherently unbalanced (due to 1-phase customer connections) so currents will flow in both the neutral conductor and earth, leading to

voltages appearing on the neutral conductor. It is important to note that most load flow software packages return phase-to-ground voltage results whereas the voltages received by customer equipment are the voltages between phases and neutral. Care should be taken to interpret load flow results when ground and neutral are not at the same potential [81]. In addition, neutral-point shifting will cause voltage increase to occur in one phase while voltage decrease in the other two phases. Ignoring the neutral conductor in modelling will therefore lead to erroneous results [82].

5.3.2 Calculating LV Line Impedances Considering Neutral Conductor and Earth

For line impedances, the series impedances published by the suppliers (positive, negative and zero sequence) for the overhead lines and cables normally assume physical symmetry between the three phase and neutral conductors. This is generally not a true representation of the MV distribution network as 2-wire 2-phase tee-offs are common especially in rural areas, and there is no regular transposition of the three phase conductors. Where high accuracy is required MV networks should therefore be modelled as a 3-phase unbalanced system. The LV distribution system consists of single-phase, two-phase, and untransposed three-phase lines serving loads that are mostly connected between phase and neutral. For LV line impedance determination, it is necessary to retain the self and mutual impedance terms of the conductors and take into account the ground return path for the unbalanced currents. A commonly used approach to calculate line impedances are the Carson's equations. Carson assumes the earth is an infinite, uniform solid with a flat uniform upper surface and a constant resistivity. The equations of self and mutual impedances made use of conductor images; that is, every conductor at a given distance above ground has an image conductor the same distance below ground. The concept is illustrated in Figure 5.3.

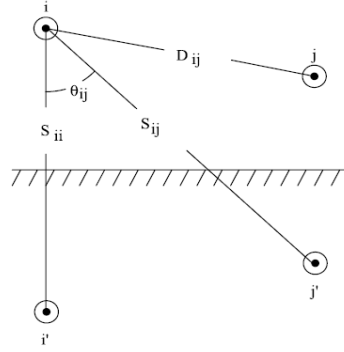


Fig. 5.3. Concepts of conductor images used in Carson's equations

The original Carson's equations [83] incorporate infinite integrals and are computationally intensive without the help of modern digital computer. Various approximations have been used to simplify the calculations and these are generally referred to as modified Carson Equations. One such approximation is given below.

The self impedance of conductor i (Z_{ii}) and the mutual impedance between conductor i and conductor j (Z_{ij}) are given by Equations 5.1 to 5.6 [33, 84].

$$Z_{ii} = (r_i + 4\omega P_{ii}) + j2\omega G \left[x_i + \ln\left(\frac{S_{ii}}{R_i}\right) + 2Q_{ii} \right] \Omega/\text{mile} \quad (5.1)$$

$$Z_{ij} = 4\omega P_{ij} + j2\omega G \left[\ln\left(\frac{S_{ij}}{D_{ij}}\right) + 2Q_{ij} \right] \Omega/\text{mile} \quad (5.2)$$

$$X_i = 2\omega G \ln\left(\frac{R_i}{GMR_i}\right) \Omega/\text{mile} \quad (5.3)$$

$$P_{ij} = \frac{\pi}{8} - \frac{1}{3\sqrt{2}} k_{ij} \cos \theta_{ij} + \frac{k_{ij}^2}{16} \cos(2\theta_{ij}) \left[0.6728 + \ln\left(\frac{2}{k_{ij}}\right) \right] + \frac{k_{ij}^2}{16} \theta_{ij} \sin(\theta_{ij}) + \frac{k_{ij}^3}{\sqrt{2} * 45} \cos(3\theta_{ij}) - \frac{\pi k_{ij}^4}{1536} \cos(4\theta_{ij}) \quad (5.4)$$

$$Q_{ij} = -0.0386 + \frac{1}{2} \ln\left(\frac{2}{k_{ij}}\right) + \frac{1}{3\sqrt{2}} k_{ij} \cos \theta_{ij} - \frac{\pi k_{ij}^2}{64} \cos(2\theta_{ij}) + \frac{k_{ij}^3}{\sqrt{2} * 45} \cos(3\theta_{ij}) - \frac{k_{ij}^4}{384} \theta_{ij} \sin(4\theta_{ij}) - \frac{k_{ij}^4}{384} \cos(4\theta_{ij}) \left[\ln\left(\frac{2}{k_{ij}}\right) + 1.0985 \right] \quad (5.5)$$

$$k_{ij} = 8.565 \times 10^{-4} S_{ij} \sqrt{\frac{f}{\rho}} \quad (5.6)$$

where $i = j = 1, 2 \dots n_{cond}$

n_{cond} = number of conductors

Z_{ii} = self impedance of conductor i in Ω/mile

Z_{ij} = mutual impedance between conductors i and j in Ω/mile

r_i = resistance of conductor i in Ω/mile

$G = 0.1609347 * 10^{-3} \Omega/\text{mile}$

$\omega = 2\pi f$ = system angular frequency in radians per second

R_i = radius of conductor i in feet

GMR_i = Geometric Mean Radius of conductor i in feet

f = system frequency in Hertz

ρ = resistivity of earth in $\Omega\text{-metres}$

D_{ij} = distance between conductors i and j in feet (see Figure 5.2)

S_{ij} = distance between conductor i and image j in feet (see Figure 5.2)

θ_{ij} = angle between a pair of lines drawn from conductor i to its own image and to the image of conductor j (see Figure 5.2)

These equations can be further modified to reduce the computational effort without sacrificing too much of accuracy [33] by reducing the number of terms in Equations 5.4 and 5.5:

$$P_{ij} = \frac{\pi}{8} \quad (5.7)$$

$$Q_{ij} = -0.0386 + \frac{1}{2} \ln\left(\frac{2}{k_{ij}}\right) \quad (5.8)$$

These modified Carson's equations, as they come to be called, are used extensively.

Applying the modified Carson's equations to a 4-wire LV line (a, b, c, n) will result in a primitive impedance matrix of [4 x 4]:

$$Z_{line} = \begin{bmatrix} Z_{aa} & Z_{ab} & Z_{ac} & Z_{an} \\ Z_{ba} & Z_{bb} & Z_{bc} & Z_{bn} \\ Z_{ca} & Z_{cb} & Z_{cc} & Z_{cn} \\ Z_{na} & Z_{nb} & Z_{nc} & Z_{nn} \end{bmatrix} \quad (5.9)$$

$$\begin{bmatrix} V_a \\ V_b \\ V_c \\ V_n \end{bmatrix} = \begin{bmatrix} Z_{aa} & Z_{ab} & Z_{ac} & Z_{an} \\ Z_{ba} & Z_{bb} & Z_{bc} & Z_{bn} \\ Z_{ca} & Z_{cb} & Z_{cc} & Z_{cn} \\ Z_{na} & Z_{nb} & Z_{nc} & Z_{nn} \end{bmatrix} \begin{bmatrix} I_a \\ I_b \\ I_c \\ I_n \end{bmatrix} \quad (5.10)$$

Kron reduction can be used to reduce Z_{line} to a 3x3 phase impedance matrix however this is not recommended as we are interested to know the voltage on the neutral conductor.

Work examples to derive line and cable parameters from manufacturer data and physical construction can be found in [33, 84].

The modelling software, as detailed in Section 5.6, uses the modified Carson's equations to derive line and cable impedance parameters and is well suited for the application described herein.

5.4 Derivation of Loads and Generation

5.4.1 Load Modelling

Customer load models are set up based on SCADA and smart meter measurements over a summer week from 15 to 21 February 2015 when the daily ambient temperature varied from 14.5°C to 35°C. This week of data is chosen in the case study because it represents a wide range of load consumption which the supply network needs to accommodate, and impact of PV generation is generally at its highest during summer months. The loads are modelled as PQ loads and are specified in base load format (kVA, constant power factor). The base loads are modified by loadshapes to gives time series variations of load over the course of the week. The methodology for the derivation of base loads and loadshapes is shown in Table 5.2.

Care has been exercised to ensure the load models closely resemble actual customer loads. Figure 5.4 shows the loadshapes used in the weekly simulation, while Figure 5.5 shows the daily loadshapes in more details for 15 February 2015.

Table 5.2 Derivation of base loads and load shapes

Loads	Method of derivation
SHM Zone Substation loads (excluding loads on 22kV feeder SHM14)	5-minutes snapshots from Supervisory Control And Data Acquisition (SCADA) system. The readings are aggregated and normalized to form 30-minute weekly load shape data. The maximum coincident demand is 18MVA.
SHM14 22kV feeder loads	5-minutes snapshots from SCADA system. The readings are aggregated and normalized to form 30-minute weekly load shape data. The maximum coincident demand is 9MVA.
Cypress-Stillia Distribution Substation Loads	Substation load shape is formed by summing the 30-minute smart meter kWh readings of all customers (except those on LV Circuit #4). The maximum coincident demand is 180kVA.
Customer 1 to 8 on LV Circuit #4	For each customer, the load shape is defined by the 30-minute smart meter kWh readings. For customers with roof-top PV systems, the smart meter readings (representing net of load and generation) are replaced with typical load readings. The maximum coincident demand of LV Circuit #4 is 38kVA.
Roof-top PV systems on LV Circuit #4	No direct measurements of PV output are available. PV output model is used based on ambient temperature and solar irradiance data. Solar irradiance data (1-minute averages) provided by the Bureau of Meteorology are aggregated to form 30-minute snapshots of irradiance data. 5-minute snapshots of ambient temperature measurements by SCADA are aggregated to form 30-minute snapshots.

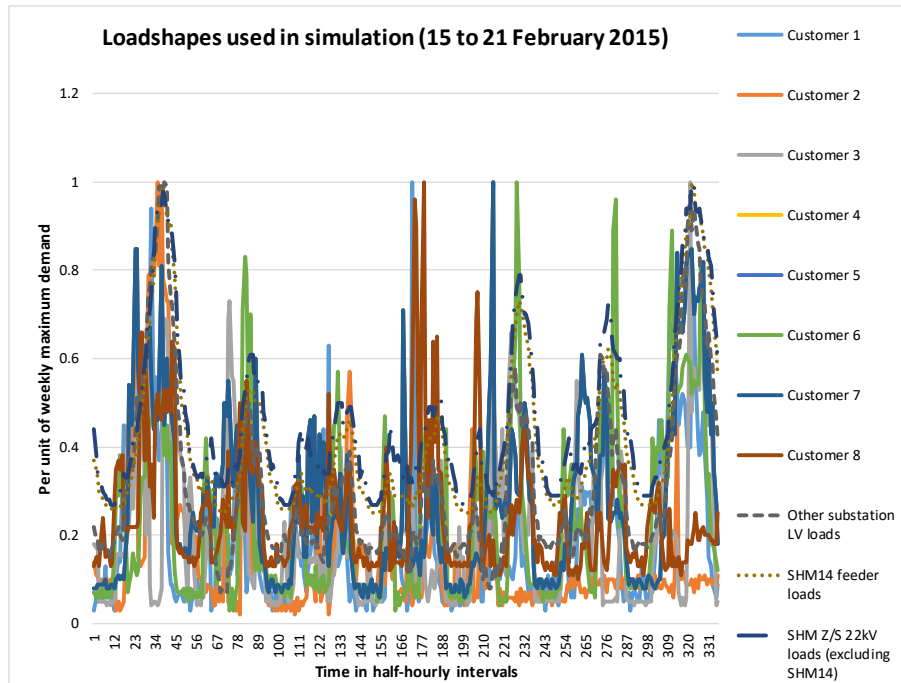


Fig. 5.4. Weekly loadshapes used in the simulation based on SCADA and smart meter

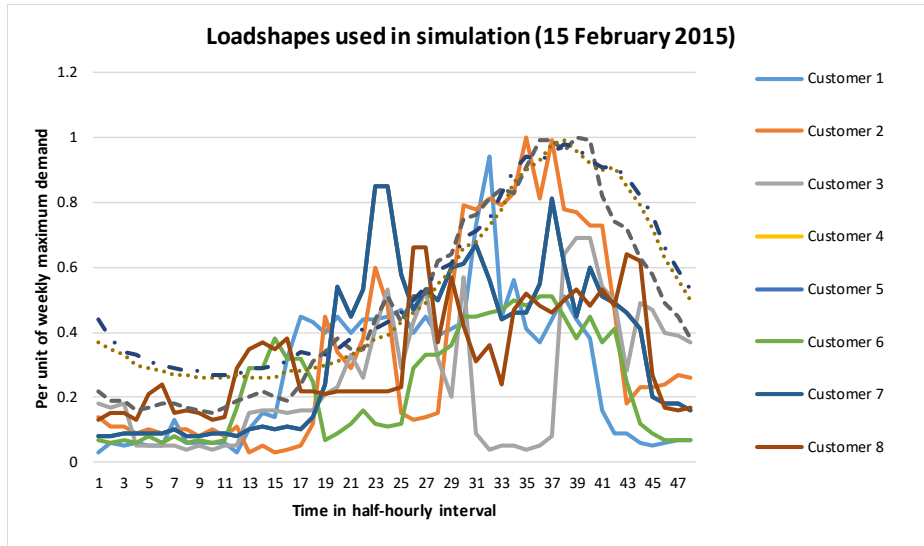


Fig. 5.5. Loadshapes used in the simulation for 15 February 2015 based on SCADA and smart meter measurements

5.4.2 Generation Modelling

Customers 5 and 7 have roof-top PV systems installed on the R-phase. Due to the use of net metering, actual outputs of the PV generators are not available. PV output model based on input parameters of solar irradiance and ambient temperature time series data is used in the computer simulation, and has been shown to be fairly accurate [85]. An example of the modelled output of the PV generator at Customer 5 is shown in Figure 5.6. Note the solar generation varies considerably during the week due to cloud coverage. The effect of solar variability is therefore reflected in the modelled results.

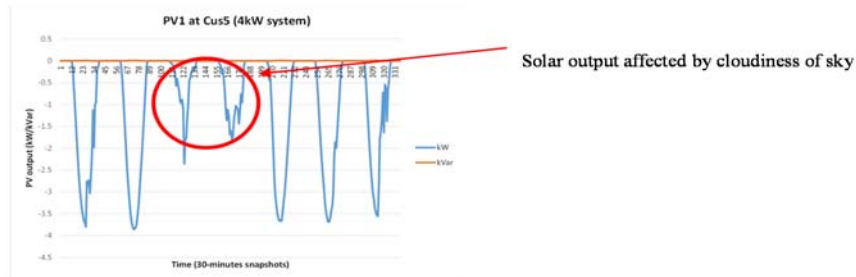


Fig. 5.6 Output of solar generator PV1 between 15 to 21 February 2015

5.5 Modelling of Voltage Control Devices

As a distribution network, JEN takes supply from the transmission substations primarily at 66kV. The voltages at the transmission substations are nominated by the distribution network service provider (in this case, JEN) and maintained by the transmission network service provider. Voltage regulation on the distribution network is achieved via a number of voltage control devices. Table 5.3 summarises the voltage control devices included in the network model. Some of these voltage control devices are currently utilized by JEN while others are being considered for future.

Table 5.3 Voltage Control Devices

Device	Function
On-load tap changer (OLTC) on 66/22kV transformer	Change the voltage on the 22kV side of the transformer by changing the ratio of the 66kV winding. The voltage control settings are implemented in the voltage regulating relay (VRR).
Substation capacitor banks	Adjust 22kV bus voltage by compensating for the reactive component of the customer loads. Arranged in two steps of 4MVar (3-ph) each.
Line capacitor banks	Adjust 22kV line voltage by switching pole-mounted capacitors to compensate for the reactive component of the customer loads flowing through the 22kV distribution line. Single step of 900kVar (3-ph) each.
22/0.433kV distribution transformer	The transformer is fitted with off-load tap changer on the 22kV side. It is generally set on tap 1 (22.55/0.433kV) at time of commissioning.
22/0.415kV smart grid distribution transformer (future)	The transformer is fitted with on-load tap changer on the 22kV side. The transformer specification used in the simulation consists of off-load tap +/- 5% with 5 taps, and on-load tap +/- 5% with 5 taps.
Smart PV inverter (future)	Smart inverters fitted to PV generators to reduce their impact on network voltage while generating and/or to assist network voltage by acting as a DSTATCOM.
Storage battery (future)	Storage battery can assist with voltage changes caused by PV generation, by charging from excess PV generation during the day and discharging during the evening peak load period.

5.6 Modelling Software

The network model is set up in the Open Distribution System Simulator™ (OpenDSS), an open-source electrical system simulation tool for utility distribution systems, made available by the Electric Power Research Institute, Inc. (EPRI) [86]. OpenDSS includes comprehensive library of power delivery elements such as generators, transformers, lines, PV generators, storage batteries as well as control elements such as regulator control and capacitor bank control. Scripting is performed using text files. The flexibility and versatility of OpenDSS is further expanded by the use of an in-process Component Object Model (COM) interface which allows an external program to drive the various OpenDSS

functions, provides external analytical capabilities as well as graphics for displaying results. In this research, MATLAB® is used to drive OpenDSS through the COM interface.

The network model is set up in OpenDSS based on the network characteristics of Table 5.1 and load characteristics of Table 5.2. For line impedances, OpenDSS uses two different methods to represent line impedances: LineCode objects requires input of impedance characteristics while LineGeometry objects uses wire data and positions of the conductors to compute the impedance matrix using modified Carson's equations. A simple example of an OpenDSS program to compute the impedance matrix for a typical 4-wire LV line using 19/3.25AAC conductors is shown in Figure 5.7. The program output is shown in Figure 5.8 and the impedance matrix is reproduced in Table 5.4 for clarity.

```
CLEAR
New circuit.My_4W_circuit
New Wiredata.19/3.25AAC GMR=0.006347 DIAM=0.01630 RAC=0.000196 NormAmps=250.0 Runits=m radunits=m g
New Wiredata.7/3.0AAC GMR=0.003505 DIAM=0.00900 RAC=0.000614 NormAmps=150.0 Runits=m radunits=m gm
New Wiredata.7/064Cu GMR=0.001904 DIAM=0.00489 RAC=0.001308 NormAmps=130.0 Runits=m radunits=m gm

New Linegeometry.4W-19/3.25AAC nconds=4 nphases=3
~ cond=1 Wire=19/3.25AAC x=-0.95 h=8 units=m ! R-phase
~ cond=2 Wire=19/3.25AAC x=0.35 h=8 units=m ! W-phase
~ cond=3 Wire=19/3.25AAC x=0.95 h=8 units=m ! B-phase
~ cond=4 Wire=19/3.25AAC x=-0.35 h=8 units=m ! N-phase

Show lineconstants freq=50 units=km
```

Fig. 5.7. Example OpenSS codes for converting a 4-wre LV line construction into impedance matrix

```
Frequency = 50 Hz, Earth resistivity = 100 ohm-m
Earth Model = Deri

-----
Geometry Code = 4w-19/3.25aac

R MATRIX, ohms per km
0.241234,
0.0486496, 0.241234,
0.0486496, 0.0486497, 0.241234,
0.0486497, 0.0486497, 0.0486496, 0.241234,

jX MATRIX, ohms per km
0.75306,
0.418661, 0.75306,
0.394817, 0.467242, 0.75306,
0.467242, 0.457556, 0.418661, 0.75306,
```

Fig. 5.8. Output of OpenDSS codes for a 4-wire LV line

Table 5.4 Impedance Matrix for 4-wire 19/3.25AAC LV Overhead Line

Phase a	Phase b	Phase c	Neutral	
$0.241234 + j0.75306$	$0.0486496 + j0.418661$	$0.0486496 + j0.394817$	$0.0486497 + j0.467242$	Phase a
$0.0486496 + j0.418661$	$0.241234 + j0.75306$	$0.0486497 + j0.467242$	$0.0486497 + j0.457556$	Phase b
$0.0486496 + j0.394817$	$0.0486497 + j0.467242$	$0.241234 + j0.75306$	$0.0486496 + j0.418661$	Phase c
$0.0486497 + j0.467242$	$0.0486497 + j0.457556$	$0.0486496 + j0.418661$	$0.241234 + j0.75306$	Neutral

The circuit in OpenDSS allows explicit modelling of the ground connections and this feature is used in modelling the MEN LV network.

Figure 5.9 shows the single-line representation of the network model that has been set up in OpenDSS. Monitors have been allocated to various line terminals and buses to record power parameters during simulation studies.

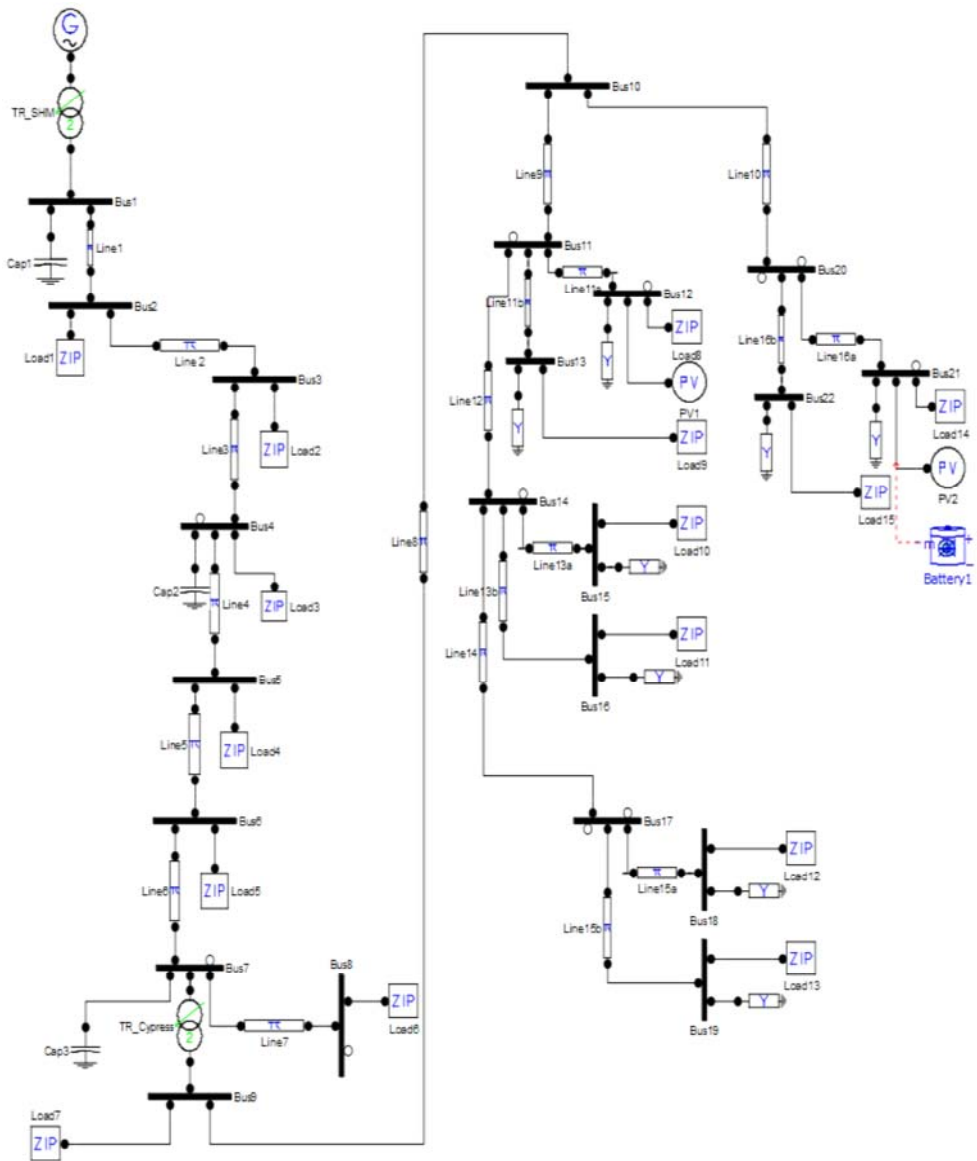


Fig. 5.9. Single-line presentation of network model

5.7 Network Scenarios Modelled

The set of network scenarios (1 to 8) considers the effectiveness of various MV voltage control schemes in regulating the voltage on the 433V side of the Cypress-Stillia distribution transformer (Table 5.5). The voltage control schemes as outlined in Table 5.3 are considered except smart grid distribution transformer, smart PV inverter and storage battery. These MV voltage control schemes are commonly deployed by distribution

utilities and their fine tuning generally represents a low-cost approach to increase the hosting capacity of PV generators by the distribution networks.

The loads served by SHM 66/22kV transformer are primarily residential in nature and so are the loads on SHM14 22kV feeder, as revealed by the SCADA readings (Figure 5.10). It is, however, not unusual for a 66/22kV substation to serve a mixture of residential, commercial and industrial customers. The network scenarios 7 and 8 consider assigning different load types (Figure 5.11) to the remaining loads served by the 66/22kV substation while keeping the SHM14 22kV feeder load as residential. These scenarios explore the balancing act of meeting the needs of different classes of customers.

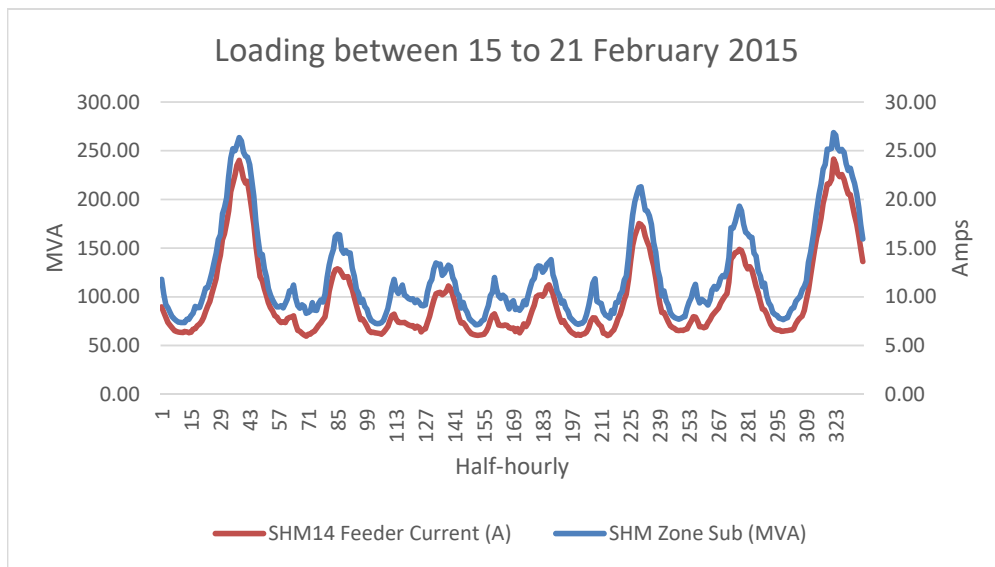


Fig. 5.10. SCADA readings of loads on SHM Zone Substation and SHM14 feeder

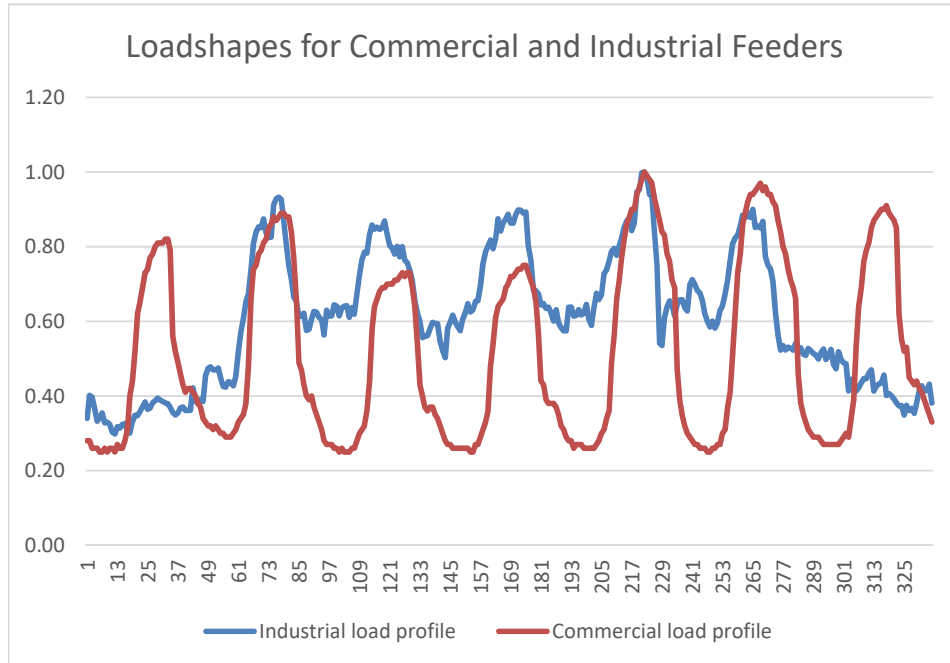


Fig. 5.11. Commercial and industrial loadshapes for the period 15 to 21 Feb 2015

The second set of network scenarios (9 to 11) considers the effectiveness of various new LV voltage control schemes to regulate the voltage on the LV distribution circuit #4. These include smart grid distribution transformer, smart PV inverter and storage battery (Table 5.6), with MV voltage control as per scenario 6. These new smart grid technologies are being investigated in various simulations and field trials around the world. They hold great promise in increasing the capacity of the distribution network to host embedded generators and facilitate other customer innovations such as peer-to-peer energy trading, demand response and electric vehicle charging, but will require significant capital investment.

Table 5.5 Network Scenarios for MV Voltage Control

	Network Scenario	Remarks
(1)	No voltage control, with SHM 66kV voltage kept at 67kV	This forms the base case where the effectiveness of various MV voltage control schemes can be compared.
(2)	VRR control for SHM 66/22kV transformer OLTC – flat voltage control	Flat voltage control is the standard control scheme applied by Jemena Electricity Networks.
(3)	VRR control for SHM 66/22kV transformer OLTC, with Line Drop Compensation (LDC)	LDC set to compensate for voltage drop along the SHM14 22kV distribution line to Cypress-Stillia distribution transformer (Bus7).
(4)	Voltage control by switching of SHM 22kV capacitor bank (Cap1) – 2 steps of 4MVar each	Cap bank control is based on Var setting, with voltage override.
(5)	Voltage control by switching of SHM14 line capacitors (Cap 2 & Cap 3) – 900kVar each	Cap bank control is based on voltage setting.
(6)	All control schemes (2, 4 & 5) in service	Standard operational practice of Jemena Electricity Networks
(7)	Repeat (6) with SHM 22kV bus loads modelled as commercial loads	
(8)	Repeat (6) with SHM 22kV bus loads modelled as industrial loads	

Table 5.6 Network Scenarios for LV Voltage Control

	Network Scenario	Remarks
(9)	Distribution transformer replaced by 22/0.415kV smart grid distribution transformer with OLTC controlled by VRR	This scenario moves the automatic voltage control function closer to LV customers.
(10)	Smart PV inverters fitted to the two PV generators	Two types of smart PV inverter control are simulated: Volt-Var control and Volt-Watt control. For Volt-Var control two options are considered: (a) where the V-V control occurs when the PV inverter is outputting active power, and (b) where the V-V control occurs throughout the day.
(11)	Storage battery applied to the PV installation	A charging profile is applied where the excess PV output is used to charge up the battery, and a discharging profile to support peak evening load.

Three-phase unbalanced load flow simulations are carried out, at 30-minute intervals, over the week from 15 to 22 February 2015. There are 336 load flow solutions per network scenario. Automatic voltage regulation (such as tap change on OLTC transformer) is allowed to take place during the 30-minute time block when the conditions are satisfied. Each load flow solution returns the phase voltages (to earth) and the phase currents at selected network locations. For the 4-wire LV network, the solution also

contains the neutral voltage and neutral current. The solution allows the derivation of the phase-to-neutral voltages and voltage unbalance.

5.8 Summary

The availability of smart meter data has improved the accuracy of network simulation results by providing dataset that closely resemble the network characteristics and the behaviour of customer electricity usage. One area that has not received sufficient attention is the modelling of the LV distribution network comprised of four conductors (three phases and neutral) supplying loads between phases and neutral, with multiple earthed neutrals (MEN) and extensive LV feeder runs. This network design requires the correct line impedances to be applied which are different from the data supplied by manufacturers. The network design also results in voltages appearing on the supply neutrals. This neutral-point shifting affects the voltages seen by customer equipment, and creates voltage unbalance that may affect customer 3-phase equipment. To ensure the validity of the simulation results, it is therefore crucial that the network model is set up correctly in the first place.

There is no lack of choices for network simulation software packages. The simulation software chosen for this project is Open Distribution System Simulator™ (OpenDSS). Apart from being fit-for-purpose, an additional bonus is OpenDSS is an open-source electrical system simulation tool specifically designed with utility distribution systems in mind. On-going improvement to the functions of the tool is achieved via an active on-line community.

Finally, this chapter outlines the scenarios of voltage control that will be simulated and presented in Chapter 6. The voltage control devices include existing deployments as well as new smart grid technologies.

Chapter 6 - Analysis of Simulation Results

This Chapter is based on the following publication:

Peter K.C. Wong, Akhtar Kalam and Robert Barr, “Modelling and Analysis of Practical Options to Improve the Hosting Capacity of Low Voltage Networks for Embedded Photo-Voltaic Generation”, accepted for publication in the IET (Institution of Engineering & Technology) Journal of Renewable Power Generation. Doi: 10.1049/iet-rpg.2016.0770.

6.1 Overview

Computer simulation is an important tool for utility engineers and even more so with the increasing complexity of the power system. With the continued increase of residential roof-top grid connected PV generators, utility engineers are keen to understand the tipping point, if any, of the number of PV installations before significant security, reliability or power quality issues arise. They would also want to know the effectiveness of various operational measures and technologies in mitigating the negative impacts of PV generators. The answers to these questions lie within the realm of computer simulation, as many utilities have not reached the tipping point and it is important to predict the future issues so proactive, rather than reactive, measures are taken now to anticipate for the future. In this regard accurate network models are a pre-requisite for dependable computer simulation results.

In Chapter 5 we presented the case study of a LV distribution circuit and demonstrate how to establish the various components of a network model using SCADA and smart meter data. We put a lot of emphasis on the need to establish a 4-wire unbalance LV network model where loads and generators are connected between phase to neutral and the neutral is earthed at multiple points. In this chapter the simulation results for the various network scenarios are analysed. Section 6.2 presents the simulation results of the voltage on the MV network using existing voltage control schemes. Simulation results of the voltage on the LV network is given in Section 6.3. Voltage unbalance arising from mismatch between loads and generation on each phase and its effect is discussed in Section 6.4. Section 6.5 proposes a new planning approach and the simulation results of

allocating PV generators to the appropriate supply phases to reduce the network voltage unbalance factor which will, in turn, reduce both voltage rise and voltage unbalance caused by the PV generators. Section 6.6 presents the simulation results of a number of smart grid technologies in mitigating the voltage quality impact of PV generators. The chapter is then summarised in Section 6.7.

6.2 Effect of MV Voltage Regulation Control

6.2.1 OLTC Flat Voltage Control

A number of voltage control schemes are used in the MV network. Power factor correction capacitors (Caps 1, 2 & 3) are used to compensate for voltage drop due to reactive component of loads whereas the OLTC of SHM 66/22kV transformer changes the ratio of transformation to keep the 22kV voltage constant at the setting of the Voltage Regulation Relay (VRR). The voltage control settings are shown in Table 6.1.

The simulation results for Scenario 1, 2, 4, 5 & 6 (Table 5.5) for distribution substation Cypress-Stillia is shown in Figure 6.1. As these voltage control schemes affect all three supply phases, for the sake of clarity we have shown only the red-phase voltage on the 433V side of distribution substation (Bus9). It can be seen that while OLTC (dotted yellow line) has the most beneficial effect in regulating voltage to within a narrower range, OLTC and capacitor combination (solid yellow line) results in a much ‘flattened’ voltage profile. From a voltage control perspective, this is the ideal situation as it allows utilities to utilise the full range of allowable voltage in network planning to supply its LV customers. This voltage control combination is adopted by the electricity distribution company Jemena and is used in the simulations unless otherwise stated.

One notices from Figure 6.1 that the LV supply voltage in this network is biased towards the high end of the allowable range, with the voltage hovering around 250V most of the time and approaching the upper regulatory limit of 253V at some instants of time. This reflects the design of the network to cater for peak load condition, a common approach in Australian electricity distribution networks. Figure 6.2 is the voltage at the end of the LV distribution circuit #4 (Bus17) which shows lower voltages during peak usage period (compared with Bus9 at the beginning of the feeder run) but is still appreciably higher than the lower regulatory limit due to the relatively short feeder run. One can also notice that the voltage on the red phase has exceeded the upper limit occasionally. As we shall

see from the analysis conducted in Section 6.3, this is caused by the embedded PV generators.

Table 6.1 Voltage Control Settings

Voltage control devices	Control Settings	Remarks
VRR for OLTC of 66/22kV transformer	Flat Voltage Control – Target 22kV bus voltage at 65.3V, deadband=1.5V, ptratio=200, time delay=90 seconds Line Drop Compensation – Target voltage = 63.5V, deadband=1.5V, ptratio=200, C _T prim=1200 R=1.16 X=1.97, time delay=90 seconds	LDC set to achieve the target voltage at the 22kV side of Cypress-Stillia distribution transformer (Bus7).
Substation capacitor bank Cap1	Var control – ONsetting=5000kVar OFFsetting=-1000kVar Delay=900 seconds DelayOFF=300 seconds Deadtime=300 seconds	Cap1 is arranged in two steps of 4MVar each
Distribution capacitor bank Cap2	Voltage control – PTratio=200 ONsetting=63.5V OFFsetting=67.3V Delay=300 seconds DelayOFF=300 seconds Deadtime=300 seconds	900kVar single step. Between Cap2 and Cap3, Cap2 is given the priority to switch on first and to switch off last
Distribution capacitor bank Cap3	Voltage control – PTratio=200 ONsetting=63.5V OFFsetting=67.3V Delay=400 seconds DelayOFF=200 seconds Deadtime=300 seconds	900kVar single step.

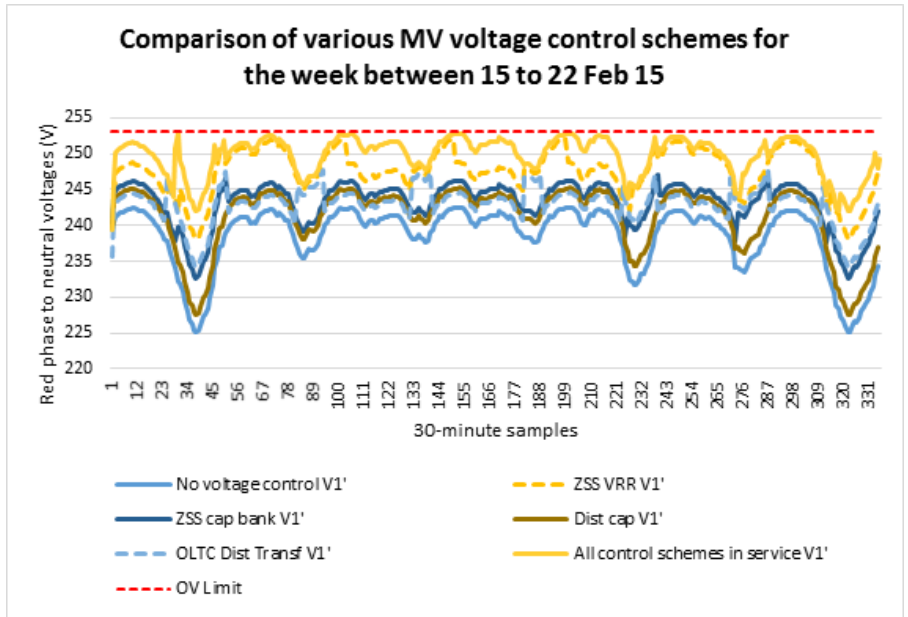


Fig. 6.1. Red phase voltage on 433V side of distribution substation showing the effect of various MV voltage control schemes (Scenarios 1, 2, 4, 5 & 6)

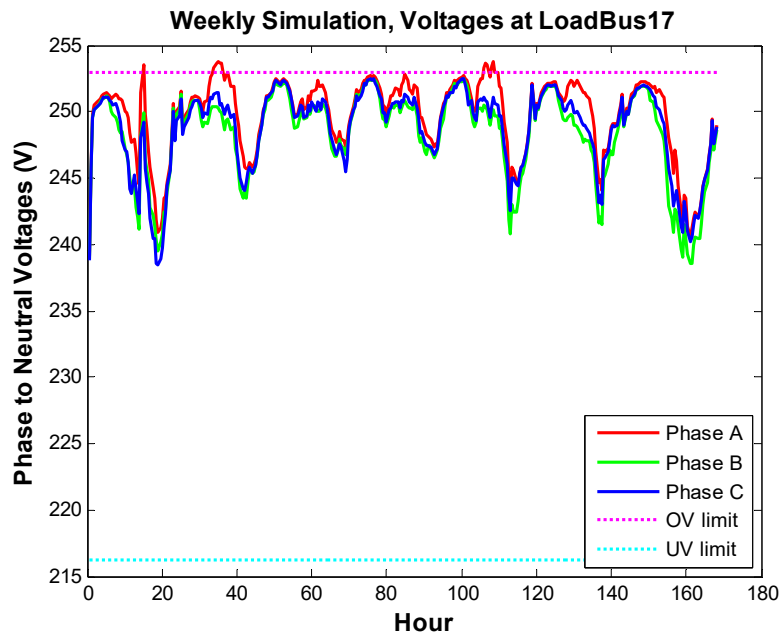


Fig. 6.2. Voltages at the end of LV distribution circuit #4

6.2.2 Line Drop Compensation

As an alternative to setting a high base voltage to cater for peak load condition, Scenario 3 explores the use of Line Drop Compensation (LDC) to provide a dynamic voltage set point for the SHM 66/22kV transformer OLTC control. The voltage set point is increased in proportion to load increase to keep the delivered voltage constant at a network location, generally the load centre of an outgoing MV feeder. In this scenario we have set the LDC to keep the voltage at the 22kV side of Cypress-Stillia distribution substation (Bus7) at the target value. The resultant voltage profile is shown in Figure 6.3. The voltages at the end of LV distribution circuit (Bus17) have also improved, as can be seen in Figure 6.4. LDC has been effective in lowering the supply voltage during light load period while keeping the voltage at a sufficiently high level during peak load period.

A dynamic voltage regulation scheme is conceptually superior to flat voltage control as it has the potential to optimise the voltage delivery in accordance with parameters that affect voltage drops along the distribution circuit. In practice the application of LDC requires careful planning when distribution feeders from the same substation are not homogenous (from load/generation distribution and impedance characteristics perspective). One possible approach is to supplement the LDC with local voltage control strategies such as LV shunt capacitors and voltage regulating distribution transformers, in accordance with the local conditions [50, 55].

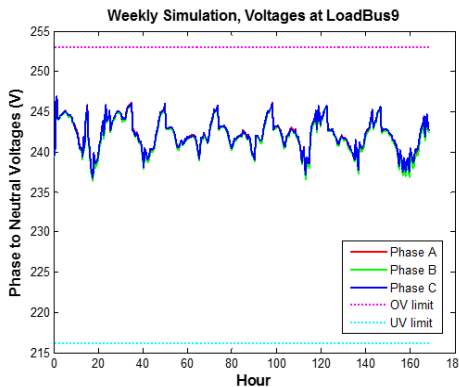


Fig. 6.3. The use of Line Drop Compensation has improved the voltage at the 433V side of the distribution substation (Bus9)

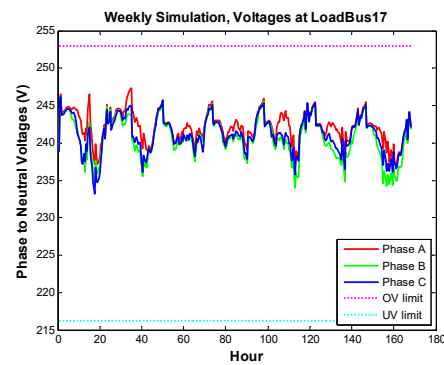


Fig. 6.4. The use of Line Drop Compensation has improved the voltage at the end of LV circuit #4 (Bus17)

6.2.3 Mixed Load Types

It should be noted that the SHM 66/22kV transformer loads and SHM14 22kV feeder loads are residential and have similar weekly cyclic patterns. The voltage control schemes that are mainly influenced by the SHM load characteristic (Cap1 and transformer OLTC) have similar beneficial effect on the voltage profile on SHM14 feeder. This is not the case when SHM load pattern changes to commercial or industrial (Scenarios 7 and 8). Figure 6.5 shows the voltage profiles at the 433V side of distribution substation Cypress-Stillia (Bus9), with all existing MV voltage control schemes in service, and options of residential, commercial or industrial SHM loads. In this particular case, the mismatch load types result in a lower minimum voltage recorded during the 7-day period.

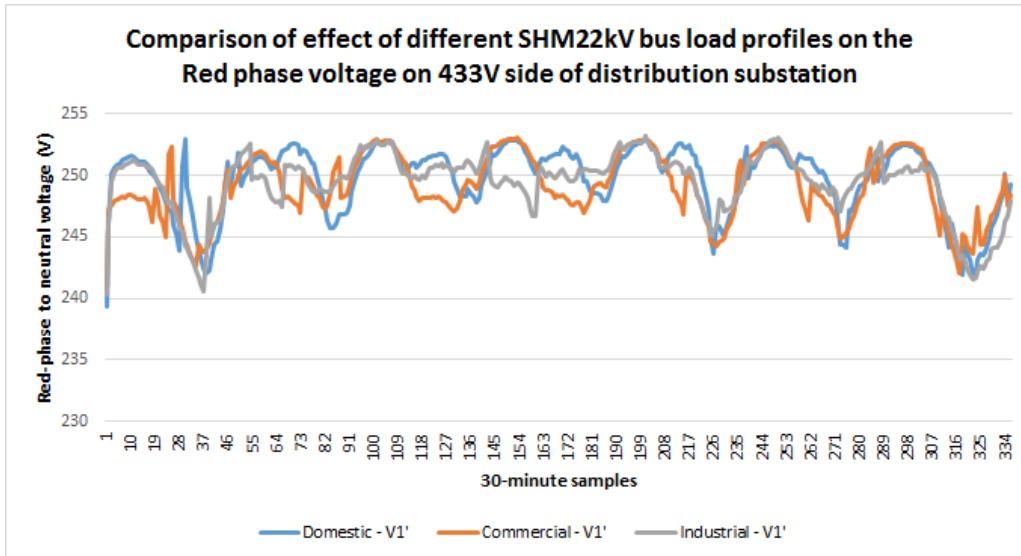


Fig. 6.5. Red phase voltage on 433V side of distribution substation showing the effect of different load profiles on SHM 22kV bus

6.3 Effect of LV Voltage Regulation Control

6.3.1 LV Model to Include Effects of Circuit unbalance, Load Unbalance and Ground Connections

As discussed in Section 5.3, it is important to model the LV distribution network as 4-wire (R, W, B & N) and include the Multiple Earthed Neutral (MEN) ground connections at the customer points of connection. Figure 6.6 provides an example of the load flow result when the network is modelled as 3-wire balanced circuit, which is very different to that in Figure 6.2 for a 4-wire unbalanced circuit.

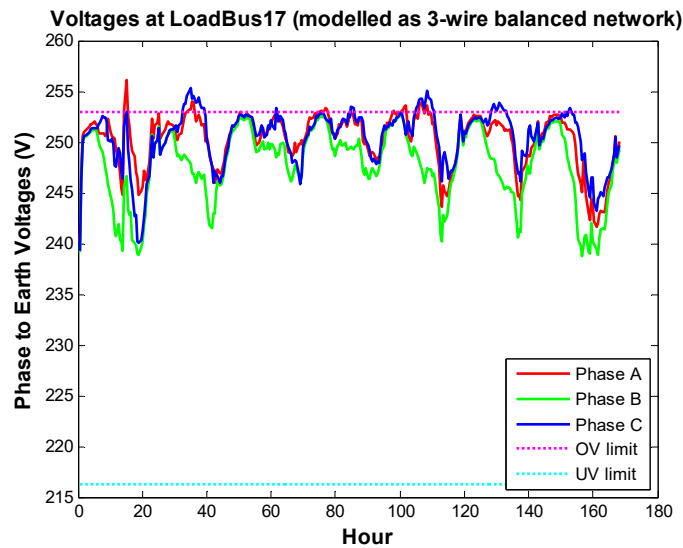


Fig. 6.6. Voltages at the end of LV distribution circuit #4, with MV and LV network modelled as 3-wire balanced network

6.3.2 LV PV Generation Caused Localized Voltage Rise and Voltage Unbalance

Excess generated power from a PV system will travel along the distribution network until it is consumed by load, while raising the voltage along the way. The voltage rise is therefore superimposed upon the network voltage. As the two PV generators in distribution circuit #4 are all connected to the red phase, one would expect the voltage rise effect to be more pronounced on the red phase of sparsely loaded buses. This is clearly seen on Bus17 as shown in Figure 6.7.

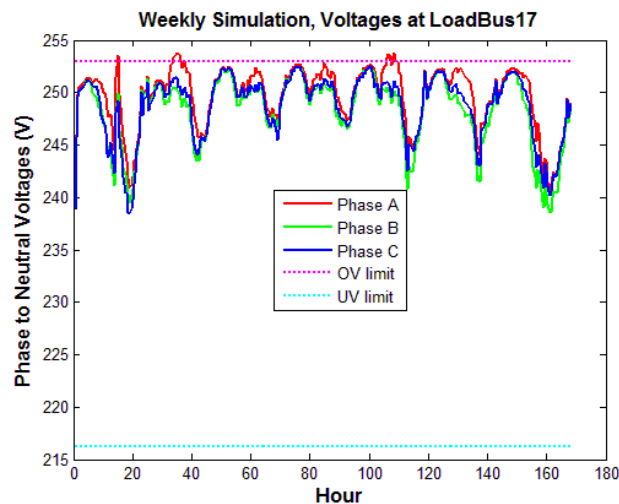


Fig. 6.7. Voltages at the end of LV distribution circuit #4

As the voltage in this distribution network is already on the high side, there are occasions during the week when the localized voltage rises have exceeded the prescribed overvoltage limit (shown dotted in Figure 6.7). When this occurs, PV inverters can trip on over-voltage and customer equipment may malfunction or their life span shortened. The difference between the voltages on the three phases also gives rise to voltage unbalance.

6.4 Phase Voltage Unbalance, Its Effect and Applicable Standards

Unbalance between the three phases in the 4-wire LV network is magnified by the difference between loads and generations in each phase, and unbalanced phase geometry (lack of transposition and 1/2-phase supply spurs). This results in voltage appearing on the neutral connection (zero sequence voltage V_0), and phase voltages that are different

in magnitude and no longer 120 degrees apart. Under these conditions the supply voltages can be resolved into positive (V_1), negative (V_2) and zero sequence (V_0) voltages for the purpose of analysis.

A number of standards exist for defining voltage unbalance using either phase-to-neutral (V_{an}, V_{bn}, V_{cn}) or phase-to-phase voltages (V_{ab}, V_{bc}, V_{ca}) [25, 87]:

- IEEE Standard 936 (1987): Phase voltage unbalance rate ($PVUR$)

$$PVUR = \frac{\text{Maximum } \{V_{an}, V_{bn}, V_{cn}\} - \text{Minimum } \{V_{an}, V_{bn}, V_{cn}\}}{\text{Mean } \{V_{an}, V_{bn}, V_{cn}\}} \times 100\% \quad (6.1)$$

- IEEE Standard 112 (1991): Modified phase voltage unbalance rate ($PVUR_{mod}$)

$$PVUR_{mod} = \frac{\text{Maximum deviation from Mean } \{V_{an}, V_{bn}, V_{cn}\}}{\text{Mean } \{V_{an}, V_{bn}, V_{cn}\}} \times 100\% \quad (6.2)$$

- NEMA (National Electric Manufacturers Associations of the USA) Standard (1993): Line voltage unbalance rate ($LVUR$)

$$LVUR = \frac{\text{Maximum deviation from Mean } \{V_{ab}, V_{bc}, V_{ca}\}}{\text{Mean } \{V_{ab}, V_{bc}, V_{ca}\}} \times 100\% \quad (6.3)$$

- IEEE Standard (1996), IEC Standard 61000-4-27 and Australian Standard TR IEC 61000.3.13: Voltage unbalance true definition (VU_{TD})

$$VU_{TD} = \frac{\text{Negative Sequence Voltage } V_2}{\text{Positive Sequence Voltage } V_1} \times 100\% \quad (6.4)$$

- CIGRE report (1986): Voltage unbalance (VU_{CIGRE})

$$VU_{CIGRE} = \sqrt{\frac{1 - \sqrt{3 - 6\beta}}{1 + \sqrt{3 - 6\beta}}}$$

$$\text{where } \beta = \frac{|V_{ab}|^4 + |V_{bc}|^4 + |V_{ca}|^4}{(|V_{ab}|^2 + |V_{bc}|^2 + |V_{ca}|^2)^2} \quad (6.5)$$

- [87] defines a voltage unbalance factor that specifically takes into account zero sequence voltage that is unavoidable in 4-wire unbalance LV networks with grounded neutral ($VU\%$):

$$VU\% = \frac{\sqrt{|V_2|^2 + |V_0|^2}}{|V_1|} \times 100\% \quad (6.6)$$

where V_1 , V_2 and V_0 are the positive sequence, negative sequence and zero sequence voltages respectively.

For a three-phase, four-wire LV feeder with equally sized phase and neutral conductors, it can be shown that $LVUR$ and VU_{TD} are equivalent, while $VU\%$ is higher than VU_{TD} but lower than $PVUR$ and $PVUR_{mod}$.

Negative sequence voltages affect the performance and life expectancy of customer 3-phase equipment (such as 3-phase motors), and zero sequence currents (caused by zero sequence voltages) affect the rating of network equipment and increase network losses [87, 88]. In addition, the neutral voltage shift caused by zero sequence voltages will further compound the overvoltage and undervoltage problems as it will cause one phase voltage to go higher while the other two phases will go lower [82]. As such both the negative and zero sequence voltages should be controlled in addition to voltage magnitudes.

This thesis uses $VU\%$ defined by Equation 6.6 to calculate voltage unbalance on the 4-wire LV network.

6.5 Optimal Solar Generator Placement to Reduce Voltage Unbalance

Under automatic connection policy, supply utilities do not generally select the phases for the connection of solar generators. For customers on single-phase supply, solar generators are connected to the same supply phase. For customers on a three-phase supply, the solar generators are connected to the phase deemed suitable by the solar installers. The localized voltage rise, however, will be dependent on the phases where the solar generators are connected as well as the distribution of loads among the three phases. Balancing loads and solar generation across all three phases will increase the capacity of the network to accommodate more solar generators without expensive network augmentation or implementation of new smart grid technologies. Customer loads and solar generation, however, are stochastic in nature hence we need a methodology to allocate loads and solar generation.

To tackle the issues of phase voltage rise and unbalance voltages, we propose that loads and generators are allocated to the three supply phases of the LV network based on minimizing voltage unbalance taking into account both negative and zero sequence

voltages, subject to the constraint that voltages on each LV supply node/bus are within the regulated limits.

For a LV network with multiple nodes where voltage unbalance can be calculated, we define a composite index, the network voltage unbalance factor $f(x)$, as the average of the weighted, maximum voltage unbalance, on each supply node/bus over the period of simulation. This can be expressed mathematically as

$$f(x) = \frac{1}{M} \sum_{n=1}^M W_n * (VU\%_{\max})_n \quad (6.7)$$

The aim is to minimize $f(x)$ subject to $216V \leq V_n \leq 253V$, where

$(VU\%_{\max})_n$ = maximum voltage unbalance at the n^{th} mode over the period of simulation

V_n = voltage on the n^{th} mode

M = number of node/bus

W_n = weight coefficient allocated to the n^{th} mode

W_n is normally set to 1 but can be set higher for the node/bus where 3-phase customer equipment, susceptible to voltage unbalance, have been installed.

Equation 6.7 uses the average of the weighted maximum voltage unbalance on each supply node/bus, not the weighted maximum voltage unbalance. This is based on the reasoning that voltage unbalance has an undesirable effect on customer equipment and hence the voltage unbalance on all supply nodes/buses should be taken into consideration in the optimisation effort.

The methodology is applied to the network model where there are two PV generators, PV1 and PV2. Keeping the load allocation constant, the PV generators can each be connected to the red, white or blue phase of the three-phase supply network, resulting in nine combinations. For each combination, load flow calculation is carried out and voltage unbalance determined for each LV bus using Equation 6.6. The network voltage unbalance factor, $f(x)$, can then be calculated using Equation 6.7. Table 6.2 summarizes the result of the network voltage unbalance factor calculated for the nine combinations, with W_i set to 1 for each bus. It can be seen that minimum network voltage unbalance occurs when PV1 is connected to white phase and PV2 to blue phase. The current PV

connection arrangement (both PV1 and PV2 connected to red phase) results in the largest network voltage unbalance factor.

Table 6.2 Network Voltage Unbalance Factor for Different Combinations of Phase Connection of Generators PV1 and PV2

Case number	PV1 connection	PV2 connection	Network voltage unbalance $f(x)$
1	R	R	0.869
2	R	W	0.557
3	R	B	0.617
4	W	R	0.547
5	W	W	0.795
6	W	B	0.436
7	B	R	0.634
8	B	W	0.438
9	B	B	0.719

The variation of the voltage unbalance for the various load buses is shown in Figures 6.8 (a) and 6.9 (a). By allocating the PV generators to minimise voltage unbalance, the voltage profiles are also improved as shown in Figures 6.8 (b) and 6.9 (b). While at present this phase balancing can only be carried out manually, with the advent of power electronics, dynamic switching of customer loads and PV generators among three phases may become economically feasible [25].

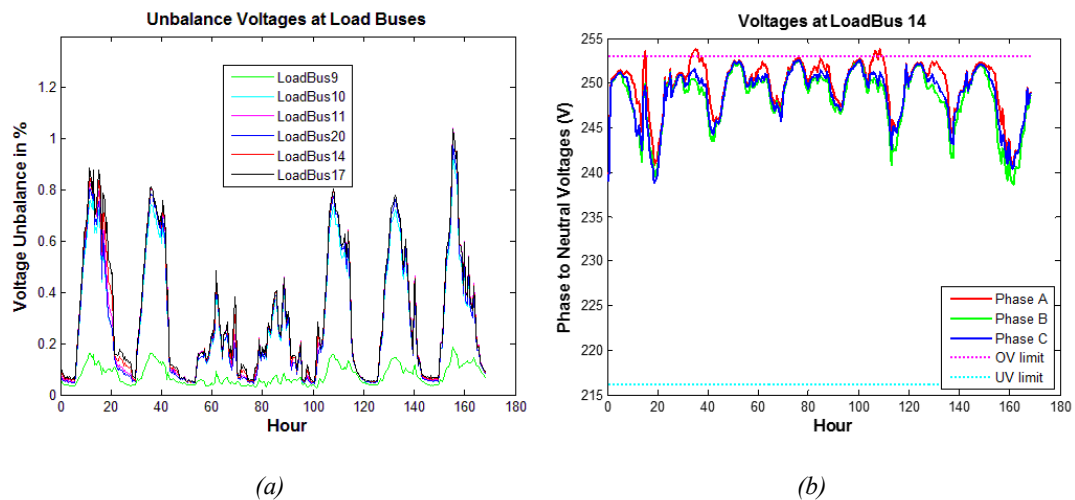


Fig. 6.8. Modelled results with PV1 and PV2 both connected to red phase

(a) shows the voltage unbalance on various load buses while (b) shows the voltages at Bus14. This combination of PV allocations results in the highest voltage unbalance factor and voltages on Bus14 exceed the over voltage limits some of the time during the period of simulation.

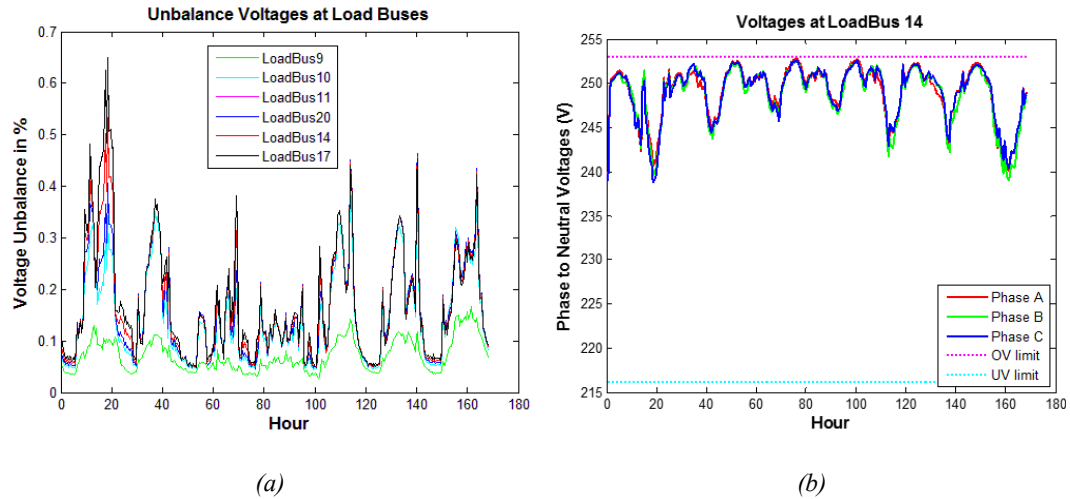


Fig. 6.9. Modelled results with PV1 connected to white phase and PV2 connected to blue phase

(a) shows the voltage unbalance on various load buses while (b) shows the voltages at Bus14. This combination of PV allocations results in the lowest voltage unbalance factor and voltages on Bus14 are within limits during the period of simulation.

6.6 Smart Grid Voltage Control Technologies

6.6.1 Smart Grid Distribution Transformer fitted with On-load Tap Changer (OLTC) and Automatic Voltage Control Scheme

Instead of relying on MV automatic voltage regulation control, this scenario introduces automatic tap changer control in the distribution transformer to regulate the voltage of its downstream LV distribution network. As the degree of load diversity is less at the distribution substation level, it is expected that there could be more frequent tap changes occurring each day. The tap change mechanism of OLTC distribution transformer needs to be specially designed for longevity and to reduce tap changer maintenance requirements. A number of suppliers can now supply these types of smart grid transformers, for example, reference [89].

Innovative voltage control schemes can be applied to these smart grid transformers tailoring to the specific local network characteristics. Successful pilot projects have been run where the conventional voltage control scheme is biased with a signal that takes into account environmental variables such as solar irradiance level and ambient temperature [45], and remote voltage metering [53] in order to cater for localized voltage condition that may not be detected at the distribution transformer end. In the following analysis, a conventional flat voltage control is applied (Scenario 9). Figures 6.10 and 6.11 show the

effect of installing a smart grid distribution transformer (refer Table 5.3 for transformer specifications), with OLTC control, on the voltages of 415V bus (Bus9) and at the end of the LV distribution circuit #4 (Bus17), with conventional MV voltage control schemes. It can be seen the LV voltages are regulated to a tighter band around 244V (voltage bias setting) which cannot be achieved by MV voltage control schemes alone. This is achieved, however, at the expense of more frequent transformer tap changes as can be observed from the more frequent voltage step changes. As the distribution transformer tap change operates on all three phases, there is no observable improvement to the voltage unbalance although phase voltage magnitudes have improved.

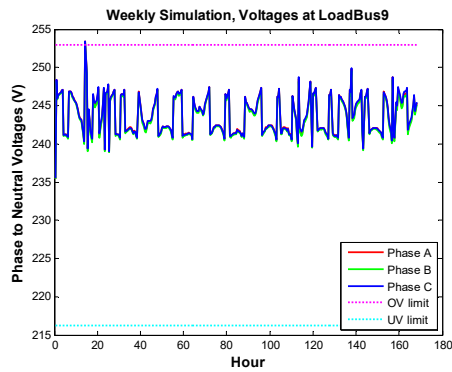


Fig. 6.10. Voltages at 415V bus (Bus9) with OLTC distribution transformer

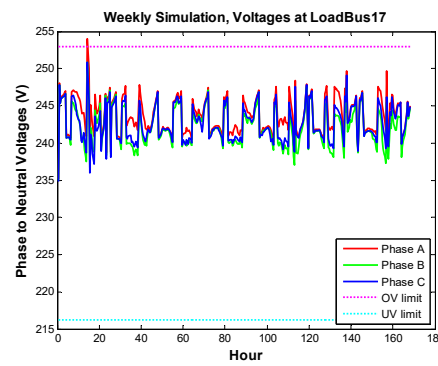


Fig. 6.11. Voltages at end of distribution circuit #4 (Bus17) with OLTC distribution transformer

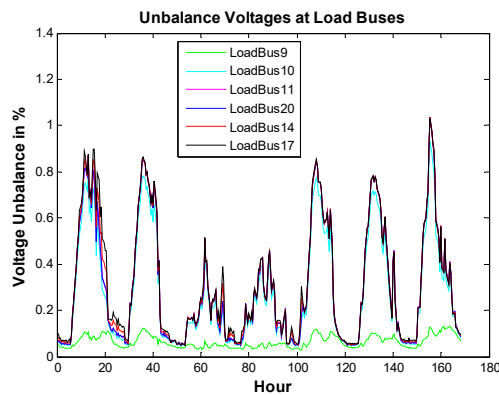


Fig. 6.12. Voltage unbalance on various load buses with OLTC distribution transformer

6.6.2 Smart PV Inverters

Up to now we have considered voltage control technologies that affect all three phases of the supply network and cannot directly mitigate the effect of PV generators that are connected to one phase. Smart PV inverters are now commercially available which act to limit the effect of PV generators on the phase(s) of the network they connect to. In some designs the smart inverter can even assist with optimizing voltage delivery by acting in a manner similar to a Distribution Static Compensator (DSTATCOM).

A number of smart inverter control algorithms are commercially available: Volt-Watt (V-W), Volt-Var (V-V) and fixed power factor (PF) [48]. In PF control, the fixed power factor is generally set to a value such that the PV system appears slightly inductive to the grid. As the PV generates active power, the inverter acts to absorb reactive power from the grid in proportion to the active power output. In V-W control, the active power output of the inverter will be curtailed when the voltage is high. In V-V control, the smart inverter is set to absorb reactive power (Var) when the voltage is high, and generate reactive power when the voltage is low. A special use of V-V control is to absorb/generate reactive power to assist with voltage delivery even when the inverter is not outputting active power e.g. after the sun sets. [45] shows that dynamic power control methods such as V-W and V-V provide superior results compared with static reactive power control methods such as PF. The simulations are therefore performed with V-W and V-V control. In the absence of internationally accepted standard for the inverter control characteristics, the characteristics used in the simulation are chosen to demonstrate beneficial effect on voltage outcome.

6.6.2.1 Inverter Volt-Watt Control

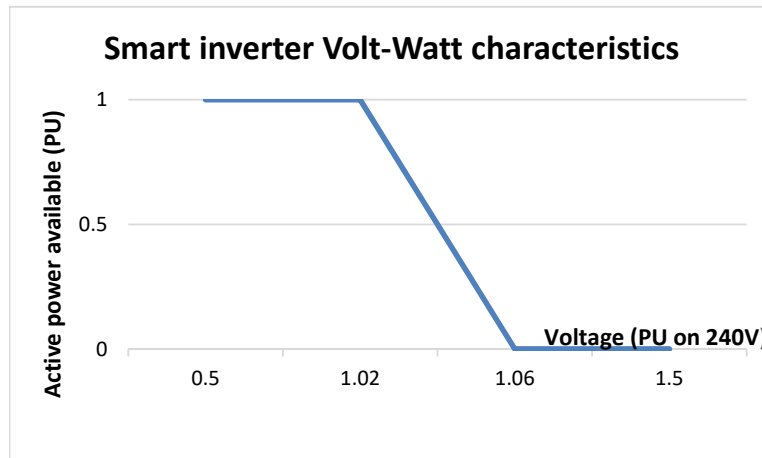


Fig. 6.13. Volt-Watt characteristics of smart inverter used in the simulation

Figure 6.13 shows the smart inverter Volt-Watt (V-W) characteristics used in the simulations. The Y-axis is the percentage of actual real power (Watt) output while the X-axis is the terminal voltage of the inverter (as percentage of reference voltage of 240V). By setting the real power output at one per unit for terminal voltage between 0.5 to 1.02 per unit, the inverter is allowed to output 100% of its generated power for terminal voltage up to 244.8V. After that, the real power output will be curtailed in a linear fashion (for example, only 50% of the PV generation is allowed to be outputted at 249.6V) until it is not allowed to generate at 254.4V.

There are a number of applications for inverter V-W control:

- Under circumstances where high PV output and low load is causing the network voltage to rise too high at certain times. The V-W functionality might be utilised to reduce active power output levels on a PV system by PV system basis;
- Under circumstances where localised service voltage may rise too high because a large number of customers have PV installed. This may result in certain PV inverters that do not turn on at all. Reducing active power output by PV systems via a V-W function may allow more of the PV to share in the capacity of the local distribution network.

The effect of V-W control on the two PV generators connected to the red phase can be seen in Figure 6.14. The occurrences of red phase voltage rise above regulatory limit have been corrected with the V-W control. As seen in Figure 6.15, voltage unbalance has also been improved.

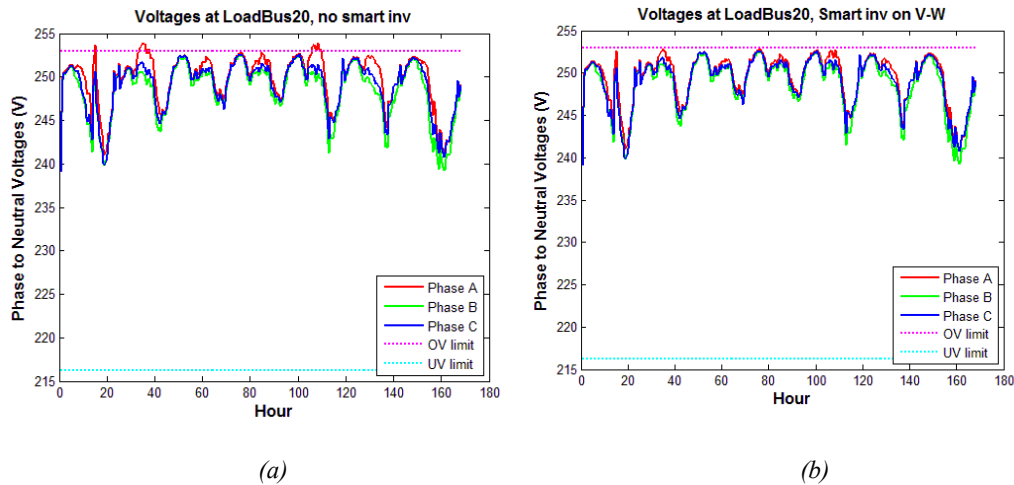


Fig. 6.14. Effect of Smart Inverter Volt-Watt control on phase voltages

- (a) No smart inverter control
- (b) PV1 and PV2 are fitted with smart inverters with Volt-Watt control as per Fig.6.13

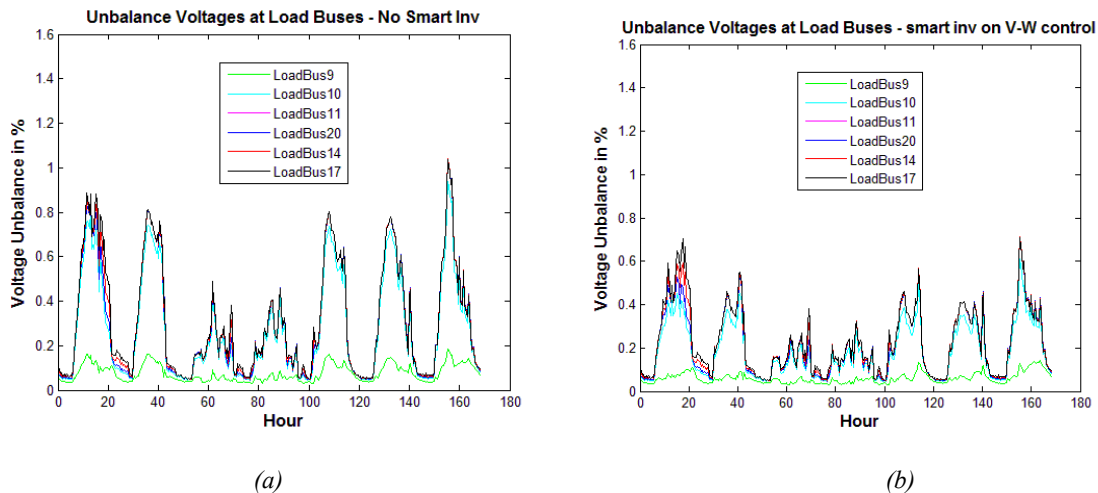


Fig. 6.15. Effect of Smart Inverter Volt-Watt control on voltage unbalance

- (a) No smart inverter control
- (b) PV1 and PV2 are fitted with smart inverters with Volt-Watt control as per Fig.6.13 characteristics

6.6.2.2 Inverter Volt-Var Control

With Volt-Var (V-V) control, reactive power is generated or absorbed depending on the terminal voltage of the inverter. The amount of reactive power output is a percentage of

available Vars given the present active power output and the full-scale apparent power rating of the inverter. In other words, active power output has been given priority and reactive support is only provided when there is excess capacity available in the inverter. This approach allows the PV customers to get the financial return on their PV investment, and only bear the cost of additional losses in the inverter when it is used to provide reactive power support. Mathematically, the available reactive power is calculated as

$$kVar_{available} = \sqrt{(kVA_{rating})^2 - (kW_{present})^2} \quad (6.8)$$

Figure 6.16 shows the smart inverter V-V characteristics used in the simulations. The Y-axis is the percentage of available reactive power (Var) output while the X-axis is the terminal voltage of the inverter (as percentage of reference voltage of 240V). Positive reactive power indicates reactive power is injected by the inverter into the network to support the voltage, while negative reactive power indicates that reactive power is being absorbed by the inverter from the network in order to reduce the voltage. For terminal voltage between 0.94 to 1.02 per unit (225.6V to 244.8V), the inverter is neither supplying or absorbing reactive power. For voltages below 0.94 per unit, the inverter will be supplying reactive power in a linear fashion until 100% of available reactive power is supplied for voltages at or below 0.9 per unit (216V). For voltages above 1.02 per unit, the inverter will be absorbing reactive power in a linear fashion until 100% of available reactive power is absorbed for voltages at or above 1.1 per unit (264V).

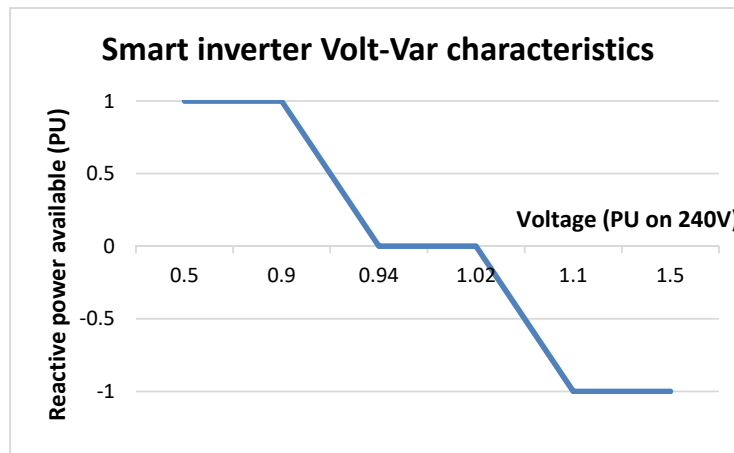


Fig. 6.16. Volt-Var characteristics of smart inverter used in the simulation

The effect of V-V control on the two PV generators connected to the red phase can be seen in Figure 6.17. Due to the use of available reactive power, V-V control has only been effective in reducing red phase voltage rise on days where there is relatively low active power output due to cloud coverage (Days 3 & 4). In Figure 6.18 PV2 inverter rating has been increased two-fold to 10kVA with the PV panel rating kept at 5kW. Reactive power support is therefore available for all the seven days resulting in consistent reduction of voltage rise in red phase. The occurrences of red phase voltage rise above regulatory limit have been satisfactorily corrected with V-V control coupled with the change to a larger size inverter. Close examination of Figure 6.18, however, reveals changes have occurred in the other two phase voltages, in particular, blue phase voltage has increased and is approaching the regulatory limit. The higher reactive power injection from PV2 on the red phase has led to increase in phase current unbalance and a corresponding neutral voltage shift that affects the voltages on the other two phases. As seen in Figure 6.19, voltage unbalance has actually deteriorated with the adoption of a larger PV inverter.

It should be noted that Volt-Var control is generally more effective when used on LV overhead distribution network where X/R ratio is higher, than when used on LV underground network [45].

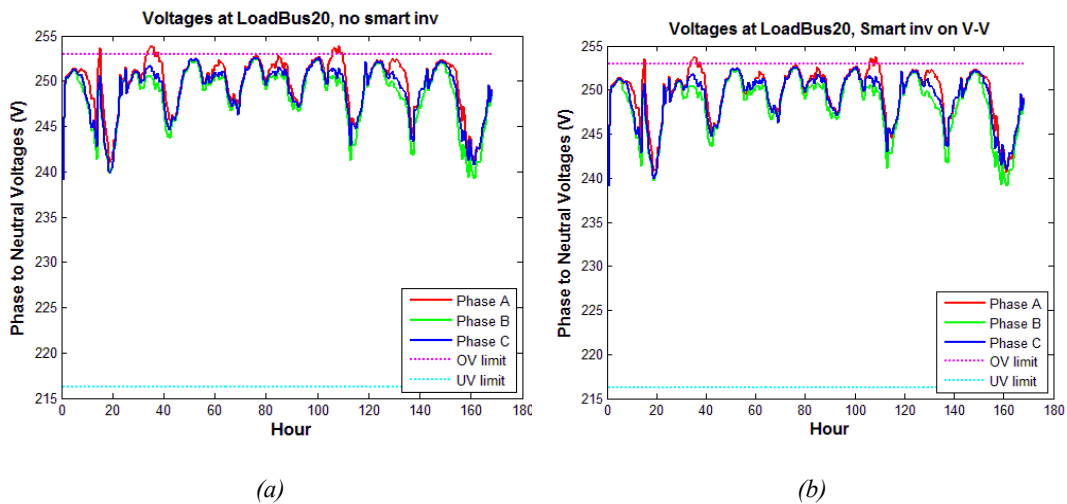


Fig. 6.17. Effect of Smart Inverter Volt-Var control on phase voltages

- (a) No smart inverter control
- (b) PV1 and PV2 are fitted with smart inverters with Volt-Var control as per Fig.6.16 characteristics

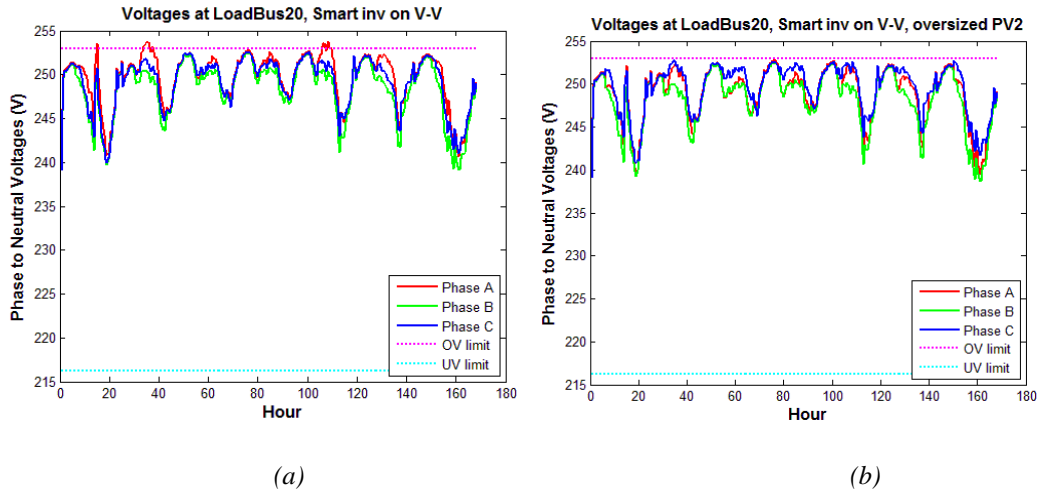


Fig. 6.18. Effect of larger inverter rating on Smart Inverter Volt-Var control

- (a) Both PV1 and PV2 are fitted with smart inverters with Volt-Var control as per Fig.6.16 characteristics. In addition, PV2 inverter has been doubled in kVA rating
- (b) Both PV1 and PV2 are fitted with smart inverters with Volt-Var control as per Fig.6.16 characteristics. In addition, PV2 inverter has been doubled in kVA rating

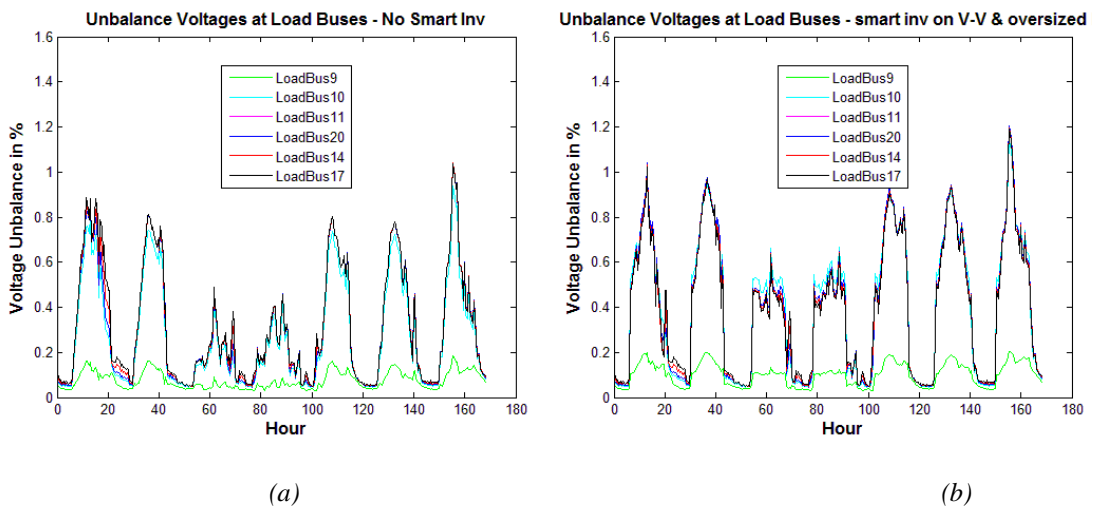


Fig. 6.19. Effect of larger inverter rating on voltage unbalance

- (a) Both PV1 and PV2 are fitted with smart inverters with Volt-Var control as per Fig.6.16 characteristics
- (b) Both PV1 and PV2 are fitted with smart inverters with Volt-Var control as per Fig.6.16 characteristics. In addition, PV2 inverter has been doubled in kVA rating

6.6.3 Connect Battery Storage to PV Generator

The effect of localized voltage rise caused by excess PV generation could be overcome if the excess generation is used to charge up a local battery. The stored energy can then be used to reduce the evening peak demand. This option has become economically feasible due to the reduction in battery cost and the continual rise in price of electricity in many parts of the world. Similar rationales have been applied to other forms of controllable loads such as water heating and space heating to absorb excess PV generation [52].

6.6.3.1 *Battery storage control algorithms*

The ideal charging strategy of a storage battery is to direct all surplus generated power (solar generation minus local consumption) to the battery. The stored energy is then discharged at the appropriate times (generally during peak times) in line with the cost of electricity stipulated in the tariff. Battery controllers to achieve this ideal characteristics will be, by necessity, rather complex due to the need to monitor the PV generation and to provide accurate short-term forecast of load consumption, all in near real-time. Research into the ideal battery control algorithms is outside the scope of this thesis.

In order to illustrate the concept of using battery storage to manage voltage rise, we have modelled a 4.4kW/25kWh battery installed by Customer 7 who has a 5kW PV generator (PV2). The rather odd figure of 4.4kW is arrived at based on a 4kW battery with a 90% energy conversion efficiency. We have adopted a charge/discharge characteristics (Figure 6.20) where charging occurs at a rate determined by the loadshape of the solar irradiance (hence tracking closely with the loadshape of PV generation), followed by discharging at a rate of the customer load usage from 6pm onwards.

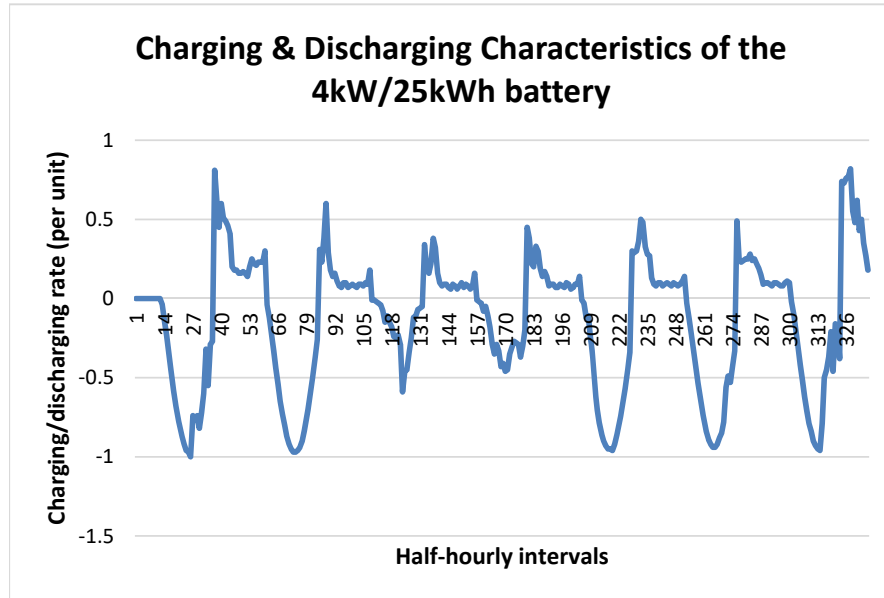


Fig. 6.20. Charging & discharging characteristics of the 4.4kW/25kWh battery.
Negative values indicate charging while positive values indicate discharging

6.6.3.2 Status of Battery Energy Content during the Simulation

The status of battery charging and energy content (kWh) during the simulation is shown in Figure 6.21. From the figure the following observations can be made:

- Day 1: The battery has an initial energy of 5kWh (20%) and starts to charge when solar irradiance is non-zero at 6am. It reaches its fully capacity of 25kWh at 2:30pm. It then idles for a while until discharging occurs at 6pm. Discharging continues until charging kicks in at 6am on Day 2, when the battery has nearly discharged back to its initial energy content of 5kWh.
- Day 2: Similar to Day 1, the battery charges to its full capacity, idles then discharges at 6pm. The customer load on Day 2, however, is lower so the battery does not discharge quite as much as Day 1.
- Day 3: Solar irradiance level is low on Day 3 due to cloud coverage. The battery does not charge to its full capacity before discharging occurs at 6pm. The customer load, however, is even lower so the battery retains significant amount of energy (15kWh or 60%) by the time when charging occurs on Day 4.
- Day 4: Solar irradiance is again down on Day 4 due to cloud coverage. With high residual storage in the battery from previous day, the battery still reaches full capacity

by the time when discharging occurs at 6pm. The load is low so the battery retains significant amount of storage (~15kWh) when charging occurs on Day 5.

- Day 5: Solar irradiance is back to the normal high level. The battery is no longer able to absorb most of the PV output due to the initial energy content. We start to see the lengthening of the idle period where the battery is fully charged.
- Day 6 and Day 7: similar to Day 5.

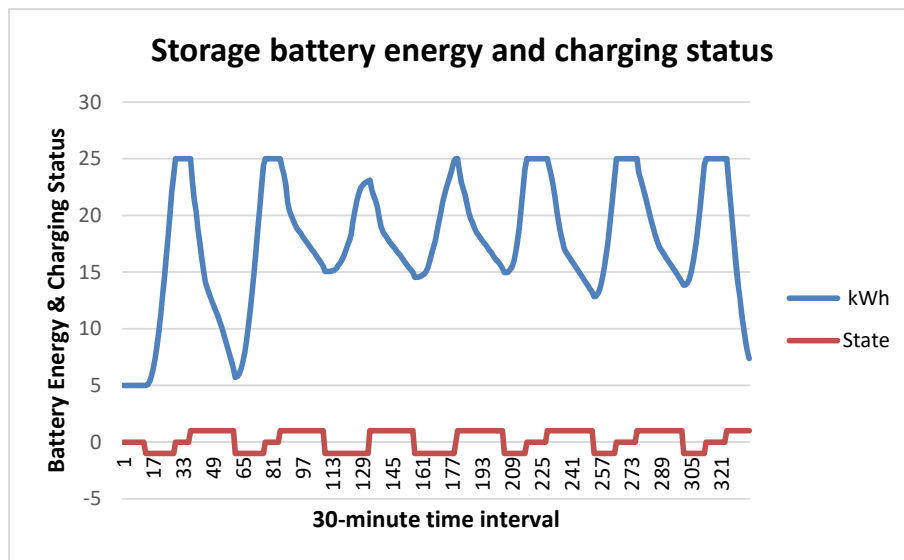


Fig. 6.21. Battery energy and charging status during the simulation.

Note State = -1 when charging, =0 when idle, =+1 when discharging

6.6.3.3 Effect of Battery on Voltage Rise

The effect of the battery storage on the voltage profile of Bus20 can be seen by comparing Figure 6.22 and Figure 6.23. Red phase overvoltage caused by PV2 generating has been reduced while the red phase voltage during peak load has improved. The voltages are now within regulatory limit except on Day 5 where there are still excursions over the limit. This is due to the battery reaching its full capacity and no longer able to absorb excess PV generation as described in 6.6.3.2. Voltage unbalance improves during the period when the battery is absorbing PV generation but deteriorates when the battery discharges. Overall there is a small improvement in voltage unbalance factor (Figure 6.24).

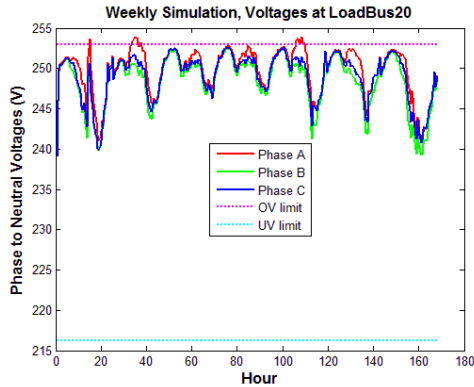


Fig. 6.22. Voltages at Bus20 without storage battery

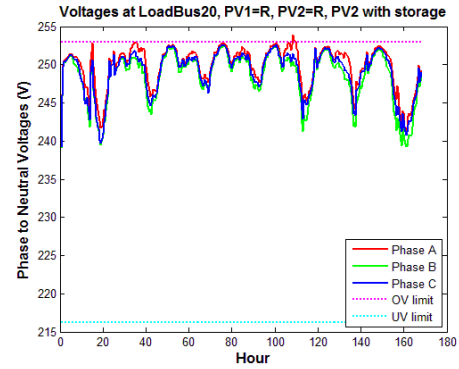


Fig. 6.23. Voltages at Bus20 with storage battery

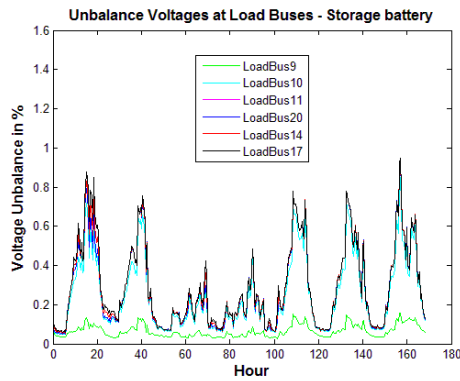


Fig. 6.24. Voltage unbalance on the load buses with storage battery

6.7 Future Scenario of Higher PV Penetration

The distribution circuit has eight customers and two PV installations representing a PV penetration of 25%. Simulation studies show that the approach of optimal PV placement to the supply phases has been effective in ensuring the supply voltages are within the regulatory limits on all the load buses. Now consider the additional installation of two PV generators of 4kW each (PV3 and PV4) bringing the PV penetration to 50% of customers. One of the worst case scenarios is the new PV generators are installed by the two single-phase customers (Customer 2 and Customer 6) as there are no choices in the phase connection. The voltage profile on the loadbuses is now over the voltage limit with the PV phase connection that is deemed to be optimal for the 2-PV case (Figure 6.25). The optimal generator placement study as detailed in Section 6.5 is repeated for the two existing PV generators (PV1 and PV2). The simulation study indicates that the

combination of PV1 connected to W-phase and PV2 to R-phase will result in the lowest network voltage unbalance factor $f(x)$ in this 4-PV situation. The result of phase allocation study is summarised in Table 6.3, and the voltage profile for the six loadbuses is shown in Figure 6.26. The voltage profile is found to be within regulatory limits with the optimal phase allocation methodology.

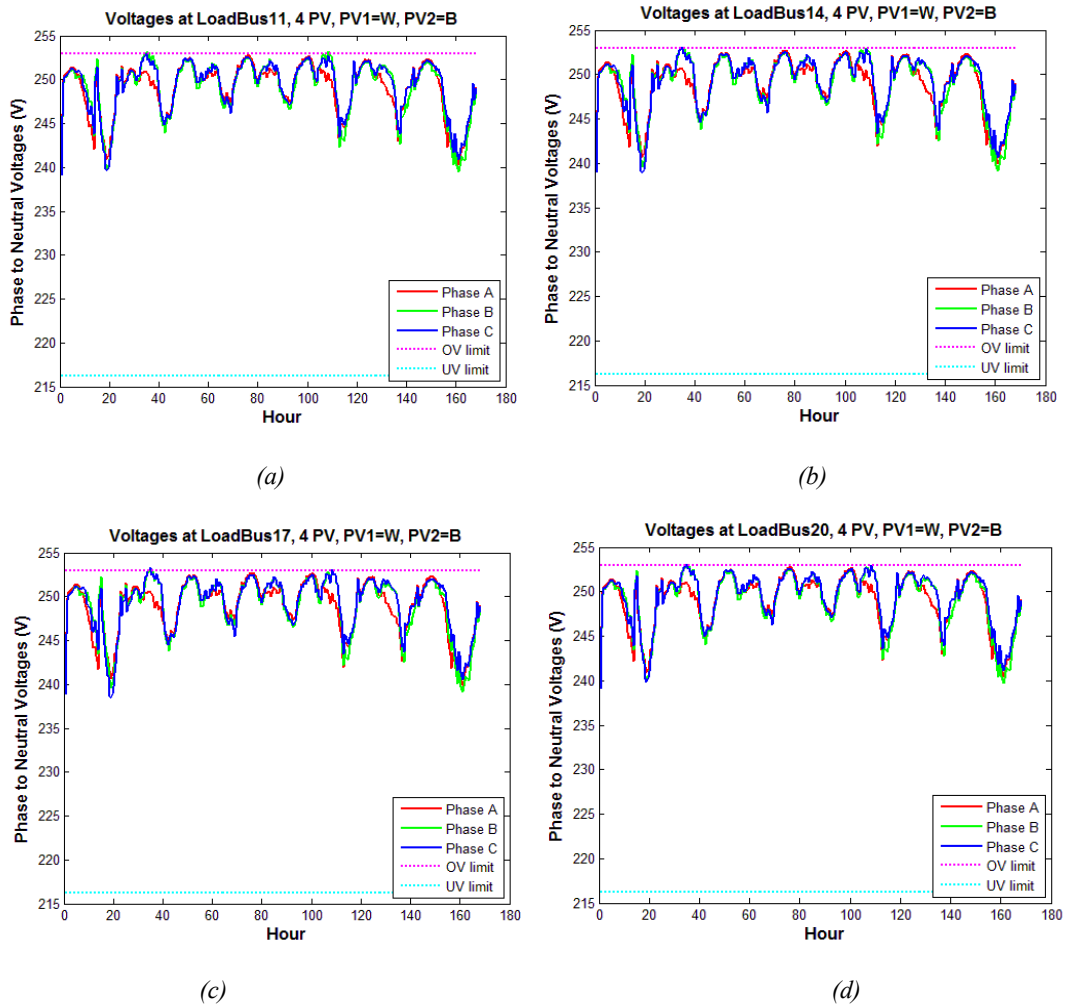


Fig. 6.25. Voltages at the various load buses with four PV

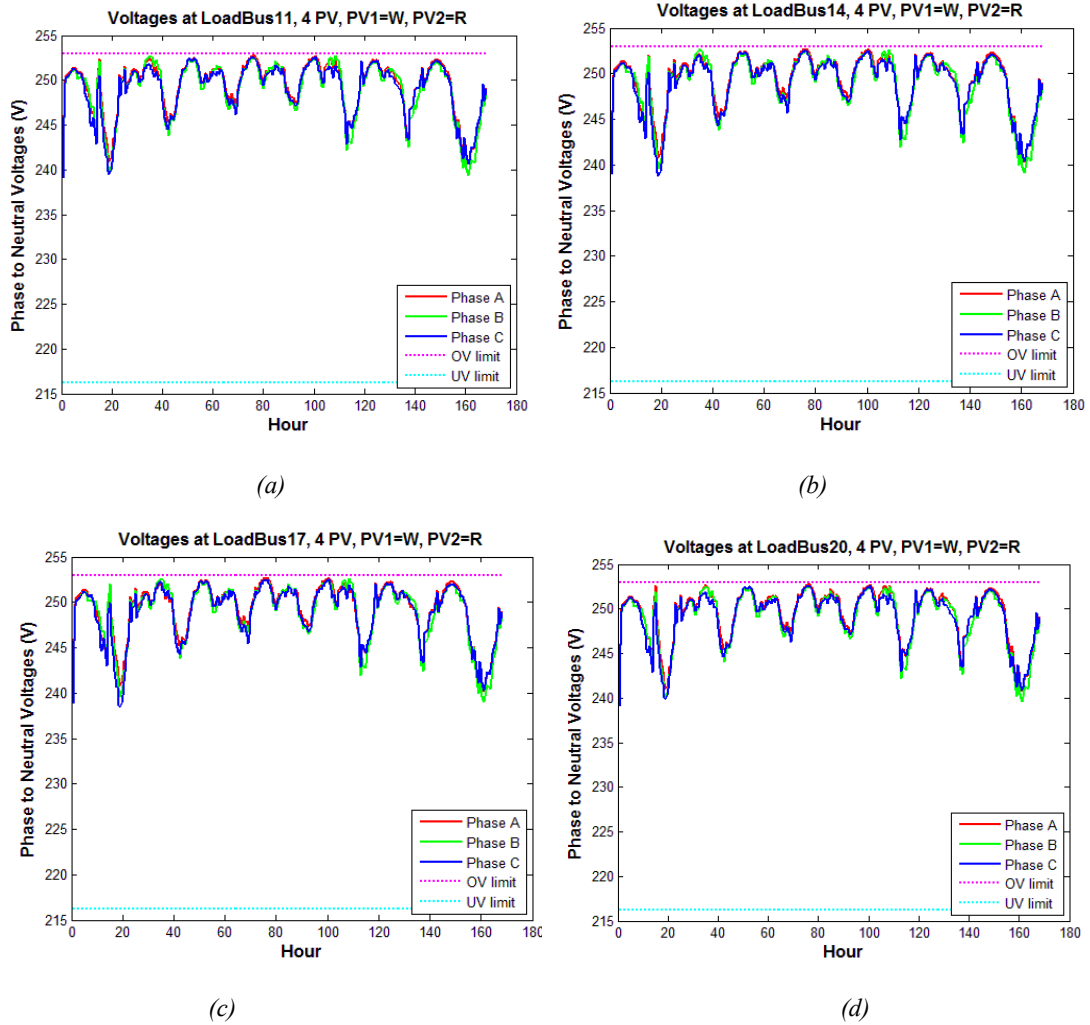


Fig. 6.26. Voltages at the various load buses with four PV and after phase optimisation

Table 6.3 Network Voltage Unbalance Factor for Different Combinations of Phase Connection of Generators PV1 and PV2, with PV3 and PV4 connected to Customer 6 (W-phase) and Customer 2 (B-phase)

Case number	PV1 connection	PV2 connection	Network voltage unbalance $f(x)$
1	R	R	0.616
2	R	W	0.510
3	R	B	0.535
4	W	R	0.469
5	W	W	0.891
6	W	B	0.647
7	B	R	0.520
8	B	W	0.636
9	B	B	0.877

Lowering the nominal supply voltage will also be effective in reducing the risk of localised voltage rise above the overvoltage limit. Figure 6.27 shows that the use of LDC in this 4-PV case brings the voltage profile within regulatory limit without the need to re-connect PV1 and PV2 to different phases. The voltage unbalance, however, is increased.

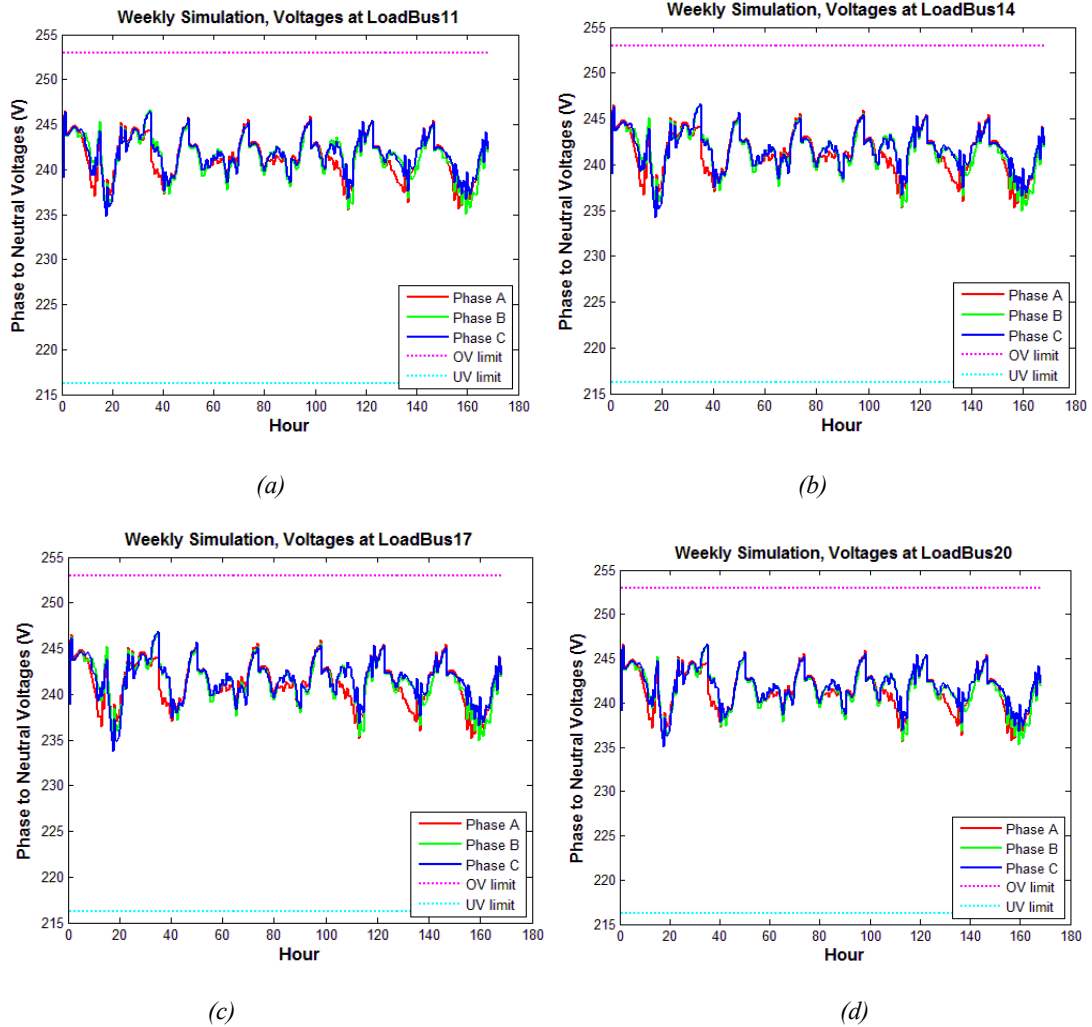


Fig. 6.27. Voltages at the various load buses with four PV and after phase optimisation and application of LDC

6.8 Summary

The establishment of an accurate LV network model provides a good foundation for carrying out computer simulation studies of voltage rise caused by embedded PV generators. As residential roof-top PV generators are generally single-phase, the voltage rise caused by the generators affect the three phases differently. Voltage unbalance also arises and can affect customer three-phase equipment. These effects are most pronounced on sparsely loaded lines farthest away from the supply source (i.e. the distribution transformer).

Automatic voltage regulation control schemes applied at MV network are traditionally biased to deliver a supply voltage that is at the high end of the allowable voltage range, to cater for large voltage drop at peak load conditions. The voltage bias leaves little headroom for the local voltage rise caused by excess PV generation. The simulation results indicate that dynamic voltage control schemes should be considered for MV voltage regulation to lower the supply voltage under light load conditions. Improvement to MV voltage regulation control will improve the hosting capacity of the LV network for embedded PV generators. It is, however, ineffective in addressing the phase discrepancy caused by the mismatch of PV generation and load on the three supply phases.

To address the effect of PV generation on different phases of the supply network, an operational approach can be taken to identify the optimal phase connection of the PV generators that will result in the lowest voltage unbalance. The thesis proposes an allocation methodology based on minimising the network voltage unbalance factor, and demonstrate the beneficial effect of such an approach in the simulation results.

Investing in smart grid technologies will further increase the hosting capacity of the LV network for embedded PV generators. The thesis has studied and demonstrated the beneficial effects of on-load tap changing distribution transformer, smart inverters with Volt-Watt and Volt-Var control, and battery storage. Careful planning in the selection of control characteristics and battery size, however, is required so these smart grid technologies can deliver the benefits as modelled.

Chapter 7 - Conclusions and Future Research

7.1 Overview

This chapter draws an overarching commentary of the dissertation including the research undertaken and the subsequent findings. Section 7.2 provides an overall conclusion and outlines the main findings of this thesis. Section 7.3 closes the thesis with recommendations for future research directions.

7.2 Conclusions

The aim of this thesis is to identify practical, cost effective measures that can be taken by supply utilities to accommodate the increasing penetration of grid connected, residential roof-top photo-voltaic generation systems. It achieves its purpose by firstly examining the present status of voltage quality delivered to LV customers and identifying the effect of PV on voltage quality. The work is then followed by establishing accurate PV generator and LV network models. Computer simulation studies are then performed on network model based on data of a realistic LV network. Various scenarios are simulated using existing voltage control schemes, new proposed planning approach and smart grid technologies, and their effect on voltage quality examined. The research is enabled by the availability of voltage quality data from smart meters that have been rolled out to all residential customers.

The main results and research contributions of this thesis can be summarised as follows:

1. Gaining a deeper insight of voltage quality delivered to end customers:
 - By performing exploratory analysis of overvoltage and undervoltage event data measured by approximately 100,000 smart meters over a 6-day period, a picture emerges that a significant number of customers have either experienced overvoltage (>12%) or undervoltage (>6%) during the period. Undervoltage events are found to be temperature dependent and occur only occasionally during hot days (>30°C maximum ambient temperature). Overvoltage events, however, are common occurrences. This result highlights the inadequacy of the existing voltage control schemes.

- By providing an electrical connectivity overlay to the overvoltage and undervoltage sites, upstream distribution substations and zone substations can be identified and targeted for more detailed voltage quality investigation.
 - The exploratory data analysis also finds that higher percentage of customer sites, with roof-top PV installations, have overvoltage events starting between 8am to 2pm than non-PV sites. On a macro level this indicates that PV generation has most likely contributed to the occurrence of overvoltage events.
 - Usefulness of the current smart meter voltage quality data can be improved by the provision of time series data of voltage, current and power factor. Resolution of the time series data would be limited by the available bandwidth of the 2-way meter communication system but 5-minute data appears to be adequate for most applications.
2. Developing a practical roof-top PV generator model that can be used in computer simulation studies by distribution utilities:
- PV generator output varies within the day, between seasons, is affected by environmental variables of ambient temperature and clearness of sky, and the orientation of the PV panel. Taking the nameplate rating as a PV generator output is not a correct representation in computer simulations.
 - Accurate silicon based PV generator models can be developed using a component approach, starting with Stockley's diode equations for the p-n junction building up to a model for individual PV cell output, followed by models for the dc/ac inverter, and solar irradiance modelling. The data required for these models are extensive and difficult to acquire for small roof-top PV generators that are generally subjected to a streamline connection process.
 - By treating the PV as a generation system, a simplified mathematical model linking time-varying inputs (ambient temperature, global solar irradiance) to electrical output has been established. Practicality of the model is further guaranteed through the analysis that demonstrates the use of global solar irradiance recorded at a nearby weather station as proxy for the irradiance measured at the PV panel. The accuracy of the simplified model was verified using smart meter data.

- The PV generator model can be used in a number of applications, including its use in computer simulations to study the effect PV generator on voltage quality.
3. Developing a network model for a 4-wire unbalanced LV distribution circuit
- A traditional lack of priority and focus means distribution utilities do not have the data required to set up an accurate LV network model. This has severely limited the capability of distribution utilities to adapt to the evolving needs of customers. In the case of roof-top PV penetration, the lack of modelling capability means most utilities do not have a clear understanding of the impact of these PV generators. They are likely to adopt a conservative approach which will unnecessarily limit the penetration of these customer installations.
 - The network sensing functions incorporated in modern smart meters have enabled distribution utilities to establish LV network parameters such as customer phase connection, supply impedance and to detect network abnormalities through big data analytics.
 - Due to the unbalanced nature of the LV 4-wire distribution network caused by the lack of phase transposition, phase-to-neutral load/generator connections and current flows in the neutral conductor and earth, we cannot apply directly the simple line/cable impedance data supplied by manufacturers. The thesis adopts the approach to calculate line impedances using the Carson's equations. Carson assumes the earth is an infinite, uniform solid with a flat uniform upper surface and a constant resistivity. The equations of self and mutual impedances made use of conductor images; that is, every conductor at a given distance above ground has an image conductor the same distance below ground. Carson's equations therefore require details about the physical construction of the distribution circuit (phase conductor spacing, distance of conductors above ground), conductor construction details (conductor radius) as well as resistance and inductance data.
 - A distribution network model, based on a real LV distribution circuit in Jemena Electricity Networks, is set up using load data from Supervisory Control and Data Acquisition (SCADA) system and smart meters, line impedance data using Carson's equations, with explicit modelling of the

neutral conductors and Multiple Earthed Neutral (MEN) system, and embedded PV generators.

- The network model is set up in OpenDSS™, an open-source electrical system simulation tool for utility distribution systems. MATLAB© is used to drive the OpenDSS through an in-process Component Object Model (COM) interface for load flow simulations and result analysis.

4. Simulating the effect of existing voltage control schemes

- This thesis has already identified, through exploratory analysis of smart meter data, that voltage supplied to LV customers tends to be at the high end of the allowable range most of the time. It has also identified that PV generators contribute to overvoltage issues experienced by LV customers. By applying the existing voltage control schemes and control settings to the network model, the same result of high voltage is observed from load flow simulations. In addition, there is voltage rise on the red phase where the two PV generators are connected, compared with the other two phases. The combination of high base voltage and further voltage rise caused by PV generation results in instances of voltage non-compliance.
- This thesis considered the scenario of applying Line Drop Compensation to provide a dynamic voltage control set point that varies based on line loading. This has the effect of lowering the voltage received by the customers during light load period and only raising the voltage when the load is high. This approach produces the desirable effect of lowering the base voltage so voltage rise caused by PV generation does not result in voltage non-compliance. Voltage unbalance caused by the mismatch of generation and load on the three phases, however, is not addressed as existing voltage control schemes act on all three phases and cannot correct single-phase issues.

5. Planning approach to address voltage unbalance issues

- Voltage unbalance often has a detrimental effect on customer 3-phase equipment. In addition, single-phase loads/PV generation in a three-phase, four-wire LV network with earthed neutral gives rise to neutral voltage shift which compounds the overvoltage and undervoltage issues. The thesis considers modifying the existing planning approach to optimize the phase connection of PV generators.

- This thesis uses the definition of voltage unbalance ($VU\%$) that incorporates both positive, negative and zero sequence voltages, and calculate $VU\%$ for each LV load bus during the load flow simulations. This thesis defines a Network Voltage Unbalance Factor $f(x)$ that takes into account the maximum value of $VU\%$ for each load bus, and sets the objective of minimizing $f(x)$ by judicious placement of the PV generators to the three supply phases. The thesis demonstrates that the approach is successful in reducing the voltage rise caused by PV generation to within the regulatory limits even though the same high base voltage is supplied. A hypothetical future case of adding two additional PV generators to the distribution circuit, raising the PV penetration to 50% of customers, is simulated. It is found that the optimal PV phase allocation approach can still contain the voltage rise to within regulatory limits in this high PV penetration scenario.

6. Simulating the effect of smart grid technologies

- Many smart grid technologies have been proposed to address the impact of embedded PV generation. OpenDSS provides a library of power delivery elements that include transformers, PV generators and battery storage. Control elements are modelled separately from the power delivery elements including smart PV inverter control, regulator control and storage control. By combining power delivery elements with the appropriate control elements (and control settings), the effect of smart grid technologies on voltage rise/voltage unbalance caused by PV generators was simulated.
- By combining a transformer element with an on-load tap changer control and using transformer specification from a supplier of smart grid transformers, this thesis establishes the scenario of adopting an on-load tap changing distribution transformer. The simulation result indicates that by extending automatic voltage control into the distribution network, the voltage delivered to the customers can be tailored to the local requirements rather than determined by the load characteristics of the upstream zone substation and the voltage drops on the MV network.
- By combining PV generators with smart inverter control, the thesis has demonstrated the effect of smart inverter Volt-Watt and Volt-Var controls on voltage rise. Volt-Watt control has the effect of curtailing the active power

output of the PV generator when the inverter terminal voltage becomes too high. Volt-Var control enables the PV inverter to absorb reactive power when the voltage is high, and supply reactive power when the voltage is low. Both smart inverter technologies are effective in reducing the voltage rise caused by PV generation to within regulatory limits.

- By fitting a battery storage element to the same premises where a PV generator is installed and applying a control strategy for the battery to absorb excess PV generated power and release the stored energy later during peak load period, the thesis has demonstrated the beneficial effect of the battery storage in reducing the voltage rise during PV generation and improving the voltage drop during the subsequent peak load period.

7. Providing recommendations to distribution utilities

- There is a pressing need to find practical, cost effective solutions that can be deployed by supply utilities to accommodate the increasing penetration of customer roof-top PV systems.
- Modifications to existing voltage regulation schemes will be required to lower the nominal voltage delivered to customers, as the current bias of high supply voltage does not leave much headroom for voltage rise caused by embedded PV generators. A relatively new Australian Standard, AS 61000.3.100 “Limits – Steady-state voltage limits in public electricity systems”, recommends that a sub-range of 230V +6%/-2% be used for planning purposes, instead of the full range of 230V+10%/-6%. This approach effectively leaves an “upper operating range” to assist the network with the absorption of embedded generation while also providing a “lower operating range” to assist with the network supply of heavy peak loads [90]. To achieve this objective, it is likely that a dynamic voltage control scheme is required.
- In addition, an effective method of dealing with voltage rise is to minimise voltage unbalance between supply phases in the LV supply network. This can be achieved by minimising the Network Voltage Unbalance Factor through judicious placement of PV generation to the appropriate supply phases.
- Central to the above proposals does require the establishment of an accurate network model that can be used to simulate the effect of different voltage regulation schemes and PV generator phase allocation. Utilities generally have

good computer models for their MV networks but LV network models are not commonly found. As disruptions to the network are primarily occurring on the LV network, the development of accurate LV network models should be a priority for utilities.

- Industry research is mostly focused on the development of smart grid technologies as mitigating measures which generally require significant additional grid investment. While transforming the supply grid performance by investing in smart grid technologies is unavoidable, customers are already financially burdened by the transition to a renewable energy future caused by initiatives such as feed-in tariffs. A prioritised approach of improving existing operational practices and implementation of smart grid technologies will help to spread the additional investment cost over a longer time horizon.

7.3 Future Work and Recommendation

After the study into intelligent distribution voltage control in the presence of intermittent embedded PV generation, there are other aspects of voltage control that can be investigated further. A few possible future research directions are suggested below:

1. Electric vehicles

Electric vehicles are increasing in popularity and will present both challenges and opportunities to the LV electricity network. The additional charging load will impact voltage quality in particular issues relating to undervoltage and voltage unbalance. Electric vehicles are also sources of energy storage. With controlled charging the energy storage capacity could be used to manage excess PV generation. The intelligent distribution voltage control investigated can be expanded to include electric vehicle charging while optimising the network's hosting capacity for PV generation.

2. Modelling of other smart grid technologies

Smart grid technologies modelled in the study include on-load tap changing distribution transformers, smart inverters and storage batteries. The study does not attempt to investigate the effect of different control characteristics of these smart grid technologies and this can form the basis of future research work. In addition, there is an emerging list of smart grid technologies that promise better control of the electricity distribution networks. Developing appropriate models of these emerging

technologies and their control characteristics will allow their effect to be assessed in computer simulation studies.

3. Automate the production of network models from asset data and spatial characteristics stored in utilities' Geographical Information Systems (GIS) to allow statistically valid conclusions be drawn based on a large number of simulation studies

In this study the production of network model has been a labour-intensive process. It is conceivable that the process can be automated beginning with the extraction of asset data (such as line construction details) and spatial characteristics (line length, line route, supply points) from the Geographical Information System into tabular format. Matching of supply points with customer meter numbers create the links between customer load information and supply points.

A simple LV distribution circuit has been modelled in the study to demonstrate the principle of various voltage control techniques. The effectiveness of the proposed approach in improving PV hosting capacity can be statistically determined when a representative sample of LV distribution circuits are used in further simulation studies. This can be undertaken when an efficient way of producing network models can be found through process automation as above.

4. Dynamic MV voltage regulation schemes

The thesis found that dynamic voltage set points, when applied to MV voltage regulation schemes, could improve voltage delivery to LV customers. Performance of Line Drop Compensation scheme, however, is affected by non-homogeneity of the MV feeders supplied by the same LDC scheme. Further research work on dynamic MV voltage regulation schemes will be useful.

7.4 Concluding Remarks

In brief, a change of customer attitude and the emergence of affordable customer technologies have necessitated a change in the way utility engineers design and operate the electricity distribution networks. In the area of roof-top photo-voltaic generation systems, Australia has topped the world in the penetration of such systems on a per capita basis. Voltage quality issues, in particular steady-state overvoltages and voltage unbalances, have been on the rise. To remain relevant to electricity customers, utilities have no option but to investigate how the existing voltage controls can be improved to

cater for these PV generators. Improvement strategies need to be prioritised to contain additional expenditure.

Appendices – OpenDSS & MatLab Codes

A. OpenDSS codes for network model

```
! Weekly power flow 15 to 21 Feb 15
! V19: revised dist transf to match 5-tap transformers commonly found in JEN, increase high voltage feeder
length from 100m to 1000m per section
! V20: revised algorithms for storage battery, volt-var and volt-watt control; revised Linecodes
! V22: added commercial and industrial load profiles
! V23: Changed O/H lines to geometry to allow Carson's Equation to be used
! V23a: Updated nomenclature of circuit elements in accordance with model schematic
! V23b: version to be used in conjunction with MATLAB

Clear
New Circuit.SHM14
Edit Vsource.Source BasekV=66 pu=1.015 ISC3=7100 ISC1=4000

! The SHM transformer should be modelled as wye/delta/wye. However to simplify modelling the transformer
has been modelled as delta/wye.
New Transformer.TR_SHM Phases=3 Windings=2 Buses=[SourceBus.1.2.3, LoadBus1.1.2.3.0] Conns=[Delta
Wye] kVs=[66 22] kVAs=[40000 40000] XHL=10
~ Wdg=1 Maxtap=1.15 Mintap=0.95 NumTaps=16 ! NumTaps is number of taps between max and min so for a
17-tap position transformer, NumTaps=16.
! Mintap<1 will boost 22kV voltage

! Define voltage regulator control on this transformer
!New RegControl.Reg1 Transformer=TR_SHM Winding=2 tapwinding=1 Bus=LoadBus2.1 Vreg=65.3 band=1.5
delay=90 ptratio=200 debugtrace=Yes !LoadBus2.1 is used as remote controlled bus
New RegControl.Reg1 Transformer=TR_SHM Winding=2 tapwinding=1 Vreg=63.5 band=1.5 delay=90
ptratio=200 CTprim=1200 R=1.16 X=1.97 PTphase=1 debugtrace=Yes !Line drop compensation
New Monitor.m1 Transformer.TR_SHM Terminal=1 Mode=2 ! Monitor transformer tap
New Monitor.m2 Transformer.TR_SHM Terminal=2 Mode=1 ! Monitor transformer kW and KVar
New Monitor.m3 Transformer.TR_SHM Terminal=2 Mode=0 ! Monitor transformer voltage and current

! Define a number of frequently used line codes
New Wiredata.19/3.25AAC GMR=0.006347 DIAM=0.01630 RAC=0.000196 NormAmps=250.0 Runits=m
radunits=m gmrunits=m
New Wiredata.7/3.0AAC GMR=0.003505 DIAM=0.00900 RAC=0.000614 NormAmps=150.0 Runits=m
radunits=m gmrunits=m
New Wiredata.7/.064Cu GMR=0.001904 DIAM=0.00489 RAC=0.001308 NormAmps=130.0 Runits=m
radunits=m gmrunits=m
New Linegeometry.4W-19/3.25AAC nconds=4 nphases=3
~ cond=1 Wire=19/3.25AAC x=-0.95 h=8 units=m ! R-phase
~ cond=2 Wire=19/3.25AAC x=0.35 h=8 units=m ! W-phase
~ cond=3 Wire=19/3.25AAC x=0.95 h=8 units=m ! B-phase
~ cond=4 Wire=19/3.25AAC x=-0.35 h=8 units=m ! N-phase
New Linegeometry.3W-19/3.25AAC nconds=3 nphases=3
~ cond=1 Wire=19/3.25AAC x=-0.900 h=10.0 units=m ! R-phase
~ cond=2 Wire=19/3.25AAC x=0 h=10.3 units=m ! W-phase
~ cond=3 Wire=19/3.25AAC x=0.900 h=10.0 units=m ! B-phase
New Linegeometry.4W-7/3.0AAC nconds=4 nphases=3
~ cond=1 Wire=7/3.0AAC x=-0.95 h=8 units=m ! R-phase
~ cond=2 Wire=7/3.0AAC x=0.35 h=8 units=m ! W-phase
~ cond=3 Wire=7/3.0AAC x=0.95 h=8 units=m ! B-phase
~ cond=4 Wire=7/3.0AAC x=-0.35 h=8 units=m ! N-phase
New Linegeometry.3W-7/3.0AAC nconds=3 nphases=3
~ cond=1 Wire=7/3.0AAC x=-0.900 h=10.0 units=m ! R-phase
~ cond=2 Wire=7/3.0AAC x=0 h=10.3 units=m ! W-phase
~ cond=3 Wire=7/3.0AAC x=0.900 h=10.0 units=m ! B-phase
```

```

New Linegeometry.4W-7/.064Cu nconds=4 nphases=3
~ cond=1 Wire=7/.064Cu x=-0.95 h=8 units=m ! R-phase
~ cond=2 Wire=7/.064Cu x=0.35 h=8 units=m ! W-phase
~ cond=3 Wire=7/.064Cu x=0.95 h=8 units=m ! B-phase
~ cond=4 Wire=7/.064Cu x=-0.35 h=8 units=m ! N-phase
New Linegeometry.3W-7/.064Cu nconds=3 nphases=3
~ cond=1 Wire=7/.064Cu x=-0.900 h=10.0 units=m ! R-phase
~ cond=2 Wire=7/.064Cu x=0 h=10.3 units=m ! W-phase
~ cond=3 Wire=7/.064Cu x=0.900 h=10.0 units=m ! B-phase

New Linecode.LVUG8 Nphases=4 R1=0.171 X1=0.081 R0=0.557 X0=0.376 Units=km ! 185mm2 Al 4c, Z0
chosen for return current in both neutral and ground in parallel
New Linecode.LVUG9 Nphases=4 R1=1.195 X1=0.1 R0=2.141 X0=1.552 Units=km ! 16mm2 Cu 4c, Z0 chosen
for return current in both neutral and ground in parallel

! Create loadshape for other loads at SHM 22kV bus, and simulate voltage delivery with different load shapes
New LoadShape.Bus_weekly npts=336 interval=0.5 Mult=[File=SHMZS_weekly.csv, Column=2, Header=Yes]
New LoadShape.Bus_commercial_weekly npts=336 interval=0.5 Mult=[File=Commercial_feeder_profile-BD10-
weekly.csv, Column=2, Header=Yes]
New LoadShape.Bus_industrial_weekly npts=336 interval=0.5 Mult=[File=Industrial_feeder_profile-AW3-
weekly.csv, Column=2, Header=Yes]
New LoadShape.SHM14_weekly npts=336 interval=0.5 Mult=[File=SHM14Profile_weekly.csv, Column=2,
Header=Yes]
New LoadShape.Cypress_weekly npts=336 interval=0.5 Mult=[File=Cypress-Stillia_weekly.csv, Column=2,
Header=Yes]
New LoadShape.Cus1_weekly npts=336 interval=0.5 Mult=[File=Customer1_weekly.csv, Column=2,
Header=Yes]
New LoadShape.Cus2_weekly npts=336 interval=0.5 Mult=[File=Customer2_weekly.csv, Column=2,
Header=Yes]
New LoadShape.Cus3_weekly npts=336 interval=0.5 Mult=[File=Customer3_weekly.csv, Column=2,
Header=Yes]
New LoadShape.Cus4_weekly npts=336 interval=0.5 Mult=[File=Customer4_weekly.csv, Column=2,
Header=Yes]
New LoadShape.Cus6_weekly npts=336 interval=0.5 Mult=[File=Customer6_weekly.csv, Column=2,
Header=Yes]
New LoadShape.Cus8_weekly npts=336 interval=0.5 Mult=[File=Customer8_weekly.csv, Column=2,
Header=Yes]

New Line.LINE1 Bus1=LoadBus1 Bus2=LoadBus2 Geometry=3W-19/3.25AAC Length=1 Units=m
New Load.LOAD1 Bus1=LoadBus2 kV=22 kVA=18000 PF=0.9 duty=Bus_weekly
New Monitor.m4 Line.LINE1 Terminal=1 Mode=0 ! Monitor voltages & currents of 22kV bus load

! Define circuit parameters supplied from the zone transformer
New Line.LINE2 Bus1=LoadBus2 Bus2=LoadBus3 Geometry=3W-19/3.25AAC Length=1000 Units=m
New Load.LOAD2 Bus1=LoadBus3 kV=22 KVA=1800 PF=0.9 duty=SHM14_weekly
New Line.LINE3 Bus1=LoadBus3 Bus2=LoadBus4 Geometry=3W-19/3.25AAC Length=1000 Units=m
New Load.LOAD3 Bus1=LoadBus4 kV=22 KVA=1800 PF=0.9 duty=SHM14_weekly
New Line.LINE4 Bus1=LoadBus4 Bus2=LoadBus5 Geometry=3W-19/3.25AAC Length=1000 Units=m
New Load.LOAD4 Bus1=LoadBus5 kV=22 KVA=1800 PF=0.9 duty=SHM14_weekly
New Line.LINE5 Bus1=LoadBus5 Bus2=LoadBus6 Geometry=3W-19/3.25AAC Length=1000 Units=m
New Load.LOAD5 Bus1=LoadBus6 kV=22 KVA=1800 PF=0.9 duty=SHM14_weekly
New Line.LINE6 Bus1=LoadBus6 Bus2=LoadBus7 Geometry=3W-19/3.25AAC Length=1000 Units=m
New Line.LINE7 Bus1=LoadBus7 Bus2=LoadBus8 Geometry=3W-19/3.25AAC Length=1000 Units=m
New Load.LOAD6 Bus1=LoadBus8 kV=22 KVA=1800 PF=0.9 duty=SHM14_weekly
New Capacitor.Cap1 Bus1=LoadBus1 Phases=3 Kvar=[8000, 8000] kV=22 Conn=wye Numsteps=2
Basefreq=50 states=[0,0] ! Define zs cap bank, 8000kvar step is considered by program to be 4000kvar (a bug)
New Capacitor.Cap2 Bus1=LoadBus4 Phases=3 kvar=900 kv=22 conn=wye Numsteps=1 Basefreq=50 states=0
! Define distribution cap (earthed star as solution does not work for unearthed star)
New Capacitor.Cap3 Bus1=LoadBus7 Phases=3 kvar=900 kv=22 conn=wye Numsteps=1 Basefreq=50 states=0

! Define LV circuit parameters supplied from distribution transformer
New Transformer.TR_Cypress Phases=3 Windings=2 Buses=[LoadBus7.1.2.3, LoadBus9.1.2.3.4] Conns=[Delta
Wye] kVs=[22 0.433] kVAs=[300 300] XHL=4
~ Wdg=1 Maxtap=1.025 Mintap=0.925 NumTaps=4 Tap=1.025

!Smart grid transformer (with on-load tap changing facility, modelled on Schneider Smart Grid Transformer)

```

!New Transformer.TR_Cypress Phases=3 Windings=2 Buses=[LoadBus7.1.2.3, LoadBus9.1.2.3.4] Conns=[Delta Wye] kVs=[22 0.415] kVAs=[400 400] XHL=4
!~ Wdg=1 Maxtap=1.05 Mintap=0.95 NumTaps=4

!New RegControl.Reg2 Transformer=TR_Cypress Winding=2 tapwinding=1 Bus=LoadBus9.1 Vreg=244
band=3 ptratio=1 debugtrace=Yes !244V=230V+6%, band=0.5tap size

New Reactor.TR_NeutReactor phases=1 bus1=LoadBus9.4 R=10 X=0
New Monitor.m5 Transformer.TR_Cypress Terminal=1 Mode=0
New Monitor.m6 Transformer.TR_Cypress Terminal=2 Mode=0
New Load.LOAD7 Bus1=LoadBus9.1.2.3.4 kV=0.415 KVA=180 PF=0.9 duty=Cypress_weekly
New Line.LINE8 Bus1=LoadBus9.1.2.3.4 Bus2=LoadBus10.1.2.3.4 Linecode=LVUG8 Length=168.6 Units=m
New Reactor.Bus10_1-5_Reactor phases=1 bus1=LoadBus10.1 bus2=LoadBus10.5 R=0.001 X=0
New Reactor.Bus10_2-6_Reactor phases=1 bus1=LoadBus10.2 bus2=LoadBus10.6 R=0.001 X=0
New Reactor.Bus10_3-7_Reactor phases=1 bus1=LoadBus10.3 bus2=LoadBus10.7 R=0.001 X=0
New Reactor.Bus10_4-8_Reactor phases=1 bus1=LoadBus10.4 bus2=LoadBus10.8 R=0.001 X=0
New Line.LINE10 Bus1=LoadBus10.1.2.3.4 Bus2=LoadBus20.1.2.3.4 Linecode=LVUG8 Length=21.5 Units=m
New Line.LINE16a Bus1=LoadBus20.1.2.3.4 Bus2=LoadBus21.1.2.3.4 Linecode=LVUG9 Length=5 Units=m
New Reactor.Bus21_NeutReactor phases=1 bus1=LoadBus21.4 R=100 X=0
New Line.LINE16b Bus1=LoadBus20.1.2.3.4 Bus2=LoadBus22.1.2.3.4 Linecode=LVUG9 Length=5 Units=m
New Reactor.Bus22_NeutReactor phases=1 bus1=LoadBus22.4 R=100 X=0
New Monitor.m17 Line.LINE10 Terminal=2 Mode=1 !Mode=1=power
New Monitor.m18 Line.LINE10 Terminal=2 Mode=0 !Mode=0=V & I !This gives the volage at Bus 20
New Monitor.m19 Line.LINE16a Terminal=2 Mode=0 !Mode=1=power
New Monitor.m20 Line.LINE16a Terminal=1 Mode=16 !Mode=0=V & I !This gives the voltage at Bus 21, PCC
for customer 7
New Load.LOAD14 Bus1=LoadBus21.1.2.3.4 kV=0.415 KVA=9 PF=0.9 duty=Cus4_weekly !Customer 7
New Load.LOAD15 Bus1=LoadBus22.1.2.3.4 kV=0.415 KVA=9 PF=0.9 duty=Cus8_weekly !Customer 8
! Define embedded PV
New LoadShape.MyIrrad npts=336 interval=0.5 Mult=[File=Solar_weekly.csv, Column=2, Header=Yes]
New TShape.MyTemp npts=336 interval=0.5 temp=[File=Temp_weekly.csv, Column=2, Header=Yes]
New XYCurve.MyPvst npts=4 xarray=[0 25 75 100] yarray=[1.2 1.0 0.8 0.6]
New XYCurve.MyEff npts=4 xarray=[0.1 0.2 0.4 1.0] yarray=[0.86 0.9 0.93 0.97]
New PVSystem.PV2 Bus1=LoadBus21.1.4 Phases=1 kV=0.24 kVA=5 Irrad=1.0 Pmpp=5 Temperature=25 PF=1
effcurve=Myeff P-TCurve=MyPvsT Duty=MyIrrad TDuty=MyTemp %Cutin=0.1 %Cutout=0.05 !Define PV
system installed by Customer 7 on R phase
New Monitor.m7 PVSystem.PV2 Terminal=1 Mode=1 !Mode=1=power
New Monitor.m8 PVSystem.PV2 Terminal=1 Mode=0 !Mode=0=V & I

! Continue to define rest of LV circuit parameters
New Line.LINE9 Bus1=LoadBus10.5.6.7.8 Bus2=LoadBus11.1.2.3.4 Linecode=LVUG8 Length=28.29 Units=m
New Line.LINE11a Bus1=LoadBus11.1.2.3.4 Bus2=LoadBus12.1.2.3.4 Linecode=LVUG9 Length=5 Units=m
New Reactor.Bus12_NeutReactor phases=1 bus1=LoadBus12.4 R=100 X=0
New Line.LINE11b Bus1=LoadBus11.1.2.3.4 Bus2=LoadBus13.1.2.3.4 Linecode=LVUG9 Length=5 Units=m
New Reactor.Bus13_NeutReactor phases=1 bus1=LoadBus13.4 R=100 X=0
New Monitor.m13 Line.LINE9 Terminal=2 Mode=1 !Mode=1=power
New Monitor.m14 Line.LINE9 Terminal=2 Mode=0 !Mode=0=V & I !This gives the volage at Bus 11
New Monitor.m15 Line.LINE11a Terminal=2 Mode=1 !Mode=1=power
New Monitor.m16 Line.LINE11a Terminal=2 Mode=0 !Mode=0=V & I !This gives the voltage at Bus 12, PCC for
customer 5
New Load.LOAD8 Bus1=LoadBus12.1.2.3.4 kV=0.415 KVA=7 PF=0.9 duty=Cus4_weekly !Customer 5
New Load.LOAD9 Bus1=LoadBus13.2.4 Phases=1 kV=0.24 KVA=5 PF=0.9 duty=Cus6_weekly !Customer 6

! Define embedded PV
New PVSystem.PV1 Bus1=LoadBus12.1.4 Phases=1 kV=0.24 kVA=4 Irrad=1.0 Pmpp=4 Temperature=25 PF=1
effcurve=Myeff P-TCurve=MyPvsT Duty=MyIrrad TDuty=MyTemp %Cutin=0.1 %Cutout=0.05 !Define PV
system installed by Customer 5 on R phase
New Monitor.m9 PVSystem.PV1 Terminal=1 Mode=1
New Monitor.m10 PVSystem.PV1 Terminal=1 Mode=0

! Continue to define rest of LV circuit parameters
New Line.LINE12 Bus1=LoadBus11.1.2.3.4 Bus2=LoadBus14.1.2.3.4 Linecode=LVUG8 Length=66.5 Units=m
New Line.LINE13a Bus1=LoadBus14.1.2.3.4 Bus2=LoadBus15.1.2.3.4 Linecode=LVUG9 Length=5 Units=m
New Reactor.Bus15_NeutReactor phases=1 bus1=LoadBus15.4 R=100 X=0
New Line.LINE13b Bus1=LoadBus14.1.2.3.4 Bus2=LoadBus16.1.2.3.4 Linecode=LVUG9 Length=5 Units=m
New Reactor.Bus16_NeutReactor phases=1 bus1=LoadBus16.4 R=100 X=0

```

New Load.LOAD10 Bus1=LoadBus15.1.2.3.4 kV=0.415 KVA=15 PF=0.9 duty=Cus3_weekly !Customer 3
New Load.LOAD11 Bus1=LoadBus16.1.2.3.4 kV=0.415 KVA=7.8 PF=0.9 duty=Cus4_weekly !Customer 4
New Line.LINE14 Bus1=LoadBus14.1.2.3.4 Bus2=LoadBus17.1.2.3.4 Linecode=LVUG8 Length=58.13 Units=m
New Line.LINE15a Bus1=LoadBus17.1.2.3.4 Bus2=LoadBus18.1.2.3.4 Linecode=LVUG9 Length=5 Units=m
New Reactor.Bus18_NeutReactor phases=1 bus1=LoadBus18.4 R=100 X=0
New Line.LINE15b Bus1=LoadBus17.1.2.3.4 Bus2=LoadBus19.1.2.3.4 Linecode=LVUG9 Length=5 Units=m
New Reactor.Bus19_NeutReactor phases=1 bus1=LoadBus19.4 R=100 X=0

```

```

New Load.LOAD12 Bus1=LoadBus18.1.2.3.4 kV=0.415 kVA=5 PF=0.9 duty=Cus1_weekly !Customer 1
New Load.LOAD13 Bus1=LoadBus19.3.4 Phases=1 kV=0.24 KVA=5 PF=0.9 duty=Cus2_weekly !Customer2
New monitor.m21 Line.LINE14 Terminal=2 Mode=0 !This gives the voltage received by the customers at the
end of the LV circuit

```

```

! Define smart PV inverter
!New XYCurve.vw_curve npts=4 xarray=[0.0, 1.04, 1.1, 2.0] yarray=[1.0, 1.0, 0.0, 0.0] ! Volt-watt curve
!New InvControl.InvPVCtrl1 mode=VOLTWATT voltage_curvex_ref=rated voltwatt_curve=vw_curve
VoltwattYAxis=PAVAILABLEPU EventLog=Yes !Smart inverter with Volt-watt control
!New XYCurve.vv_curve npts=6 xarray=[0.5, 0.9, 0.94, 1.02, 1.1, 1.5] yarray=[1.0, 1.0, 0, 0, -1.0, -1.0] ! Volt-var
curve
!New InvControl.InvPVCtrl2 mode=VOLTVAR voltage_curvex_ref=rated vvc_curve1=vv_curve EventLog=Yes
!Smart inverter with Volt-var control

```

```

! Define storage battery
!New Storage.Battery1 phases=1 Bus1=LoadBus21.1.4 kV=0.24 kW=4 kWrated=4 kWhrated=25 %stored=20
!Battery installed by Cus 7
!new monitor.m11 storage.battery1 1 ppolar=no mode=1
!new monitor.m12 storage.battery1 1 mode=3
!New LoadShape.Battery1_weekly npts=336 interval=0.5 Mult=[File=battery_charging_weekly_v1.csv,
Column=2, Header=Yes]
!New StorageController.Battctrl1 element=Line.LINE16a terminal=1 ModeCharge=Loadshape
ModeDischarge=Loadshape TimeDisChargeTrigger=18 %RatekW=20 %Ratekvar=20 Duty=Battery1_weekly
EventLog=Yes

```

```

!Define switchable capacitor control
New CapControl.CAPBank1_Ctrl Capacitor=Cap1 element=Line.LINE1 Terminal=1 Type=kvar ONsetting=5000
OFFsetting=-1000 Delay=900 DelayOFF=300 Deadtime=300 EventLog=Yes PTratio=200
New CapControl.CAPBank2_Ctrl Capacitor=Cap2 element=line.LINE3 2 Type=voltage PTratio=200
ONsetting=63.5 OFFsetting=67.3 Delay=300 DelayOFF=300 Deadtime=300 EventLog=Yes
New CapControl.CAPBank3_Ctrl Capacitor=Cap3 element=line.LINE6 2 Type=voltage PTratio=200
ONsetting=63.5 OFFsetting=67.3 Delay=400 DelayOFF=200 Deadtime=300 EventLog=Yes

```

```

CapControl.CAPBank1_Ctrl VBus=LoadBus1 Vmax=69.86 Vmin=57.16 VoltOverride=Yes ! Define VBus AFTER
doing an action that causes the OpenDSS to create the buses. In this case the operation calcvoltagebases.

```

```

New monitor.m23 Line.LINE8 Terminal=2 Mode=0 !This gives the voltage at Bus10
New monitor.m24 Line.LINE9 Terminal=2 Mode=0 !This gives the voltage at Bus11
New monitor.m25 Line.LINE12 Terminal=2 Mode=0 !This gives the voltage at Bus14

```

```

Set voltagebases="66, 22, 0.415, 0.24"

```

```

Calcvoltagebases

```

B. MATLAB Codes for Phase Voltage Analysis

```

% MatLab code for voltage analysis

```

```

% To run this MatLab code, make sure the current folder points to the
% location where all the files required by the DSS program are located

```

```

DSSObj=actxserver('OpenDSSEngine.dss');
Start=DSSObj.Start(0);
[DSSStartOK, DSSObj, DSSText] = DSSStartup;

```

```

% Set up the interface variables
DSSCircuit=DSSObj.ActiveCircuit;
DSSSolution=DSSCircuit.Solution;
DSSText.Command='Compile (C:\Program Files\OpenDSS\Examples\Jemena\SHM14_Cypress-
Stillia_V23b.dss)';

% Add an EnergyMeter object so the distances down the feeder are computed

DSSText.Command='New EnergyMeter.E1 Line.LINE1 1';

% Add a Monitor, too
DSSText.Command='New Monitor.FeederEnd Line.LINE1 1';

% New Line Drop Compensation setting default is Vreg=63.5 R=1.16 X=1.97
DSSText.Command='RegControl.Reg1.Vreg=65.3 R=0 X=0';

% Connect PV1 and PV2 to selected phases
DSSText.Command='PVSystem.PV1.Bus1=LoadBus12.1.4';
DSSText.Command='PVSystem.PV2.Bus1=LoadBus21.1.4';

% -----
% Run a weekly analysis and plot the voltages at the end of the feeder
% The 3-phase voltages are measured between the phases and neutral
% -----

DSSText.command='set mode = duty';
DSSCircuit.Solution.Number = 1;
DSSCircuit.Solution.Stepsize = 1800;
DSSCircuit.Solution.Hour = 0;

for i=1:336
DSSCircuit.Solution.Solve;

end

Hour=[0.5:0.5:168];

DSSText.Command = 'export monitors m6';
monitorFile = DSSText.Result;
MyCSV = importdata(monitorFile);
delete(monitorFile);
Hour = MyCSV.data(:,1); Second = MyCSV.data(:,2);
phaseVoltageMag = MyCSV.data(:,[3,5,7,9]);
phaseVoltageAngle = MyCSV.data(:,[4,6,8,10]);
phaseCurrent = MyCSV.data(:,[11,13,15,17]);

cosineR = cosd(phaseVoltageAngle(:,1));
sineR = sind(phaseVoltageAngle(:,1));
RphaseVoltageReal = phaseVoltageMag(:,1).*cosineR;
RphaseVoltageImag = phaseVoltageMag(:,1).*sineR;
RphaseVoltage = complex(RphaseVoltageReal,RphaseVoltageImag);

cosineW = cosd(phaseVoltageAngle(:,2));
sineW = sind(phaseVoltageAngle(:,2));
WphaseVoltageReal = phaseVoltageMag(:,2).*cosineW;
WphaseVoltageImag = phaseVoltageMag(:,2).*sineW;
WphaseVoltage = complex(WphaseVoltageReal,WphaseVoltageImag);

cosineB = cosd(phaseVoltageAngle(:,3));
sineB = sind(phaseVoltageAngle(:,3));
BphaseVoltageReal = phaseVoltageMag(:,3).*cosineB;
BphaseVoltageImag = phaseVoltageMag(:,3).*sineB;
BphaseVoltage = complex(BphaseVoltageReal,BphaseVoltageImag);

cosineN = cosd(phaseVoltageAngle(:,4));

```

```

sineN = sind(phaseVoltageAngle(:,4));
NphaseVoltageReal = phaseVoltageMag(:,4).*cosineN;
NphaseVoltageImag = phaseVoltageMag(:,4).*sineN;
NphaseVoltage = complex(NphaseVoltageReal,NphaseVoltageImag);

phaseVoltageToNeutralR = RphaseVoltage-NphaseVoltage;
phaseVoltageToNeutralW = WphaseVoltage-NphaseVoltage;
phaseVoltageToNeutralB = BphaseVoltage-NphaseVoltage;
Rphase = abs(phaseVoltageToNeutralR);
Wphase = abs(phaseVoltageToNeutralW);
Bphase = abs(phaseVoltageToNeutralB);
OVlimit = 253*ones(1,336);
UVlimit = 216.2*ones(1,336);

figure (1);
plot(Hour+Second/3600,Rphase,'Color','red','LineWidth',2);
hold on
plot(Hour+Second/3600,Wphase,'Color','green','LineWidth',2);
hold on
plot(Hour+Second/3600,Bphase,'Color','blue','LineWidth',2);
hold on
plot(Hour+Second/3600,OVlimit,'Color','magenta','LineStyle',':','LineWidth',2);
hold on
plot(Hour+Second/3600,UVlimit,'Color','cyan','LineStyle',':','LineWidth',2);

legend('Phase A', 'Phase B', 'Phase C', 'OV limit', 'UV limit', 'Location', 'southeast')
xlabel('Hour','FontSize',12,'FontWeight','bold')
ylabel('Phase to Neutral Voltages (V)','FontSize',12,'FontWeight','bold')
title('Weekly Simulation, Voltages at LoadBus9','FontSize',12,'FontWeight','bold')
hold off
saveas(gcf,'C:\Users\Peter\My Documents\PhD study\OpenDSS\Cypress-Stillia\RunCase\Volt-new\Case6-
Fig1','bmp');

DSSText.Command = 'export monitors m23';
monitorFile = DSSText.Result;
MyCSV = importdata(monitorFile);
delete(monitorFile);
Hour = MyCSV.data(:,1); Second = MyCSV.data(:,2);
phaseVoltageMag = MyCSV.data(:,[3,5,7,9]);
phaseVoltageAngle = MyCSV.data(:,[4,6,8,10]);
phaseCurrent = MyCSV.data(:,[11,13,15,17]);

cosineR = cosd(phaseVoltageAngle(:,1));
sineR = sind(phaseVoltageAngle(:,1));
RphaseVoltageReal = phaseVoltageMag(:,1).*cosineR;
RphaseVoltageImag = phaseVoltageMag(:,1).*sineR;
RphaseVoltage = complex(RphaseVoltageReal,RphaseVoltageImag);

cosineW = cosd(phaseVoltageAngle(:,2));
sineW = sind(phaseVoltageAngle(:,2));
WphaseVoltageReal = phaseVoltageMag(:,2).*cosineW;
WphaseVoltageImag = phaseVoltageMag(:,2).*sineW;
WphaseVoltage = complex(WphaseVoltageReal,WphaseVoltageImag);

cosineB = cosd(phaseVoltageAngle(:,3));
sineB = sind(phaseVoltageAngle(:,3));
BphaseVoltageReal = phaseVoltageMag(:,3).*cosineB;
BphaseVoltageImag = phaseVoltageMag(:,3).*sineB;
BphaseVoltage = complex(BphaseVoltageReal,BphaseVoltageImag);

cosineN = cosd(phaseVoltageAngle(:,4));
sineN = sind(phaseVoltageAngle(:,4));
NphaseVoltageReal = phaseVoltageMag(:,4).*cosineN;
NphaseVoltageImag = phaseVoltageMag(:,4).*sineN;
NphaseVoltage = complex(NphaseVoltageReal,NphaseVoltageImag);

```

```

phaseVtagetoNeutralR = RphaseVoltage-NphaseVoltage;
phaseVtagetoNeutralW = WphaseVoltage-NphaseVoltage;
phaseVtagetoNeutralB = BphaseVoltage-NphaseVoltage;
Rphase = abs(phaseVtagetoNeutralR);
Wphase = abs(phaseVtagetoNeutralW);
Bphase = abs(phaseVtagetoNeutralB);
OVlimit = 253*ones(1,336);
UVlimit = 216.2*ones(1,336);

figure (2);
plot(Hour+Second/3600,Rphase,'Color','red','LineWidth',2);
hold on
plot(Hour+Second/3600,Wphase,'Color','green','LineWidth',2);
hold on
plot(Hour+Second/3600,Bphase,'Color','blue','LineWidth',2);
hold on
plot(Hour+Second/3600,OVlimit,'Color','magenta','LineStyle',':','LineWidth',2);
hold on
plot(Hour+Second/3600,UVlimit,'Color','cyan','LineStyle',':','LineWidth',2);

legend('Phase A','Phase B','Phase C','OV limit','UV limit','Location','southeast')
xlabel('Hour','FontSize',12,'FontWeight','bold')
ylabel('Phase to Neutral Voltages (V)','FontSize',12,'FontWeight','bold')
title('Weekly Simulation, Voltages at LoadBus10','FontSize',12,'FontWeight','bold')
hold off
saveas(gcf,'C:\Users\Peter\My Documents\PhD study\OpenDSS\Cypress-Stillia\RunCase\Volt-new\Case6-
Fig2','bmp');

DSSText.Command = 'export monitors m24';
monitorFile = DSSText.Result;
MyCSV = importdata(monitorFile);
delete(monitorFile);
Hour = MyCSV.data(:,1); Second = MyCSV.data(:,2);
phaseVoltageMag = MyCSV.data(:,[3,5,7,9]);
phaseVoltageAngle = MyCSV.data(:,[4,6,8,10]);
phaseCurrent = MyCSV.data(:,[11,13,15,17]);

cosineR = cosd(phaseVoltageAngle(:,1));
sineR = sind(phaseVoltageAngle(:,1));
RphaseVoltageReal = phaseVoltageMag(:,1).*cosineR;
RphaseVoltageImag = phaseVoltageMag(:,1).*sineR;
RphaseVoltage = complex(RphaseVoltageReal,RphaseVoltageImag);

cosineW = cosd(phaseVoltageAngle(:,2));
sineW = sind(phaseVoltageAngle(:,2));
WphaseVoltageReal = phaseVoltageMag(:,2).*cosineW;
WphaseVoltageImag = phaseVoltageMag(:,2).*sineW;
WphaseVoltage = complex(WphaseVoltageReal,WphaseVoltageImag);

cosineB = cosd(phaseVoltageAngle(:,3));
sineB = sind(phaseVoltageAngle(:,3));
BphaseVoltageReal = phaseVoltageMag(:,3).*cosineB;
BphaseVoltageImag = phaseVoltageMag(:,3).*sineB;
BphaseVoltage = complex(BphaseVoltageReal,BphaseVoltageImag);

cosineN = cosd(phaseVoltageAngle(:,4));
sineN = sind(phaseVoltageAngle(:,4));
NphaseVoltageReal = phaseVoltageMag(:,4).*cosineN;
NphaseVoltageImag = phaseVoltageMag(:,4).*sineN;
NphaseVoltage = complex(NphaseVoltageReal,NphaseVoltageImag);

phaseVtagetoNeutralR = RphaseVoltage-NphaseVoltage;
phaseVtagetoNeutralW = WphaseVoltage-NphaseVoltage;
phaseVtagetoNeutralB = BphaseVoltage-NphaseVoltage;
Rphase = abs(phaseVtagetoNeutralR);
Wphase = abs(phaseVtagetoNeutralW);

```

```

Bphase = abs(phaseVoltageToNeutralB);
OVlimit = 253*ones(1,336);
UVlimit = 216.2*ones(1,336);

figure (3);
plot(Hour+Second/3600,Rphase,'Color','red','LineWidth',2);
hold on
plot(Hour+Second/3600,Wphase,'Color','green','LineWidth',2);
hold on
plot(Hour+Second/3600,Bphase,'Color','blue','LineWidth',2);
hold on
plot(Hour+Second/3600,OVlimit,'Color','magenta','LineStyle',':','LineWidth',2);
hold on
plot(Hour+Second/3600,UVlimit,'Color','cyan','LineStyle',':','LineWidth',2);

legend('Phase A', 'Phase B', 'Phase C','OV limit','UV limit','Location','southeast')
xlabel('Hour','FontSize',12,'FontWeight','bold')
ylabel('Phase to Neutral Voltages (V)','FontSize',12,'FontWeight','bold')
title('Weekly Simulation, Voltages at LoadBus11','FontSize',12,'FontWeight','bold')
hold off
saveas(gcf,'C:\Users\Peter\My Documents\PhD study\OpenDSS\Cypress-Stillia\RunCase\Volt-new\Case6-
Fig3','bmp');

```

```

DSSText.Command = 'export monitors m25';
monitorFile = DSSText.Result;
MyCSV = importdata(monitorFile);
delete(monitorFile);
Hour = MyCSV.data(:,1); Second = MyCSV.data(:,2);
phaseVoltageMag = MyCSV.data(:,[3,5,7,9]);
phaseVoltageAngle = MyCSV.data(:,[4,6,8,10]);
phaseCurrent = MyCSV.data(:,[11,13,15,17]);

cosineR = cosd(phaseVoltageAngle(:,1));
sineR = sind(phaseVoltageAngle(:,1));
RphaseVoltageReal = phaseVoltageMag(:,1).*cosineR;
RphaseVoltageImag = phaseVoltageMag(:,1).*sineR;
RphaseVoltage = complex(RphaseVoltageReal,RphaseVoltageImag);

cosineW = cosd(phaseVoltageAngle(:,2));
sineW = sind(phaseVoltageAngle(:,2));
WphaseVoltageReal = phaseVoltageMag(:,2).*cosineW;
WphaseVoltageImag = phaseVoltageMag(:,2).*sineW;
WphaseVoltage = complex(WphaseVoltageReal,WphaseVoltageImag);

cosineB = cosd(phaseVoltageAngle(:,3));
sineB = sind(phaseVoltageAngle(:,3));
BphaseVoltageReal = phaseVoltageMag(:,3).*cosineB;
BphaseVoltageImag = phaseVoltageMag(:,3).*sineB;
BphaseVoltage = complex(BphaseVoltageReal,BphaseVoltageImag);

cosineN = cosd(phaseVoltageAngle(:,4));
sineN = sind(phaseVoltageAngle(:,4));
NphaseVoltageReal = phaseVoltageMag(:,4).*cosineN;
NphaseVoltageImag = phaseVoltageMag(:,4).*sineN;
NphaseVoltage = complex(NphaseVoltageReal,NphaseVoltageImag);

phaseVoltageToNeutralR = RphaseVoltage-NphaseVoltage;
phaseVoltageToNeutralW = WphaseVoltage-NphaseVoltage;
phaseVoltageToNeutralB = BphaseVoltage-NphaseVoltage;
Rphase = abs(phaseVoltageToNeutralR);
Wphase = abs(phaseVoltageToNeutralW);
Bphase = abs(phaseVoltageToNeutralB);
OVlimit = 253*ones(1,336);
UVlimit = 216.2*ones(1,336);

```

```

figure (4);

```

```

plot(Hour+Second/3600,Rphase,'Color','red','LineWidth',2);
hold on
plot(Hour+Second/3600,Wphase,'Color','green','LineWidth',2);
hold on
plot(Hour+Second/3600,Bphase,'Color','blue','LineWidth',2);
hold on
plot(Hour+Second/3600,OVLimit,'Color','magenta','LineStyle',':','LineWidth',2);
hold on
plot(Hour+Second/3600,UVLimit,'Color','cyan','LineStyle',':','LineWidth',2);

legend('Phase A', 'Phase B', 'Phase C','OV limit','UV limit','Location','southeast')
xlabel('Hour','FontSize',12,'FontWeight','bold')
ylabel('Phase to Neutral Voltages (V)','FontSize',12,'FontWeight','bold')
title('Weekly Simulation, Voltages at LoadBus14','FontSize',12,'FontWeight','bold')
hold off
saveas(gcf,'C:\Users\Peter\My Documents\PhD study\OpenDSS\Cypress-Stillia\RunCase\Volt-new\Case6-
Fig4','bmp');

DSSText.Command = 'export monitors m21';
monitorFile = DSSText.Result;
MyCSV = importdata(monitorFile);
delete(monitorFile);
Hour = MyCSV.data(:,1); Second = MyCSV.data(:,2);
phaseVoltageMag = MyCSV.data(:,[3,5,7,9]);
phaseVoltageAngle = MyCSV.data(:,[4,6,8,10]);
phaseCurrent = MyCSV.data(:,[11,13,15,17]);

cosineR = cosd(phaseVoltageAngle(:,1));
sineR = sind(phaseVoltageAngle(:,1));
RphaseVoltageReal = phaseVoltageMag(:,1).*cosineR;
RphaseVoltageImag = phaseVoltageMag(:,1).*sineR;
RphaseVoltage = complex(RphaseVoltageReal,RphaseVoltageImag);

cosineW = cosd(phaseVoltageAngle(:,2));
sineW = sind(phaseVoltageAngle(:,2));
WphaseVoltageReal = phaseVoltageMag(:,2).*cosineW;
WphaseVoltageImag = phaseVoltageMag(:,2).*sineW;
WphaseVoltage = complex(WphaseVoltageReal,WphaseVoltageImag);

cosineB = cosd(phaseVoltageAngle(:,3));
sineB = sind(phaseVoltageAngle(:,3));
BphaseVoltageReal = phaseVoltageMag(:,3).*cosineB;
BphaseVoltageImag = phaseVoltageMag(:,3).*sineB;
BphaseVoltage = complex(BphaseVoltageReal,BphaseVoltageImag);

cosineN = cosd(phaseVoltageAngle(:,4));
sineN = sind(phaseVoltageAngle(:,4));
NphaseVoltageReal = phaseVoltageMag(:,4).*cosineN;
NphaseVoltageImag = phaseVoltageMag(:,4).*sineN;
NphaseVoltage = complex(NphaseVoltageReal,NphaseVoltageImag);

phaseVoltageToNeutralR = RphaseVoltage-NphaseVoltage;
phaseVoltageToNeutralW = WphaseVoltage-NphaseVoltage;
phaseVoltageToNeutralB = BphaseVoltage-NphaseVoltage;
Rphase = abs(phaseVoltageToNeutralR);
Wphase = abs(phaseVoltageToNeutralW);
Bphase = abs(phaseVoltageToNeutralB);
OVLimit = 253*ones(1,336);
UVLimit = 216.2*ones(1,336);

figure (5);
plot(Hour+Second/3600,Rphase,'Color','red','LineWidth',2);
hold on
plot(Hour+Second/3600,Wphase,'Color','green','LineWidth',2);
hold on
plot(Hour+Second/3600,Bphase,'Color','blue','LineWidth',2);

```

```

hold on
plot(Hour+Second/3600,OVLimit,'Color','magenta','LineStyle',':', 'LineWidth',2);
hold on
plot(Hour+Second/3600,UVLimit,'Color','cyan','LineStyle',':', 'LineWidth',2);

legend('Phase A', 'Phase B', 'Phase C', 'OV limit', 'UV limit', 'Location', 'southeast')
xlabel('Hour', 'FontSize', 12, 'FontWeight', 'bold')
ylabel('Phase to Neutral Voltages (V)', 'FontSize', 12, 'FontWeight', 'bold')
title('Weekly Simulation, Voltages at LoadBus17', 'FontSize', 12, 'FontWeight', 'bold')
hold off
saveas(gcf, 'C:\Users\Peter\My Documents\PhD study\OpenDSS\Cypress-Stillia\RunCase\Volt-new\Case6-
Fig5', 'bmp');

```

```

DSSText.Command = 'export monitors m18';
monitorFile = DSSText.Result;
MyCSV = importdata(monitorFile);
delete(monitorFile);
Hour = MyCSV.data(:,1); Second = MyCSV.data(:,2);
phaseVoltageMag = MyCSV.data(:,[3,5,7,9]);
phaseVoltageAngle = MyCSV.data(:,[4,6,8,10]);
phaseCurrent = MyCSV.data(:,[11,13,15,17]);

cosineR = cosd(phaseVoltageAngle(:,1));
sineR = sind(phaseVoltageAngle(:,1));
RphaseVoltageReal = phaseVoltageMag(:,1).*cosineR;
RphaseVoltageImag = phaseVoltageMag(:,1).*sineR;
RphaseVoltage = complex(RphaseVoltageReal,RphaseVoltageImag);

cosineW = cosd(phaseVoltageAngle(:,2));
sineW = sind(phaseVoltageAngle(:,2));
WphaseVoltageReal = phaseVoltageMag(:,2).*cosineW;
WphaseVoltageImag = phaseVoltageMag(:,2).*sineW;
WphaseVoltage = complex(WphaseVoltageReal,WphaseVoltageImag);

cosineB = cosd(phaseVoltageAngle(:,3));
sineB = sind(phaseVoltageAngle(:,3));
BphaseVoltageReal = phaseVoltageMag(:,3).*cosineB;
BphaseVoltageImag = phaseVoltageMag(:,3).*sineB;
BphaseVoltage = complex(BphaseVoltageReal,BphaseVoltageImag);

cosineN = cosd(phaseVoltageAngle(:,4));
sineN = sind(phaseVoltageAngle(:,4));
NphaseVoltageReal = phaseVoltageMag(:,4).*cosineN;
NphaseVoltageImag = phaseVoltageMag(:,4).*sineN;
NphaseVoltage = complex(NphaseVoltageReal,NphaseVoltageImag);

phaseVoltageToNeutralR = RphaseVoltage-NphaseVoltage;
phaseVoltageToNeutralW = WphaseVoltage-NphaseVoltage;
phaseVoltageToNeutralB = BphaseVoltage-NphaseVoltage;
Rphase = abs(phaseVoltageToNeutralR);
Wphase = abs(phaseVoltageToNeutralW);
Bphase = abs(phaseVoltageToNeutralB);
OVLimit = 253*ones(1,336);
UVLimit = 216.2*ones(1,336);

figure (6);
plot(Hour+Second/3600,Rphase,'Color','red','LineWidth',2);
hold on
plot(Hour+Second/3600,Wphase,'Color','green','LineWidth',2);
hold on
plot(Hour+Second/3600,Bphase,'Color','blue','LineWidth',2);
hold on
plot(Hour+Second/3600,OVLimit,'Color','magenta','LineStyle',':', 'LineWidth',2);
hold on
plot(Hour+Second/3600,UVLimit,'Color','cyan','LineStyle',':', 'LineWidth',2);

```

```

legend('Phase A', 'Phase B', 'Phase C', 'OV limit', 'UV limit', 'Location', 'southeast')
xlabel('Hour', 'FontSize', 12, 'FontWeight', 'bold')
ylabel('Phase to Neutral Voltages (V)', 'FontSize', 12, 'FontWeight', 'bold')
title('Weekly Simulation, Voltages at LoadBus20', 'FontSize', 12, 'FontWeight', 'bold')
hold off
saveas(gcf, 'C:\Users\Peter\My Documents\PhD study\OpenDSS\Cypress-Stillia\RunCase\Volt-new\Case6-
Fig6', 'bmp');

```

C. MATLAB Codes for Voltage Unbalance Analysis

```
% MatLab code for voltage unbalance analysis
```

```
% To run this MatLab code, make sure the current folder points to the
% location where all the files required by the DSS program are located
```

```

clear all;
DSSObj=actxserver('OpenDSSEngine.dss');
Start=DSSObj.Start(0);
[DSSStartOK, DSSObj, DSSText] = DSSStartup;

    % Set up the interface variables
    DSSCircuit=DSSObj.ActiveCircuit;
    DSSSolution=DSSCircuit.Solution;
    DSSText.Command='Compile (C:\Program Files\OpenDSS\Examples\Jemena\SHM14_Cypress-
Stillia_V23b.dss)';

    % Add an EnergyMeter object so the distances down the feeder are computed

DSSText.Command='New EnergyMeter.E1 Line.LINE1 1';

% Add a Monitor, too
    DSSText.Command='New Monitor.FeederEnd Line.LINE1 1';

% New Line Drop Compensation setting default is Vreg=63.5 R=1.16 X=1.97
DSSText.Command='RegControl.Reg1.Vreg=65.3 R=0 X=0';

% Change the load type at SHM 22kV bus
DSSText.Command='New Load.LOAD1 Bus1=LoadBus2 kV=22 kVA=18000 PF=0.9 duty=Bus_weekly';

% Connect PV1 and PV2 to selected phases
DSSText.Command='PVSystem.PV1.Bus1=LoadBus12.3.4';
DSSText.Command='PVSystem.PV2.Bus1=LoadBus21.3.4';

% -----
% Run a weekly analysis and plot the voltages and currents measured by the monitors
% The 3-phase voltages are measured between the phases and neutral
% -----

DSSText.command='set mode = duty';
DSSCircuit.Solution.Number = 1;
DSSCircuit.Solution.Stepsize = 1800;
DSSCircuit.Solution.Hour = 0;

    for i=1:336
DSSCircuit.Solution.Solve;

        end

    DSSText.Command = 'export monitors m6';
    monitorFile = DSSText.Result;
    MyCSV = importdata(monitorFile);
    delete(monitorFile);

```

```

Hour = MyCSV.data(:,1); Second = MyCSV.data(:,2);
phaseVoltageMag = MyCSV.data(:,[3,5,7,9]);
phaseVoltageAngle = MyCSV.data(:,[4,6,8,10]);

cosineR = cosd(phaseVoltageAngle(:,1));
sineR = sind(phaseVoltageAngle(:,1));
RphaseVoltageReal = phaseVoltageMag(:,1).*cosineR;
RphaseVoltageImag = phaseVoltageMag(:,1).*sineR;
RphaseVoltage = complex(RphaseVoltageReal,RphaseVoltageImag);

cosineW = cosd(phaseVoltageAngle(:,2));
sineW = sind(phaseVoltageAngle(:,2));
WphaseVoltageReal = phaseVoltageMag(:,2).*cosineW;
WphaseVoltageImag = phaseVoltageMag(:,2).*sineW;
WphaseVoltage = complex(WphaseVoltageReal,WphaseVoltageImag);

cosineB = cosd(phaseVoltageAngle(:,3));
sineB = sind(phaseVoltageAngle(:,3));
BphaseVoltageReal = phaseVoltageMag(:,3).*cosineB;
BphaseVoltageImag = phaseVoltageMag(:,3).*sineB;
BphaseVoltage = complex(BphaseVoltageReal,BphaseVoltageImag);

cosineN = cosd(phaseVoltageAngle(:,4));
sineN = sind(phaseVoltageAngle(:,4));
NphaseVoltageReal = phaseVoltageMag(:,4).*cosineN;
NphaseVoltageImag = phaseVoltageMag(:,4).*sineN;
NphaseVoltage = complex(NphaseVoltageReal,NphaseVoltageImag);

phaseVolutetoNeutralR = RphaseVoltage-NphaseVoltage;
phaseVolutetoNeutralW = WphaseVoltage-NphaseVoltage;
phaseVolutetoNeutralB = BphaseVoltage-NphaseVoltage;
Rphase = abs(phaseVolutetoNeutralR); % phase-to-neutral voltage magnitude
Wphase = abs(phaseVolutetoNeutralW);
Bphase = abs(phaseVolutetoNeutralB);

RphaseAngle = angle(phaseVolutetoNeutralR); % in radians
WphaseAngle = angle(phaseVolutetoNeutralW);
BphaseAngle = angle(phaseVolutetoNeutralB);

RWphaseAngle = RphaseAngle-WphaseAngle; % in radians
WBphaseAngle = WphaseAngle-BphaseAngle;
BRphaseAngle = BphaseAngle-RphaseAngle;

VoltageUnbalance_Num =
sqrt((Rphase.^2+Wphase.^2+Bphase.^2)*2+Rphase.*Wphase.*cos(RWphaseAngle+1.0472)*2+Wphase.*Bphase.*cos(WBphaseAngle+1.0472)*2+Bphase.*Rphase.*cos(BRphaseAngle+1.0472)*2);
VoltageUnbalance_Dem = sqrt((Rphase.^2+Wphase.^2+Bphase.^2)+Rphase.*Wphase.*cos(RWphaseAngle-2.0944)*2+Wphase.*Bphase.*cos(WBphaseAngle-2.0944)*2+Bphase.*Rphase.*cos(BRphaseAngle-2.0944)*2);
VoltageUnbalance_bus9 = 100*(VoltageUnbalance_Num./VoltageUnbalance_Dem); % voltage balance in %

xlswrite('C:\Users\Peter\My Documents\PhD study\OpenDSS\Cypress-Stillia\RunCase\Unbalance-new\Phase allocation\Monitors-phase allocation.xlsx',VoltageUnbalance_bus9,'Case9','A2:A337');

clear('phaseVoltageMag','phaseVoltageAngle');

DSSText.Command = 'export monitors m23';
monitorFile = DSSText.Result;
MyCSV = importdata(monitorFile);
delete(monitorFile);
Hour = MyCSV.data(:,1); Second = MyCSV.data(:,2);
phaseVoltageMag = MyCSV.data(:,[3,5,7,9]);
phaseVoltageAngle = MyCSV.data(:,[4,6,8,10]);

cosineR = cosd(phaseVoltageAngle(:,1));
sineR = sind(phaseVoltageAngle(:,1));
RphaseVoltageReal = phaseVoltageMag(:,1).*cosineR;

```

```

RphaseVoltageImag = phaseVoltageMag(:,1).*sineR;
RphaseVoltage = complex(RphaseVoltageReal,RphaseVoltageImag);

cosineW = cosd(phaseVoltageAngle(:,2));
sineW = sind(phaseVoltageAngle(:,2));
WphaseVoltageReal = phaseVoltageMag(:,2).*cosineW;
WphaseVoltageImag = phaseVoltageMag(:,2).*sineW;
WphaseVoltage = complex(WphaseVoltageReal,WphaseVoltageImag);

cosineB = cosd(phaseVoltageAngle(:,3));
sineB = sind(phaseVoltageAngle(:,3));
BphaseVoltageReal = phaseVoltageMag(:,3).*cosineB;
BphaseVoltageImag = phaseVoltageMag(:,3).*sineB;
BphaseVoltage = complex(BphaseVoltageReal,BphaseVoltageImag);

cosineN = cosd(phaseVoltageAngle(:,4));
sineN = sind(phaseVoltageAngle(:,4));
NphaseVoltageReal = phaseVoltageMag(:,4).*cosineN;
NphaseVoltageImag = phaseVoltageMag(:,4).*sineN;
NphaseVoltage = complex(NphaseVoltageReal,NphaseVoltageImag);

phaseVoltageToNeutralR = RphaseVoltage-NphaseVoltage;
phaseVoltageToNeutralW = WphaseVoltage-NphaseVoltage;
phaseVoltageToNeutralB = BphaseVoltage-NphaseVoltage;
Rphase = abs(phaseVoltageToNeutralR); % phase-to-neutral voltage magnitude
Wphase = abs(phaseVoltageToNeutralW);
Bphase = abs(phaseVoltageToNeutralB);

RphaseAngle = angle(phaseVoltageToNeutralR); % in radians
WphaseAngle = angle(phaseVoltageToNeutralW);
BphaseAngle = angle(phaseVoltageToNeutralB);

RWphaseAngle = RphaseAngle-WphaseAngle; % in radians
WBphaseAngle = WphaseAngle-BphaseAngle;
BRphaseAngle = BphaseAngle-RphaseAngle;

VoltageUnbalance_Num =
sqrt((Rphase.^2+Wphase.^2+Bphase.^2)*2+Rphase.*Wphase.*cos(RWphaseAngle+1.0472)*2+Wphase.*Bphase.*cos(WBphaseAngle+1.0472)*2+Bphase.*Rphase.*cos(BRphaseAngle+1.0472)*2);
VoltageUnbalance_Dem = sqrt((Rphase.^2+Wphase.^2+Bphase.^2)+Rphase.*Wphase.*cos(RWphaseAngle-2.0944)*2+Wphase.*Bphase.*cos(WBphaseAngle-2.0944)*2+Bphase.*Rphase.*cos(BRphaseAngle-2.0944)*2);
VoltageUnbalance_bus10 = 100*(VoltageUnbalance_Num./VoltageUnbalance_Dem); % voltage balance in %

xlswrite('C:\Users\Peter\My Documents\PhD study\OpenDSS\Cypress-Stillia\RunCase\Unbalance-
new\Phase allocation\Monitors-phase allocation.xlsx',VoltageUnbalance_bus10,'Case9','B2:B337');

clear('phaseVoltageMag','phaseVoltageAngle');

DSSText.Command = 'export monitors m24';
monitorFile = DSSText.Result;
MyCSV = importdata(monitorFile);
delete(monitorFile);
Hour = MyCSV.data(:,1); Second = MyCSV.data(:,2);
phaseVoltageMag = MyCSV.data(:,[3,5,7,9]);
phaseVoltageAngle = MyCSV.data(:,[4,6,8,10]);

cosineR = cosd(phaseVoltageAngle(:,1));
sineR = sind(phaseVoltageAngle(:,1));
RphaseVoltageReal = phaseVoltageMag(:,1).*cosineR;
RphaseVoltageImag = phaseVoltageMag(:,1).*sineR;
RphaseVoltage = complex(RphaseVoltageReal,RphaseVoltageImag);

cosineW = cosd(phaseVoltageAngle(:,2));
sineW = sind(phaseVoltageAngle(:,2));
WphaseVoltageReal = phaseVoltageMag(:,2).*cosineW;
WphaseVoltageImag = phaseVoltageMag(:,2).*sineW;

```

```

WphaseVoltage = complex(WphaseVoltageReal,WphaseVoltageImag);

cosineB = cosd(phaseVoltageAngle(:,3));
sineB = sind(phaseVoltageAngle(:,3));
BphaseVoltageReal = phaseVoltageMag(:,3).*cosineB;
BphaseVoltageImag = phaseVoltageMag(:,3).*sineB;
BphaseVoltage = complex(BphaseVoltageReal,BphaseVoltageImag);

cosineN = cosd(phaseVoltageAngle(:,4));
sineN = sind(phaseVoltageAngle(:,4));
NphaseVoltageReal = phaseVoltageMag(:,4).*cosineN;
NphaseVoltageImag = phaseVoltageMag(:,4).*sineN;
NphaseVoltage = complex(NphaseVoltageReal,NphaseVoltageImag);

phaseVoltageToNeutralR = RphaseVoltage-NphaseVoltage;
phaseVoltageToNeutralW = WphaseVoltage-NphaseVoltage;
phaseVoltageToNeutralB = BphaseVoltage-NphaseVoltage;
Rphase = abs(phaseVoltageToNeutralR); % phase-to-neutral voltage magnitude
Wphase = abs(phaseVoltageToNeutralW);
Bphase = abs(phaseVoltageToNeutralB);

RphaseAngle = angle(phaseVoltageToNeutralR); % in radians
WphaseAngle = angle(phaseVoltageToNeutralW);
BphaseAngle = angle(phaseVoltageToNeutralB);

RWphaseAngle = RphaseAngle-WphaseAngle; % in radians
WBphaseAngle = WphaseAngle-BphaseAngle;
BRphaseAngle = BphaseAngle-RphaseAngle;

VoltageUnbalance_Num =
sqrt((Rphase.^2+Wphase.^2+Bphase.^2)*2+Rphase.*Wphase.*cos(RWphaseAngle+1.0472)*2+Wphase.*Bphase.*cos(WBphaseAngle+1.0472)*2+Bphase.*Rphase.*cos(BRphaseAngle+1.0472)*2);
VoltageUnbalance_Dem = sqrt((Rphase.^2+Wphase.^2+Bphase.^2)+Rphase.*Wphase.*cos(RWphaseAngle-2.0944)*2+Wphase.*Bphase.*cos(WBphaseAngle-2.0944)*2+Bphase.*Rphase.*cos(BRphaseAngle-2.0944)*2);
VoltageUnbalance_bus11 = 100*(VoltageUnbalance_Num./VoltageUnbalance_Dem); % voltage balance in %

xlswrite('C:\Users\Peter\My Documents\PhD study\OpenDSS\Cypress-Stillia\RunCase\Unbalance-new\Phase allocation\Monitors-phase allocation.xlsx',VoltageUnbalance_bus11,'Case9','C2:C337');

clear('phaseVoltageMag','phaseVoltageAngle');

DSSText.Command = 'export monitors m18';
monitorFile = DSSText.Result;
MyCSV = importdata(monitorFile);
delete(monitorFile);

Hour = MyCSV.data(:,1); Second = MyCSV.data(:,2);
phaseVoltageMag = MyCSV.data(:,[3,5,7,9]);
phaseVoltageAngle = MyCSV.data(:,[4,6,8,10]);

cosineR = cosd(phaseVoltageAngle(:,1));
sineR = sind(phaseVoltageAngle(:,1));
RphaseVoltageReal = phaseVoltageMag(:,1).*cosineR;
RphaseVoltageImag = phaseVoltageMag(:,1).*sineR;
RphaseVoltage = complex(RphaseVoltageReal,RphaseVoltageImag);

cosineW = cosd(phaseVoltageAngle(:,2));
sineW = sind(phaseVoltageAngle(:,2));
WphaseVoltageReal = phaseVoltageMag(:,2).*cosineW;
WphaseVoltageImag = phaseVoltageMag(:,2).*sineW;
WphaseVoltage = complex(WphaseVoltageReal,WphaseVoltageImag);

cosineB = cosd(phaseVoltageAngle(:,3));
sineB = sind(phaseVoltageAngle(:,3));
BphaseVoltageReal = phaseVoltageMag(:,3).*cosineB;
BphaseVoltageImag = phaseVoltageMag(:,3).*sineB;

```

```

BphaseVoltage = complex(BphaseVoltageReal,BphaseVoltageImag);

cosineN = cosd(phaseVoltageAngle(:,4));
sineN = sind(phaseVoltageAngle(:,4));
NphaseVoltageReal = phaseVoltageMag(:,4).*cosineN;
NphaseVoltageImag = phaseVoltageMag(:,4).*sineN;
NphaseVoltage = complex(NphaseVoltageReal,NphaseVoltageImag);

phaseVoltageToNeutralR = RphaseVoltage-NphaseVoltage;
phaseVoltageToNeutralW = WphaseVoltage-NphaseVoltage;
phaseVoltageToNeutralB = BphaseVoltage-NphaseVoltage;
Rphase = abs(phaseVoltageToNeutralR); % phase-to-neutral voltage magnitude
Wphase = abs(phaseVoltageToNeutralW);
Bphase = abs(phaseVoltageToNeutralB);

RphaseAngle = angle(phaseVoltageToNeutralR); % in radians
WphaseAngle = angle(phaseVoltageToNeutralW);
BphaseAngle = angle(phaseVoltageToNeutralB);

RWphaseAngle = RphaseAngle-WphaseAngle; % in radians
WBphaseAngle = WphaseAngle-BphaseAngle;
BRphaseAngle = BphaseAngle-RphaseAngle;

VoltageUnbalance_Num =
sqrt((Rphase.^2+Wphase.^2+Bphase.^2)*2+Rphase.*Wphase.*cos(RWphaseAngle+1.0472)*2+Wphase.*Bphase.*cos(WBphaseAngle+1.0472)*2+Bphase.*Rphase.*cos(BRphaseAngle+1.0472)*2);
VoltageUnbalance_Dem = sqrt((Rphase.^2+Wphase.^2+Bphase.^2)+Rphase.*Wphase.*cos(RWphaseAngle-2.0944)*2+Wphase.*Bphase.*cos(WBphaseAngle-2.0944)*2+Bphase.*Rphase.*cos(BRphaseAngle-2.0944)*2);
VoltageUnbalance_bus20 = 100*(VoltageUnbalance_Num./VoltageUnbalance_Dem); % voltage balance in %

xlswrite('C:\Users\Peter\My Documents\PhD study\OpenDSS\Cypress-Stillia\RunCase\Unbalance-new\Phase allocation\Monitors-phase allocation.xlsx',VoltageUnbalance_bus20,'Case9','F2:F337');

clear('phaseVoltageMag','phaseVoltageAngle');

DSSText.Command = 'export monitors m25';
monitorFile = DSSText.Result;
MyCSV = importdata(monitorFile);
delete(monitorFile);
Hour = MyCSV.data(:,1); Second = MyCSV.data(:,2);
phaseVoltageMag = MyCSV.data(:,[3,5,7,9]);
phaseVoltageAngle = MyCSV.data(:,[4,6,8,10]);

cosineR = cosd(phaseVoltageAngle(:,1));
sineR = sind(phaseVoltageAngle(:,1));
RphaseVoltageReal = phaseVoltageMag(:,1).*cosineR;
RphaseVoltageImag = phaseVoltageMag(:,1).*sineR;
RphaseVoltage = complex(RphaseVoltageReal,RphaseVoltageImag);

cosineW = cosd(phaseVoltageAngle(:,2));
sineW = sind(phaseVoltageAngle(:,2));
WphaseVoltageReal = phaseVoltageMag(:,2).*cosineW;
WphaseVoltageImag = phaseVoltageMag(:,2).*sineW;
WphaseVoltage = complex(WphaseVoltageReal,WphaseVoltageImag);

cosineB = cosd(phaseVoltageAngle(:,3));
sineB = sind(phaseVoltageAngle(:,3));
BphaseVoltageReal = phaseVoltageMag(:,3).*cosineB;
BphaseVoltageImag = phaseVoltageMag(:,3).*sineB;
BphaseVoltage = complex(BphaseVoltageReal,BphaseVoltageImag);

cosineN = cosd(phaseVoltageAngle(:,4));
sineN = sind(phaseVoltageAngle(:,4));
NphaseVoltageReal = phaseVoltageMag(:,4).*cosineN;
NphaseVoltageImag = phaseVoltageMag(:,4).*sineN;
NphaseVoltage = complex(NphaseVoltageReal,NphaseVoltageImag);

```

```

phaseVoltageToNeutralR = RphaseVoltage-NphaseVoltage;
phaseVoltageToNeutralW = WphaseVoltage-NphaseVoltage;
phaseVoltageToNeutralB = BphaseVoltage-NphaseVoltage;
Rphase = abs(phaseVoltageToNeutralR); % phase-to-neutral voltage magnitude
Wphase = abs(phaseVoltageToNeutralW);
Bphase = abs(phaseVoltageToNeutralB);

RphaseAngle = angle(phaseVoltageToNeutralR); % in radians
WphaseAngle = angle(phaseVoltageToNeutralW);
BphaseAngle = angle(phaseVoltageToNeutralB);

RWphaseAngle = RphaseAngle-WphaseAngle; % in radians
WBphaseAngle = WphaseAngle-BphaseAngle;
BRphaseAngle = BphaseAngle-RphaseAngle;

VoltageUnbalance_Num =
sqrt((Rphase.^2+Wphase.^2+Bphase.^2)+Rphase.*Wphase.*cos(RWphaseAngle+1.0472)*2+Wphase.*Bpha
se.*cos(WBphaseAngle+1.0472)*2+Bphase.*Rphase.*cos(BRphaseAngle+1.0472)*2);
VoltageUnbalance_Dem = sqrt((Rphase.^2+Wphase.^2+Bphase.^2)+Rphase.*Wphase.*cos(RWphaseAngle-
2.0944)*2+Wphase.*Bphase.*cos(WBphaseAngle-2.0944)*2+Bphase.*Rphase.*cos(BRphaseAngle-2.0944)*2);
VoltageUnbalance_bus14 = 100*(VoltageUnbalance_Num./VoltageUnbalance_Dem); % voltage balance in %

xlswrite('C:\Users\Peter\My Documents\PhD study\OpenDSS\Cypress-Stillia\RunCase\Unbalance-
new\Phase allocation\Monitors-phase allocation.xlsx',VoltageUnbalance_bus14,'Case9','d2:d337');

clear('phaseVoltageMag','phaseVoltageAngle');

DSSText.Command = 'export monitors m21';
monitorFile = DSSText.Result;
MyCSV = importdata(monitorFile);
delete(monitorFile);
Hour = MyCSV.data(:,1); Second = MyCSV.data(:,2);
phaseVoltageMag = MyCSV.data(:,[3,5,7,9]);
phaseVoltageAngle = MyCSV.data(:,[4,6,8,10]);

cosineR = cosd(phaseVoltageAngle(:,1));
sineR = sind(phaseVoltageAngle(:,1));
RphaseVoltageReal = phaseVoltageMag(:,1).*cosineR;
RphaseVoltageImag = phaseVoltageMag(:,1).*sineR;
RphaseVoltage = complex(RphaseVoltageReal,RphaseVoltageImag);

cosineW = cosd(phaseVoltageAngle(:,2));
sineW = sind(phaseVoltageAngle(:,2));
WphaseVoltageReal = phaseVoltageMag(:,2).*cosineW;
WphaseVoltageImag = phaseVoltageMag(:,2).*sineW;
WphaseVoltage = complex(WphaseVoltageReal,WphaseVoltageImag);

cosineB = cosd(phaseVoltageAngle(:,3));
sineB = sind(phaseVoltageAngle(:,3));
BphaseVoltageReal = phaseVoltageMag(:,3).*cosineB;
BphaseVoltageImag = phaseVoltageMag(:,3).*sineB;
BphaseVoltage = complex(BphaseVoltageReal,BphaseVoltageImag);

cosineN = cosd(phaseVoltageAngle(:,4));
sineN = sind(phaseVoltageAngle(:,4));
NphaseVoltageReal = phaseVoltageMag(:,4).*cosineN;
NphaseVoltageImag = phaseVoltageMag(:,4).*sineN;
NphaseVoltage = complex(NphaseVoltageReal,NphaseVoltageImag);

phaseVoltageToNeutralR = RphaseVoltage-NphaseVoltage;
phaseVoltageToNeutralW = WphaseVoltage-NphaseVoltage;
phaseVoltageToNeutralB = BphaseVoltage-NphaseVoltage;
Rphase = abs(phaseVoltageToNeutralR); % phase-to-neutral voltage magnitude
Wphase = abs(phaseVoltageToNeutralW);
Bphase = abs(phaseVoltageToNeutralB);

```

```

RphaseAngle = angle(phaseVoltageToNeutralR); % in radians
WphaseAngle = angle(phaseVoltageToNeutralW);
BphaseAngle = angle(phaseVoltageToNeutralB);

RWphaseAngle = RphaseAngle-WphaseAngle; % in radians
WBphaseAngle = WphaseAngle-BphaseAngle;
BRphaseAngle = BphaseAngle-RphaseAngle;

VoltageUnbalance_Num =
sqrt((Rphase.^2+Wphase.^2+Bphase.^2)*2+Rphase.*Wphase.*cos(RWphaseAngle+1.0472)*2+Wphase.*Bphase.*cos(WBphaseAngle+1.0472)*2+Bphase.*Rphase.*cos(BRphaseAngle+1.0472)*2);
VoltageUnbalance_Dem = sqrt((Rphase.^2+Wphase.^2+Bphase.^2)+Rphase.*Wphase.*cos(RWphaseAngle-2.0944)*2+Wphase.*Bphase.*cos(WBphaseAngle-2.0944)*2+Bphase.*Rphase.*cos(BRphaseAngle-2.0944)*2);
VoltageUnbalance_bus17 = 100*(VoltageUnbalance_Num./VoltageUnbalance_Dem); % voltage balance in %

xlswrite('C:\Users\Peter\My Documents\PhD study\OpenDSS\Cypress-Stillia\RunCase\Unbalance-new\Phase allocation\Monitors-phase allocation.xlsx',VoltageUnbalance_bus17,'Case9','e2:e337');

clear('phaseVoltageMag','phaseVoltageAngle');

figure (9);
plot(Hour+Second/3600,VoltageUnbalance_bus9,'Color','green','LineWidth',1);
hold on
plot(Hour+Second/3600,VoltageUnbalance_bus10,'Color','cyan','LineWidth',1);
hold on
plot(Hour+Second/3600,VoltageUnbalance_bus11,'Color','magenta','LineWidth',1);
hold on
plot(Hour+Second/3600,VoltageUnbalance_bus20,'Color','blue','LineWidth',1);
hold on
plot(Hour+Second/3600,VoltageUnbalance_bus14,'Color','red','LineWidth',1);
hold on
plot(Hour+Second/3600,VoltageUnbalance_bus17,'Color','black','LineWidth',1);
legend('LoadBus9','LoadBus10','LoadBus11','LoadBus20','LoadBus14','LoadBus17','Location','best')
xlabel('Hour','FontSize',12,'FontWeight','bold')
ylabel('Voltage Unbalance in %','FontSize',12,'FontWeight','bold')
ylim([0 1.4])
title('Unbalance Voltages at Load Buses','FontSize',12,'FontWeight','bold')
hold off

saveas(gcf,'C:\Users\Peter\My Documents\PhD study\OpenDSS\Cypress-Stillia\RunCase\Unbalance-New\Phase allocation\Scenario6Case9-all load buses','bmp');

```

References

1. Ochoa, L.F. and P. Mancarella. *Low-carbon LV networks: Challenges for planning and operation*. in *Power and Energy Society General Meeting, 2012 IEEE*. 2012. IEEE.
2. Elphick, S., et al. *The Australian Long Term Power Quality Survey project update*. in *Proceedings of 14th International Conference on Harmonics and Quality of Power - ICHQP 2010*. 2010.
3. Navarro, A., et al. *Impacts of photovoltaics on low voltage networks: A case study for the North West of England*. in *22nd International Conference and Exhibition on Electricity Distribution (CIRED 2013)*. 2013.
4. Inc, R.W.B., *Distributed Renewable Energy Operating Impacts and Valuation Study*. 2009, Arizona Public Service.
5. Shafiullah, G.M., et al., *Prospects of renewable energy – a feasibility study in the Australian context*. *Renewable Energy*, 2012. **39**(1): p. 183-197.
6. McConnell, D., et al., *Retrospective modeling of the merit-order effect on wholesale electricity prices from distributed photovoltaic generation in the Australian National Electricity Market*. *Energy Policy*, 2013. **58**: p. 17-27.
7. Marinopoulos, A.G., M.C. Alexiadis, and P.S. Dokopoulos, *Energy losses in a distribution line with distributed generation based on stochastic power flow*. *Electric Power Systems Research*, 2011. **81**(10): p. 1986-1994.
8. Medina, A., J.C. Hernandez, and F. Jurado. *Optimal Placement and Sizing Procedure for PV Systems on Radial Distribution Systems*. in *2006 International Conference on Power System Technology*. 2006.
9. Marinopoulos, A.G., M.C. Alexiadis, and P.S. Dokopoulos, *A Correlation Index to Evaluate Impact of PV Installation on Joule Losses*. *IEEE Transactions on Power Systems*, 2011. **26**(3): p. 1564-1572.
10. Barbeiro, P.N.P., et al. *Evaluation of the impact of large scale integration of micro-generation units in low and Medium Voltage distribution networks*. in *2010 IEEE Conference on Innovative Technologies for an Efficient and Reliable Electricity Supply*. 2010.
11. Ropp, M., et al. *Review of potential problems and utility concerns arising from high penetration levels of photovoltaics in distribution systems*. in *2008 33rd IEEE Photovoltaic Specialists Conference*. 2008.
12. Gonzalez, C., et al. *LV distribution network feeders in Belgium and power quality issues due to increasing PV penetration levels*. in *2012 3rd IEEE PES Innovative Smart Grid Technologies Europe (ISGT Europe)*. 2012.
13. Eltawil, M.A. and Z. Zhao, *Grid-connected photovoltaic power systems: Technical and potential problems—A review*. *Renewable and Sustainable Energy Reviews*, 2010. **14**(1): p. 112-129.
14. Braun, M., et al., *Is the distribution grid ready to accept large-scale photovoltaic deployment? State of the art, progress, and future prospects*. *Progress in Photovoltaics: Research and Applications*, 2012. **20**(6): p. 681-697.
15. Purvins, A. and B. Klebow, *Technical grid connection guides for distributed electricity generation systems: a new DERlab database has come alive*. *IET Renewable Power Generation*, 2015. **9**(8): p. 1087-1092.
16. Kimmo Lummi, P.T., Antti Rautiainen, Pertti Järventausta. *Implementation possibilities of power-based distribution tariff by using smart metering technology*. in *CIRED*. 2015. Lyon, France.
17. *Electricity distribution investment - what regulatory framework do we need*. 2014, Eurelectric.
18. Ramos, S. and Z. Vale. *Data Mining techniques to support the classification of MV electricity customers*. in *2008 IEEE Power and Energy Society General Meeting - Conversion and Delivery of Electrical Energy in the 21st Century*. 2008.
19. Haben, S., C. Singleton, and P. Grindrod, *Analysis and Clustering of Residential Customers Energy Behavioral Demand Using Smart Meter Data*. *IEEE Transactions on Smart Grid*, 2016. **7**(1): p. 136-144.
20. Pan, E., D. Wang, and Z. Han, *Analyzing Big Smart Metering Data Towards Differentiated User Services: A Sublinear Approach*. *IEEE Transactions on Big Data*, 2016. **2**(3): p. 249-261.

21. Valigi, E. and E.d. Marino. *Networks optimization with advanced meter infrastructure and smart meters*. in *CIREC 2009 - 20th International Conference and Exhibition on Electricity Distribution - Part 1*. 2009.
22. Han, S., et al., *An Automated Impedance Estimation Method in Low-Voltage Distribution Network for Coordinated Voltage Regulation*. IEEE Transactions on Smart Grid, 2015: p. 1-9.
23. Pezeshki, H. and P.J. Wolfs. *Consumer phase identification in a three phase unbalanced LV distribution network*. in *2012 3rd IEEE PES Innovative Smart Grid Technologies Europe (ISGT Europe)*. 2012.
24. Satya Jayadev P, A.R., Nirav P Bhatt, Ramkrishna Pasumarthy, *A Novel Approach for Phase Identification in Smart Grids Using Graph Theory and Principal Component Analysis.pdf*, in *2016 American Control Conference*. 2016: Boston Marriott Copley Place. Boston, MA, USA.
25. Shahnia, F., P.J. Wolfs, and A. Ghosh, *Voltage Unbalance Reduction in Low Voltage Feeders by Dynamic Switching of Residential Customers Among Three Phases*. IEEE Transactions on Smart Grid, 2014. **5**(3): p. 1318-1327.
26. Lim, Y.S. and J.H. Tang, *Experimental study on flicker emissions by photovoltaic systems on highly cloudy region: A case study in Malaysia*. Renewable Energy, 2014. **64**: p. 61-70.
27. Cameron, C.P., W.E. Boyson, and D.M. Riley. *Comparison of PV system performance-model predictions with measured PV system performance*. in *2008 33rd IEEE Photovoltaic Specialists Conference*. 2008.
28. Chatterjee, A., A. Keyhani, and D. Kapoor, *Identification of Photovoltaic Source Models*. IEEE Transactions on Energy Conversion, 2011. **26**(3): p. 883-889.
29. Bo, Z., et al. *Research on model for photovoltaic system power forecasting*. in *CICED 2010 Proceedings*. 2010.
30. Ciric, R.M., A.P. Feltrin, and L.F. Ochoa, *Power flow in four-wire distribution networks-general approach*. IEEE Transactions on Power Systems, 2003. **18**(4): p. 1283-1290.
31. Sunderland, K.M. and M.F. Conlon. *4-Wire load flow analysis of a representative urban network incorporating SSEG*. in *2012 47th International Universities Power Engineering Conference (UPEC)*. 2012.
32. Urquhart, A.J. and M. Thomson, *Series impedance of distribution cables with sector-shaped conductors*. IET Generation, Transmission & Distribution, 2015. **9**(16): p. 2679-2685.
33. Kersting, W.H. and R.K. Green. *The application of Carson's equation to the steady-state analysis of distribution feeders*. in *2011 IEEE/PES Power Systems Conference and Exposition*. 2011.
34. Shahnia, F., et al., *Voltage imbalance analysis in residential low voltage distribution networks with rooftop PVs*. Electric Power Systems Research, 2011. **81**(9): p. 1805-1814.
35. Alam, M.J.E., K.M. Muttaqi, and D. Sutanto, *A SAX-Based Advanced Computational Tool for Assessment of Clustered Rooftop Solar PV Impacts on LV and MV Networks in Smart Grid*. IEEE Transactions on Smart Grid, 2013. **4**(1): p. 577-585.
36. Navarro, A., L.F. Ochoa, and D. Randles. *Monte Carlo-based assessment of PV impacts on real UK low voltage networks*. in *2013 IEEE Power & Energy Society General Meeting*. 2013.
37. Ruiz-Rodriguez, F.J., J.C. Hernández, and F. Jurado, *Probabilistic load flow for photovoltaic distributed generation using the Cornish-Fisher expansion*. Electric Power Systems Research, 2012. **89**: p. 129-138.
38. Rigoni, V., et al., *Representative Residential LV Feeders: A Case Study for the North West of England*. IEEE Transactions on Power Systems, 2016. **31**(1): p. 348-360.
39. Fila, M., et al. *Flexible voltage control to support Distributed Generation in distribution networks*. in *2008 43rd International Universities Power Engineering Conference*. 2008.
40. Vincent Thornley, N.J., Peter Reay, Jonathan Hill, Christine Barbier. *Field experience with active network management of distribution networks with distributed generation*. in *CIREC*. 2007. Vienna, Austria.
41. Alnaser, S.W. and L.F. Ochoa, *Advanced Network Management Systems: A Risk-Based AC OPF Approach*. IEEE Transactions on Power Systems, 2015. **30**(1): p. 409-418.
42. Harrison, G.P., et al., *Hybrid GA and OPF evaluation of network capacity for distributed generation connections*. Electric Power Systems Research, 2008. **78**(3): p. 392-398.

43. Hengsrirawat, V., T. Tayjasanant, and N. Nimpitiwan, *Optimal sizing of photovoltaic distributed generators in a distribution system with consideration of solar radiation and harmonic distortion*. International Journal of Electrical Power & Energy Systems, 2012. **39**(1): p. 36-47.
44. Ballanti, A., et al. *Assessing the benefits of PV var absorption on the hosting capacity of LV feeders*. in *IEEE PES ISGT Europe 2013*. 2013.
45. T. Stetz, W.Y., M. Braun. *Voltage Control in Distribution Systems with High Level PV Penetration-Improving Absorption Capacity for PV Systems by Reactive Power Supply*. in *25th European Photovoltaic Solar Energy Conference and Exhibition / 5th World Conference on Photovoltaic Energy Conversion*. 2010. Valencia, Spain.
46. Herman, L., B. Blažič, and I. Papič. *Voltage profile support in LV distribution networks with distributed generation*. in *2009 44th International Universities Power Engineering Conference (UPEC)*. 2009.
47. Demirok, E., et al. *Clustered PV inverters in LV networks: An overview of impacts and comparison of voltage control strategies*. in *2009 IEEE Electrical Power & Energy Conference (EPEC)*. 2009.
48. Wes Sunderman, J.S., Lindsey Rogers, Huijuan Li. *Smart grid inverters to support photovoltaics in distribution systems*. in *CIREC*. 2015. Lyon, France.
49. Shahnia, F., et al. *Sensitivity analysis of voltage imbalance in distribution networks with rooftop PVs*. in *IEEE PES General Meeting*. 2010.
50. Chao Long, L.F.O., Geraldine Bryson, Dan Randles. *Adoption of capacitors in LV networks with PV systems*. in *CIREC*. 2015. Lyon, France.
51. Alnaser, S.W. and L.F. Ochoa. *Hybrid controller of energy storage and renewable DG for congestion management*. in *2012 IEEE Power and Energy Society General Meeting*. 2012.
52. Richard Tokle Schytte, K.S., Rolf Erlend Grundt. *Use cases for efficient integration of smart homes PV*. in *CIREC*. 2015. Lyon, France.
53. Peter Hauße, C.W., Maximilian Arnold, Wolfram H. Wellssow. *Techno-economic assessment of planning principles for low voltage grids in the presence of massive distributed PV generation*. in *CIREC*. 2015. Lyon, France.
54. Claas Matrose, M.C., Armin Schnettler, Thomas Smolka, Manuel Sojer, Robert Frings. *Control algorithms for voltage regulated distribution transformers – maximum grid-integration of PV and minimal wear*. in *CIREC*. 2015. Lyon, France.
55. Yves Chollot, P.D., Arthur Jourdan, Sandeep Mishra. *New approach to regulate low voltage distribution network*. in *CIREC*. 2015. Lyon, France.
56. Olivia Leitermann, V.M., James Simonelli. *A comparison of field results with modeled behavior for a power electronics regulator used to manage dynamic voltage variation on a feeder with high PV content*. in *CIREC*. 2015. Lyon, France.
57. Kabiri, R., et al., *LV Grid Voltage Regulation Using Transformer Electronic Tap Changing, With PV Inverter Reactive Power Injection*. IEEE Journal of Emerging and Selected Topics in Power Electronics, 2015. **3**(4): p. 1182-1192.
58. Thomas Drizard, C.L., Benoit Chazottes. *Integration of distributed PV generation - the Nice Grid Project*. in *CIREC*. 2015. Lyon, France.
59. Alnaser, S.W. and L.F. Ochoa. *Distribution network management system: An AC OPF approach*. in *2013 IEEE Power & Energy Society General Meeting*. 2013.
60. Hollingworth, D., et al. *Demonstrating enhanced automatic voltage control for today's low carbon network*. in *CIREC 2012 Workshop: Integration of Renewables into the Distribution Grid*. 2012.
61. *Advanced Metering Infrastructure - Minimum AMI functionality Specification (Victoria) September 2008*. 2008.
62. *Electricity Distribution Code*. 2014.
63. Australia, S., *Australian/New Zealand Standard: Electromagnetic compatibility (EMC) Part 4.30: Testing and measurement techniques - Power quality measurement methods*. 2012, SAI Global.

64. Augustin McEvoy, T.M., Luis Castaner, *Practical Handbook of Photovoltaics Fundamentals and Applications*. Edition 2 ed.: Elsevier.
65. Skoplaki, E. and J.A. Palyvos, *On the temperature dependence of photovoltaic module electrical performance: A review of efficiency/power correlations*. Solar Energy, 2009. **83**(5): p. 614-624.
66. Maria Carmela Di Piazza, A.R., Gianpaolo Vitale. *Identification of photovoltaic array model parameters by robust linear regression methods*. in *International Conference on Renewable Energies and Power Quality (ICREPO'09)*. 2009. Valencia, Spain.
67. Chenni, R., et al., *A detailed modeling method for photovoltaic cells*. Energy, 2007. **32**(9): p. 1724-1730.
68. Di Piazza, M.C., et al., *A dynamic model of a photovoltaic generator based on experimental data*. Renew Energy Power Qual J. ISSN, 2010.
69. Mondol, J.D., Y.G. Yohanis, and B. Norton, *Comparison of measured and predicted long term performance of grid a connected photovoltaic system*. Energy Conversion and Management, 2007. **48**(4): p. 1065-1080.
70. Macêdo, W.N. and R. Zilles, *Operational results of grid-connected photovoltaic system with different inverter's sizing factors (ISF)*. Progress in Photovoltaics: Research and Applications, 2007. **15**(4): p. 337-352.
71. Tan, Y.T., D.S. Kirschen, and N. Jenkins, *A Model of PV Generation Suitable for Stability Analysis*. IEEE Transactions on Energy Conversion, 2004. **19**(4): p. 748-755.
72. Hohm, D. and M.E. Ropp, *Comparative study of maximum power point tracking algorithms*. Progress in photovoltaics: Research and Applications, 2003. **11**(1): p. 47-62.
73. Alves, M.d.C., et al., *Effects of Sky Conditions Measured by the Clearness Index on the Estimation of Solar Radiation Using a Digital Elevation Model*. Atmospheric and Climate Sciences, 2013. **03**(04): p. 618-626.
74. A.Q. Jakhrani, A.K.O., A. R. H. Rigit, S. R. Samo, L. P. Ling, R. Bains. *Evaluation of Incident Solar Radiation on Inclined Plane by Empirical Models at Kuching Sarawak Malaysia*. in *International Conference on Renewable Energies and Power Quality - ICREPO*. 2011. Las Palmas de Gran Canaria, Spain.
75. Thomson, M. and D.G. Infield, *Impact of widespread photovoltaics generation on distribution systems*. IET Renewable Power Generation, 2007. **1**(1): p. 33.
76. Wandhare, R.G. and V. Agarwal. *Novel control scheme to reduce the effect of intermittent solar radiation on the grid connected PV system power output without losing MPPT*. in *2012 Twenty-Seventh Annual IEEE Applied Power Electronics Conference and Exposition (APEC)*. 2012.
77. Dobos, A.P., *PVWatts Version 1 Technical Reference*. 2013, National Renewable Energy Laboratory.
78. *Australian Government Bureau of Meteorology* Available from: <http://www.bom.gov.au/climate/data-services/>.
79. Wu, J., et al., *Prediction of solar radiation with genetic approach combing multi-model framework*. Renewable Energy, 2014. **66**: p. 132-139.
80. Pezeshki, H. and P. Wolfs. *Correlation based method for phase identification in a three phase LV distribution network*. in *2012 22nd Australasian Universities Power Engineering Conference (AUPEC)*. 2012.
81. Tsai-Hsiang, C. and Y. Wen-Chih, *Analysis of multi-grounded four-wire distribution systems considering the neutral grounding*. IEEE Transactions on Power Delivery, 2001. **16**(4): p. 710-717.
82. Degroote, L., et al. *Neutral-point shifting and voltage unbalance due to single-phase DG units in low voltage distribution networks*. in *2009 IEEE Bucharest PowerTech*. 2009.
83. Carson, J.R., *Wave propagation in overhead wires with ground return*. The Bell System Technical Journal, 1926. **5**(4): p. 539-554.
84. Kersting, W.H., *Distribution system modeling and analysis*. 2001: CRC Press.
85. Peter K.C. Wong, R.A.B., Akhtar Kalam, *Generation modelling of residential rooftop photovoltaic systems and its applications in practical electricity distribution networks*. Australian Journal of Electrical and Electronics Engineering, 2015. **12.4**: p. 332-341.

86. *Open Distribution System Simulator [Online]*. EPRI.
87. Bina, M.T. and A. Kashefi, *Three-phase unbalance of distribution systems: Complementary analysis and experimental case study*. International Journal of Electrical Power & Energy Systems, 2011. **33**(4): p. 817-826.
88. Gnacinski, P., *Windings Temperature and Loss of Life of an Induction Machine Under Voltage Unbalance Combined With Over- or Undervoltages*. IEEE Transactions on Energy Conversion, 2008. **23**(2): p. 363-371.
89. *Smart Grid Transformers*. [cited 2016 19 May]; Available from: <http://www.schneider-electric.com/en/product-range/62109-minera-sgrid/>.
90. Barr, R.A., P. Wong, and A. Baitch. *New concepts for steady state voltage standards*. in *2012 IEEE 15th International Conference on Harmonics and Quality of Power*. 2012.